THE NUCLEAR STRUCTURE OF ARSENIC, BROMINE, RUBIDIUM AND SCANDIUM ISOTOPES(Dissertation_全文)

AUTHOR(S):

Imanishi, Nobutsugu

THE NUCLEAR STRUCTURE OF ARSENIC, BROMINE, RUBIDIUM AND SCANDIUM ISOTOPES

N. Imanishi

December 1969

THE NUCLEAR STRUCTURE
OF
ARSENIC, BROMINE, RUBIDIUM AND SCANDIUM ISOTOPES

NOBUTSUGU IMANISHI

KYOTO UNIVERSITY

December 1969

THE NUCLEAR STRUCTURE
OF
ARSENIC, BROMINE, RUBIDIUM AND SCANDIUM ISOTOPES

CONTENTS

ABSTRACT

The nuclear structures of some off-magic isotopes ^{71}As, ^{73}As, ^{75}As, ^{77}As, ^{77}Br, ^{79}Br, ^{81}Br, ^{81}Rb, ^{83}Rb, ^{45}Sc and ^{47}Sc have been studied. Here, it is assumed that each nucleus subjects to a quadrupole distortion and is composed of a doubly-even core plus an un-paired quasi-particle. Then a non-adiabatic model is introduced, where the motion of the quasiparticle moving in Nilsson's deformed orbital is coupled by a Coriolis force with the rotational motion.

First, the level spectra of these isotopes are calculated and compared with experiment. In this calculation, it is necessary to know about the quasiparticle motion. We reveal, therefore, the single particle energy and the wave function as well as the chemical potential and the energy gap, which are determined accurately as a function of deformation. It is found that the quasiparticle formalism leads to a reduction of the coupling term as well as a compression of the low energy spectrum, when compared with the single particle picture. The model spectra are obtained by diagonalizing the Coriolis interaction with the rotational wave functions built on a number of intrinsic quasiparticle states. These states are attributed to the motion of a single "quasi-proton" in No. 15, 16, 17, 19, 20 or 26 orbital for so called $p_{3/2}$ or $f_{5/2}$ shell nuclei

and in No. 10, 12, 13, or 14 orbital for so called $f_{7/2}$ shell nuclei. These calculations are done by using only two parameters; deformation and rotational constant.

For ^{75}As, ^{79}Br, ^{45}Sc and ^{47}Sc, which are most established experimentally among the nuclei of interest, the best fit procedures are carried out between the calculated and the observed level locations. Some characteristic features appeared in the level spectra as well as the overall level locations are reproduced. For other nuclei, only the tentative level spectra are presented. These represent well the levels established experimentally. For comparison, the results of other models are also presented.

Second, to check the validity of the present wave functions, a comparison is made for the experimental and the theoretical reduced electric quadrupole transition probabilities. The experimental E2 transition probabilities are obtained for some nuclei by the Coulomb excitation experiment using nitrogen ions as projectiles. In the extraction procedure, stopping power data are needed and a semiempirical method is proposed to evaluate the stopping powers.

The theoretical transition probability is composed of the collective and the quasiparticle parts and is calculated using the present wave functions. It is found that the pairing effect diminishes the contribution of quasiparticles and a major part of the transition probability

comes from the collective part. An overall agreement is obtained between the theoretical and experimental results except for a few transitions. Since the calculation is done without effective charges, the overall agreement seems worth noting.

Third, the calculated intrinsic and electric quadrupole moment are treated. They are found to agree well with the experimental Q_o values for the nearest doubly-even-mass nuclei and also with the experimental ground state Q values, respectively.

It is concluded that the non-adiabatic model with quasiparticle formalism gives a correct description of the structure of some off-magic nuclei.

CHAPTER 1. INTRODUCTION

The investigation of nuclear structure is one of the most important branches in the field of nuclear study. Very many investigators have endeavoured to understand the nuclear properties from both experimental and theoretical points of view, but it has been quite difficult to establish a complete model----the properties of some nuclei or their groups have been partly explained.

Among the facts hitherto discovered, the existence of magic numbers and large quadrupole moments are the most distinct. When the number of protons (neutrons) reaches to 2, 8, 20, 28, 50, 82 and 126, the nucleus shows abruptly distinguished properties in neutron energy, level spacing, reaction cross section, nuclear radius, etc. To explain the discovered magic numbers and the properties of magic and near-magic nuclei, a shell model has been proposed. Mayer, Haxel, Jensen and Suess (Ma49,Ha49) succeeded in reproducing the appearance of magic numbers by introducing a large amount of spin-orbit coupling.

After this success, many theorists have improved the original shell model--- independent particle model--- in order to explain the accumulated experimental facts. Some of them assumed a detailed residual interaction and radial wave functions of the independent particle shell model states, and then calculated the interaction matrix elements between states of arbitrarily many configurations. Others de[illegible]e

considered rigorous configurations, and used the interaction matrix elements which were determined from experiments. These shell model calculations have been applied to the magic and near-magic nuclei and succeeded in explaining many nuclear properties, such as locations and spins of energy levels, transition probabilities, reduced width, etc.

The nuclei far from the magic numbers have very large quadrupole moments. It is also distinguished that these nuclei have large electric quadupole transition probabilities and distinct rotational energy spectra. The facts suggest that far-magic nuclei are deformed and ready to rotate when they are excited. Bohr, Mottelson and others (Bo52,53,62) have treated these in great detail by a collective model, and succeeded in explaining various properties of the nuclei in the regions of $A=150\sim190$ and $A\gtrsim220$ and those arround $A\sim24$.

The shell model and the collective model seem to be incompatible in first sight, but the truth is more complicated. Each model predicts only one aspect of the real nuclei. Even in deformed nuclei, the nucleons moves in a deformed well and some independent particle motions would still hold. Therefore Bohr and Mottelson have proposed an unified model by combining the deformed shell model with the collective model. In this model the nucleus is composed of a core and a few extra particles--- the former causing a collective motion and the latter producing an intrinsic motion. Thus

the odd-mass nuclei in the well known deformed region have been successfully represented(Mo59).

The off-magic nuclei, which exist in the middle region between the near-magic and far-magic nuclei, show neither clear independent particle picture nor rotational spectra. Thus the theoretical treatments were difficult. But fortunately Bohr, Mottelson and Pines (Bo58) have succeeded in explaining the well known energy gap by introducing the pairing effect, and this gave a key to treat the off-magic nuclei. The systematic study was first done by Kisslinger and Sorensen (Ki63). They started from a spherical shell model, considering a pairing plus quadrupole force as residual interaction and using the quasiparticle random phase approximation. A fairly well success was reported, over a wide range of periodic table, in reproducing the systematic trend of various nuclear properties such as level energies, electric and magnetic transition probabilities, nuclear binding energies, etc. However, they also pointed out that their model might be inadequate to represent nuclei in some regions (for example, the $32 \leq Z \leq 36$ region) other than the well established deformed regions. Because in these regions, their model does not reproduce the detailed variation of the first 2+ energy states in the doubly-even nuclei seen in a particular sequence of isotopes, and the theoretical trend of the variation is similar to that found in the well established deformed regions. Kisslinger and Kumar (Ki67) also modified

the model and predicted the level spectra of some odd-mass nuclei, by considering the anharmonisity of doubly-even system, but the result was not always satisfactory.

In nuclei, there are two important residual interactions, that is, pairing and field effects. The pairing force tends nuclei to form spherical shapes, while the field force causes nuclei to deform. Therefore, the shapes of nuclei are determined by the competition of two forces. Again, the pairing or field force bedomes predominant as an isotope lies nearer to or farther from a closed shell, respectively. Then those nuclei of $32 \leq Z \leq 36$ may be considerably deformed. This is suggested by the experimental facts about nuclear quadrupole moments, nuclear radii, etc. and by the Kisslinger and Sorensen's theoretical work.

As stated above, the nuclei of the present interest are off-magic and the pairing and field forces would compete, but showing considerably deformed shapes. The theoretical treatments have not been done since Kisslinger and Sorensen's work. Therefore we investigate odd-mass nuclei in this region from a point of deformation, considering both Coriolis and pairing interactions, and the satisfactory results are obtained for ^{71}As, ^{73}As, ^{75}As, ^{77}As, ^{79}Br, ^{81}Br and ^{83}Rb. This model is applied also to ^{45}Sc and ^{47}Sc nuclei. The idea of Coriolis coupling was first introduced by Kerman(Ke56). Fig.1-1 shows the locations of these nuclei against magic numbers.

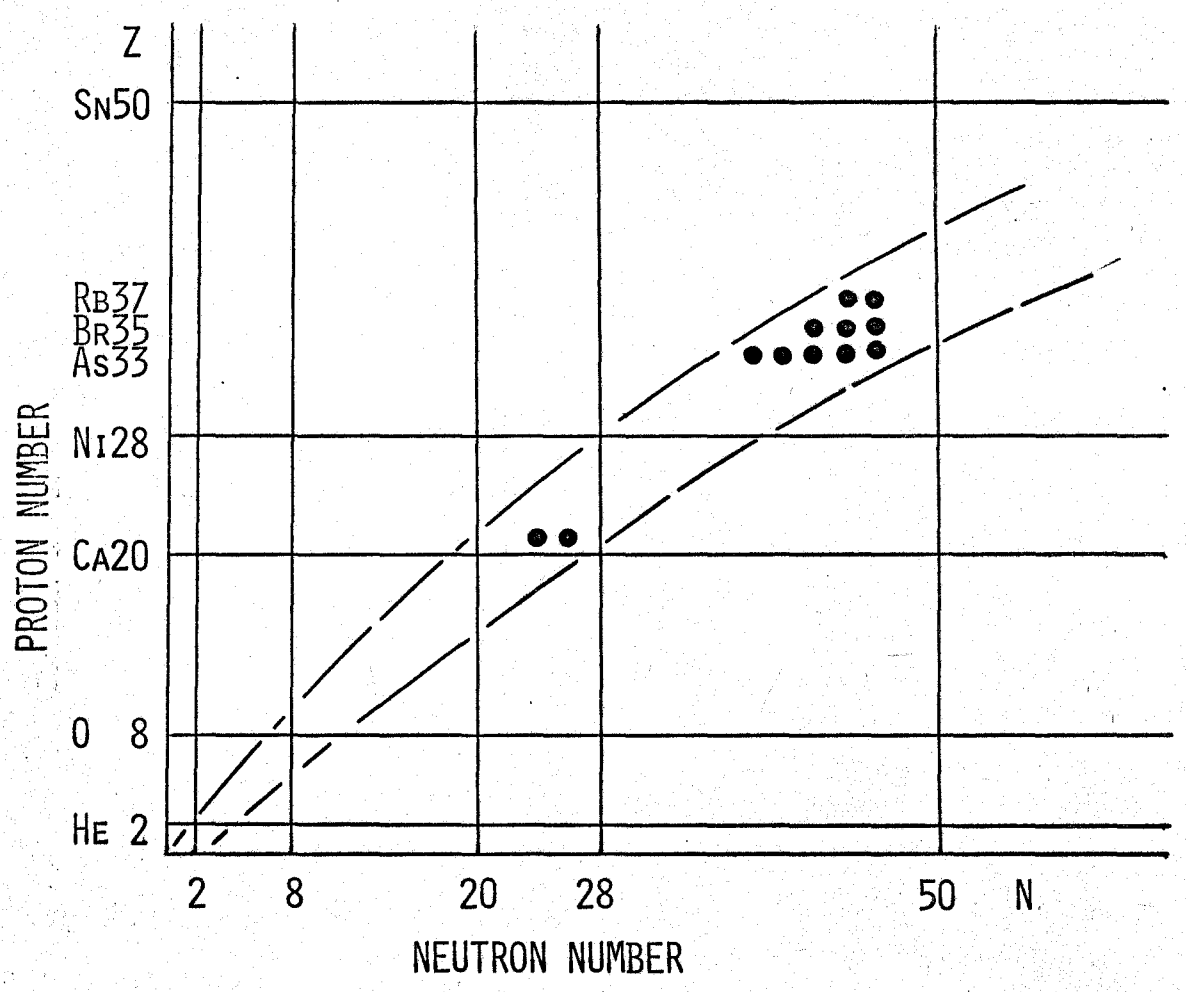

Fig. 1-1. The location of present nuclei.

In Chap. 2, the outline of the present model is proposed. Here, the nucleus is assumed to be axially symmetric and has a reflection symmetry with respect to the symmetry axis. Though the deformation is predominant, the pairing effect still exists. Therefore the zeroth order Hamiltonian for the system is given by a composition of a rotational part and an intrinsic quasiparticle part. In addition to this, a Coriolis force is considered as a perturbation in order to couple an unpaired quasiparticle motion with a rotational motion.

We use Nillson model to represent a single particle motion in a quadrupole field. This model is summarized in the first half of Chap. 3. For odd-mass nuclei with $31 \leq Z \leq 37$ and $21 \leq Z \leq 25$, the unpaired proton or hole is situated mainly in the N=3 shell. Therefore it is necessary to determine accurately the single particle energy and wave function for the N=3 shell. We determined them, referring to the observed single particle energy spectrum of a nucleus which is composed of a doubly magic core plus one nucleon. This procedure is given in the second half of Chap. 3.

In Chap. 4, we describe a method how to obtain values of a gap parameter and a chemical potential as a function of deformation. Many figures are presented.

In Chap. 5, we determine the theoretical level energies and wave functions for ^{71}As, ^{73}As, ^{75}As, ^{77}As, ^{77}Br, ^{79}Br, ^{81}Br, ^{81}Rb and ^{83}Rb. Similar treatments are done for ^{45}Sc

and ^{47}Sc. These theoretical level spectra are first calculated as functions of deformation and rotational constant, and are fitted with the experimental spectra. The fittness and the validity of the obtained rotational constant are also discussed in this chapter. As the deformation parameter is related to the intrinsic quadrupole moment, we calculate it for the ground state and compare it with the measured value in Chap. 6.

We discuss, in Chap. 6, the electric properties of these nuclei. As is well known, the nuclear deformation leads to an enhancement of electric quadrupole transition compared with the rate for the single particle model. Then the comparison of the theoretical electric quadrupole transition probabilities with the experimental data is another test of the present nuclear wave functions. The Coulomb excitation experiment of Sc and As by using 12 MeV nitrogen ions and the extraction of B(E2) values are described. Their quadrupole moments are also discussed.

CHAPTER 2. MODEL

In the long course of the investigation about nuclear structure, considerable attention has been payed to the shapes of nuclei. Many nuclei in the neighbourhood of closed shells are believed to be spherical, and this is characterized by the small intrinsic quadrupole moment and large excitation energies. The success of ordinary shell model spectra also supports the exsistence of spherical nuclei. On the contrary, those nuclei which locate distant from the closed shells are found to be strongly deformed with axially symmetric and prolate shapes. The illustrations are reported about the nuclei in the neighbourhood of $A \sim 24$, and in the regions of $A = 150 - 190$ and $A \gtrsim 220$.

Baranger (Ba60) has tried a Hartree-Fock calculation without residual interaction and found that it gives a deformation for many spherical nuclei. However, there are two important types of residual nuclear interactions, i.e., pairing and field effects. The former tends nuclei to form spherical shapes, while the latter causes deforming effect. The shapes of nuclei are thus determined by the fact that which effect is superior to the other. The stronger pairing is expected to an isotope which lies nearer to a closed shell, whereas the stronger field effect is found in what locates more distant from a closed nucleus.

As is pointed out in the introduction, the recent

experimental facts suggest that the nuclei in the region of the present interest would be considerably deformed, though they do not show as clear rotational spectra as do nuclei in the well established deformed regions. Therefore the investigation of above nuclei from a point of deformation would be quite important.

First, we assume that the nucleus in question is axially symmetric and has a reflection symmetry with respect to the symmetry axis. Though the deformation is introduced, the pairing effect still remains and the nucleons would move in the background of it. Then the excitation energy of a quasiparticle differs from that of a single particle. Especially the low-lying quasiparticle states suffer the pairing effect strongly and locate densely just above the energy gap.

In addition to this, when an unpaired quasiparticle moves arround a doubly-even core, its motion is coupled by the Coriolis force with the rotational motion. This term must be considered and is introduced as the first order perturbation in this report.

The zeroth order Hamiltonian for the system is then described as

$$H_o = \frac{\hbar^2}{2\mathcal{I}} I^2 + E_\nu(\alpha_\nu^+ \alpha_\nu + \beta_\nu^+ \beta_\nu), \qquad (2\text{-}1)$$

and the corresponding low energy wave function is

$$|IMK\nu\rangle = \sqrt{\frac{2I+1}{16\pi^2}}\left[D^I_{MK}|q=1,\nu\rangle + (-1)^{I+K}D^I_{M-K}|q=1,\bar{\nu}\rangle\right]. \tag{2-2}$$

Here I is the total angular momentum, $\mathcal{J}$ the moment of inertia, E_ν the excitation energy associated with quasiparticles α_ν^+ and β_ν^+, respectively. The abbreviation ν means quantum numbers which characterize the intrinsic state. The D^I_{MK} are usual rotational wave functions (Ni55) characterized by I, M and K. The quantum numbers I, M and K are the total angular momentum, its projection on the space fixed axis and its projection on the nuclear symmetry axis, respectively as shown in Fig. 2-1.

The functions $|q=1,\nu\rangle$ and $|q=1,\bar{\nu}\rangle$ which represent the ground and the low-lying intrinsic excited states are described by the equations (Be59)

$$\begin{aligned} |q=1,\nu\rangle &= \alpha_\nu^+|q=0\rangle \\ |q=1,\bar{\nu}\rangle &= \beta_\nu^+|q=0\rangle, \end{aligned} \tag{2-3}$$

where the function $|q=0\rangle$ is the well known BCS wave function (Ba57), and the notation q = 1 and q = 0 are used to clarify the one quasiparticle state and the vacuum with respect to quasiparticles, respectively. The above two functions $|q=1,\nu\rangle$ and $|q=1,\bar{\nu}\rangle$ compose a conjugate pair and are assumed to correspond to the single particle Nilsson states $|\nu\rangle$ and $|\bar{\nu}\rangle$, respectively.

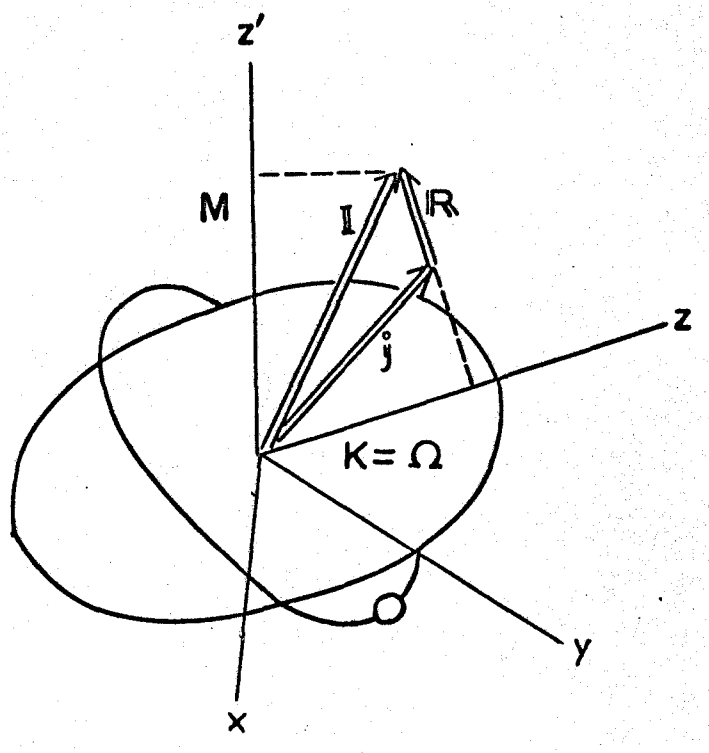

$\mathbb{I}$; the total angular momentum

$\mathbb{R}$; the angular momentum of the roter

j ; the angular momentum of the un-paired particle

M ; the component of the total angular momentum on the space fixed axis z

K ; the component of the total angular momentum on the body fixed axis z'

Fig. 2-1. Angular momentum diagram.

Without Coriolis couplig, Ω the component of the angular momentum j of an unpaired quasiparticle on the nuclear symmetry axis is a good quantum number. Therefore we denote explicitly the intrinsic Nilsson states $|\nu\rangle$ and $|\bar{\nu}\rangle$ as

$$|\nu\rangle \equiv |\Omega\xi\rangle \qquad |\bar{\nu}\rangle \equiv |-\Omega\xi\rangle \tag{2-4}$$

and represent the corresponding quasiparticle states as

$$|q = 1,\nu\rangle \equiv |q = 1,\Omega\xi\rangle$$

$$|q = 1,\bar{\nu}\rangle \equiv |q = 1,-\Omega\xi\rangle .$$

Here the extra index ξ is introduced to distinguish the different intrinsic Nilsson states with same Ω. Considering $\Omega = K$, we also rewrite the wave function in Eq. (2-2) as

$$|IMK\nu\rangle \equiv |IMK\Omega\xi\rangle \equiv |IMK\xi\rangle .$$

The quasiparticle excitation energy E_ν in Eq. (2-1) is connected with the single particle Nilsson energy ε_ν as (Be59)

$$E_\nu = [(\varepsilon_\nu - \lambda)^2 + \Delta^2]^{1/2}. \tag{2-6}$$

Two parameters λ and Δ are well known chemical potential and gap parameter, respectively, and they must be obtained by solving the following equations:

$$\Delta = G\sum_{\nu} U_\nu V_\nu \tag{2-7}$$

$$n = 2\sum_{\nu} V_\nu^2. \tag{2-8}$$

Here G is the strength parameter for the pairing force and n is the true particle number in the system. The meaning of V_ν and U_ν is well known as follows: V_ν^2 is the probability of $(\nu,\bar{\nu})$ pair being found in the ground state, while U_ν^2 the probability of non-occupancy. Explicitly, U_ν^2 and V_ν^2 are given as

$$\begin{aligned} U_\nu^2 &= \frac{1}{2}\left(1 + \frac{\varepsilon_\nu - \lambda}{E_\nu}\right) \\ V_\nu^2 &= \frac{1}{2}\left(1 - \frac{\varepsilon_\nu - \lambda}{E_\nu}\right). \end{aligned} \tag{2-9}$$

They are shown schematically in Fig. 2-2.

One must consider a blocking effect on these parameters. Due to this effect, the λ and Δ values for the excited states differ somewhat from those for the ground state, and consequently U_ν and V_ν are necessary to be adjusted (Ni64). In the present work, however, we calculate the values λ and Δ only for the ground state and use these values for all the excited states considered, because in the present region, the correction arising from blocking is generally small and affects only slightly on the final energy spectra.

In addition to H_o, we now consider a Coriolis interaction of the form

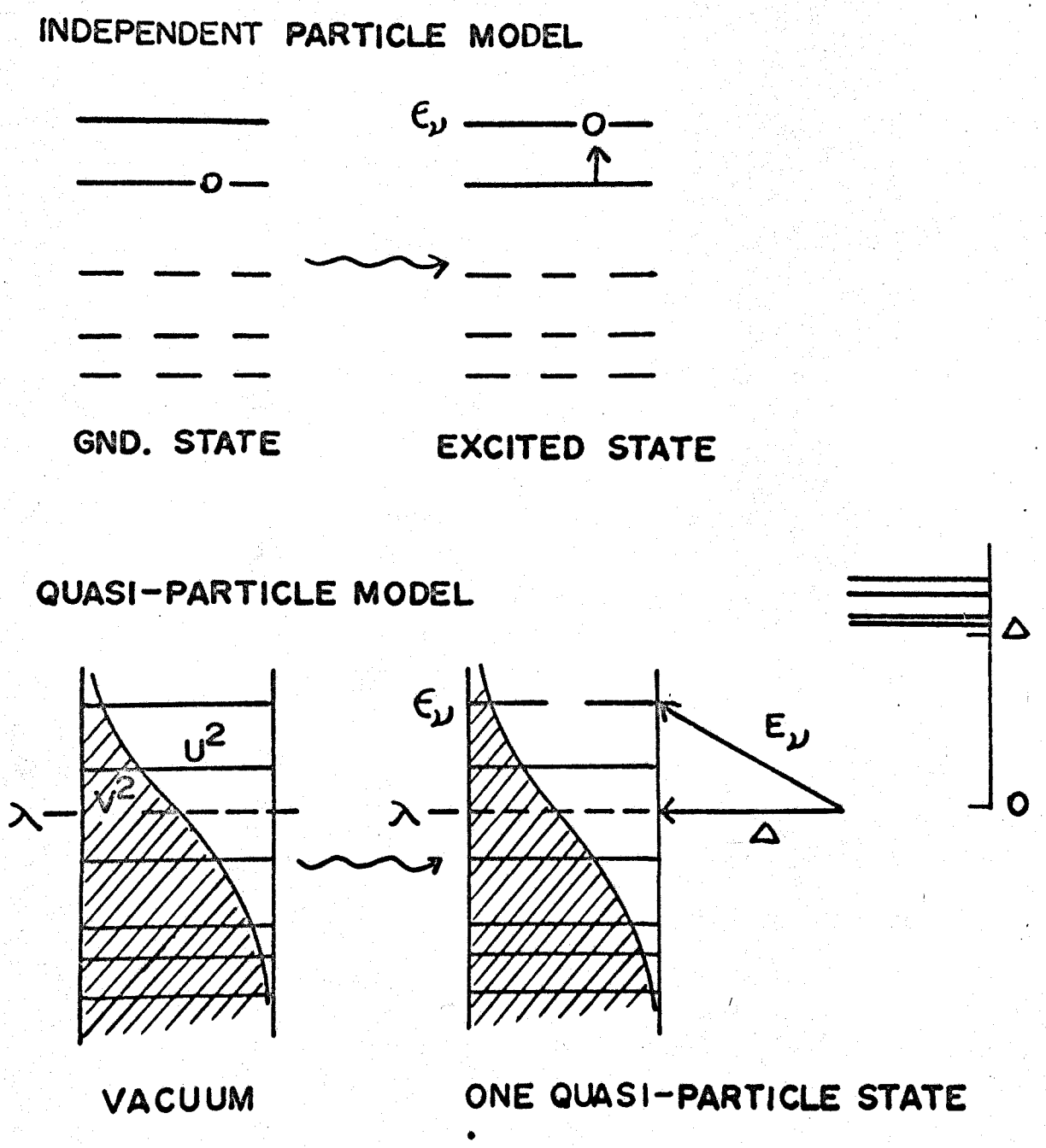

Fig. 2-2. Connection between the quasiparticle excitation energy and the single particle Nilsson energy.

$$H' = -\frac{\hbar^2}{\mathcal{J}}\mathbb{I}\cdot j. \qquad (2\text{-}10)$$

This Coriolis term connects the rotational bands of $|\Delta K| = 1$ with each other, and this effect would be of major importance for the present cases because the levels belonging to different quasiparticle states become very close to one another, as shown in Fig. 2-3.

The Hamiltonian for the system is then

$$\begin{aligned} H &= H_o + H' \\ &= \frac{\hbar^2}{2\mathcal{J}}I(I+1) + \sum_\nu \Big\{E_\nu(\alpha_\nu^+\alpha_\nu + \beta_\nu^+\beta_\nu) \\ &\quad - \frac{\hbar^2}{\mathcal{J}}K^2(\alpha_\nu^+\alpha_\nu - \beta_\nu^+\beta_\nu)\Big\} + \sum_{\nu\nu'} H_{coup}, \end{aligned} \qquad (2\text{-}11)$$

where H_{coup} is represented as

$$H_{coup} = -\frac{\hbar^2}{2\mathcal{J}}\langle I_+ j_- + I_- j_+\rangle (U_\nu U_{\nu'} + V_\nu V_{\nu'})(\alpha_\nu^+\alpha_{\nu'} - \beta_{\nu'}^+\beta_\nu). \qquad (2\text{-}12)$$

For the state with $K = 1/2$, the diagonal element of H_{coup} is

$$\langle IM\tfrac{1}{2}\xi | H_{coup} | IM\tfrac{1}{2}\xi\rangle = \frac{\hbar^2}{2\mathcal{J}}a(-1)^{I+\frac{1}{2}}(I+\tfrac{1}{2}) \qquad (2\text{-}13)$$

where a is the decoupling parameter and is given by

$$a = -\sum_j (-1)^{j+\frac{1}{2}}(j+\tfrac{1}{2})|c_{j1/2}|^2 \qquad (2\text{-}14)$$

in the $j\Omega$ representation of Nilsson wave function.

The diagonal element of the Hamiltonian (2-11) is expressed as

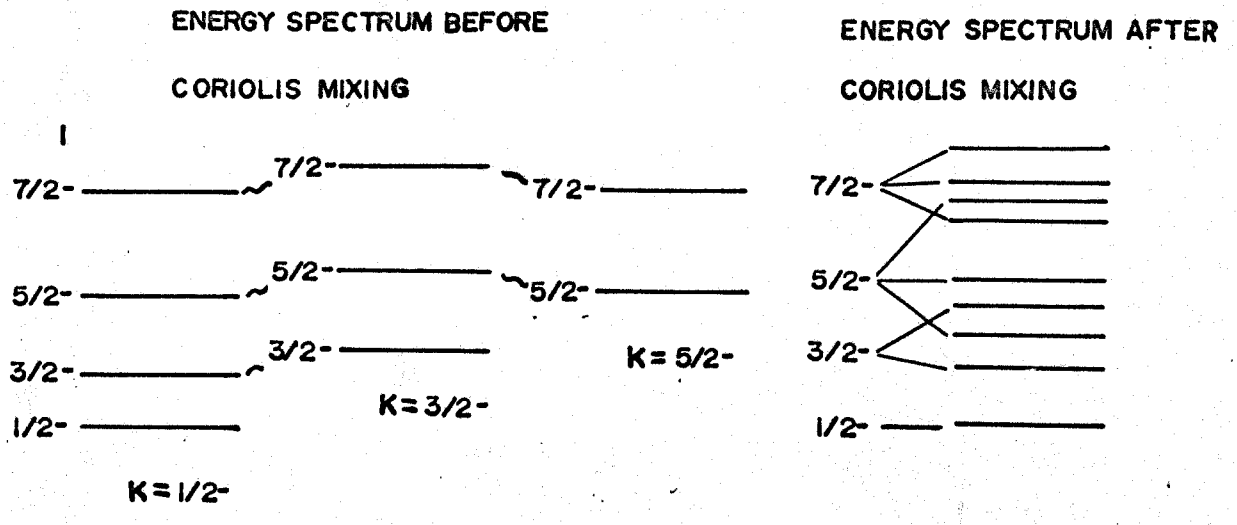

Fig. 2-3. Coriolis effect.

$$\langle H\rangle_{dia} = E_\nu + \left(\frac{\hbar^2}{2\mathcal{J}}\right)[I(I+1) - 2K^2 + \delta_{K1/2}a(-1)^{I+\frac{1}{2}}(I+\tfrac{1}{2})]. \tag{2-15}$$

The off-diagonal element of H_{coup} between the states of different rotational bands with $|\Delta K| = 1$ does not vanish and

$$\begin{aligned}\langle IMK \pm 1\xi'|H_{coup}|IMK\xi\rangle &= \langle IMK\xi|H_{coup}|IMK \pm 1\xi'\rangle \\ &= -\frac{\hbar^2}{2\mathcal{J}}(U_{K\pm1\xi'}U_{K\xi} + V_{K\pm1\xi'}V_{k\xi})\langle\Omega \pm 1\xi'|j_\pm|\Omega\xi\rangle \\ &\quad\cdot[(I \pm K + 1)(I \mp K)]^{1/2},\end{aligned} \tag{2-16}$$

where the matrix element for the particle state is evaluated as follows:

$$\langle\Omega \pm 1\xi'|j_\pm|\Omega\xi\rangle = \sum c_{j\Omega\pm1}c_{j\Omega}(-1)^{I-\frac{1}{2}}[(j \mp \Omega)(j \pm \Omega + 1)]^{1/2}. \tag{2-17}$$

Therefore, the quasiparticle formalism leads to a reduction of the off-diagonal elements of H_{coup}. A compression of the low-energy spectrum would be also expected, when compared with the independent particle picture.

When the Coriolis interaction in the Hamiltonian (2-11) is treated as a perturbation, we can expand the total wave function as

$$|IM\rangle = \sqrt{\frac{2I+1}{16\pi^2}}\sum_{K=\Omega\xi}\sum C^I_{K\xi}[D^I_{MK}|q = 1,\Omega\xi\rangle + (-1)^{I+K}D^I_{M-K}|q = 1,-\Omega\xi\rangle] \tag{2-18}$$

where the mixing amplitudes $C^{I}_{K\xi}$ are determined by the Jacobi diagonalization procedure.

Finally, we carry out a least-squares fitting to the experimental energy spectrum by selecting the adequate and reasonable parameters, and obtain the total wave functions as well as the theoretical energy spectrum.

CHAPTER 3. MODIFICATION OF NILSSON LEVEL ENERGY AND WAVE FUNCTION

3-1. General

In the preceding chapter, we proposed the outline of the present model, but in practice; more precise treatments are necessary. In this chapter, some modifications of Nilsson level energy and wave function are presented.

As previously mentioned, the pairing and field effects play important role on nuclear shapes. The deformed nuclei are seen in far- and off-magic regions, where the field effect overcomes the pairing one. Practically, it has turned out that the most predominant shape of deformed nuclei is a quadrupole one. This is supported by the level spectra of the nuclei with $150 < A < 190$ (Mo59).

Nilsson (Ni55) has treated a motion of single particle in this quadrupole field. He assumes a single particle Hamiltonian H_n of the form

$$H_n = \overset{o}{H}_o + \kappa\hbar\,\overset{o}{\omega}_o R. \qquad (3\text{-}1)$$

Here $\overset{o}{H}_o$ represents a spherically symmetric part and

$$\overset{o}{H}_o = \hbar\omega_o(\delta)\tfrac{1}{2}[-\Delta^2 + r^2] \qquad (3\text{-}2)$$

where r is a radial distance of the single particle in polar coordinates and δ is a shape parameter.

For the sake of simplisity we first adopt this spherical

Hamiltonian oscillator potential. The second term in Eq. (3-1) is a kind of deformation coupling and

$$R = \eta(-\frac{4}{3}\sqrt{\frac{\pi}{5}}\, r^2 Y_{20}) - 2\bar{l}\bar{s} - \mu\bar{l}^2 \qquad (3\text{-}3)$$

Here η represents the deformation of the potential well. The $l*s$ term is a spin-orbit coupling and is introduced to account for the magic numbers. The l^2 term serves to depressthe high angular momentum states. These terms are reasonable and are necessary to reproduce the observed level spacing.

The parameters in Eqs. (3-1), (3-2) and (3-3) are related to the parameters as follows:

$$\omega_o(\delta) = \overset{o}{\omega}_o(1 - \frac{4}{3}\delta^2 - \frac{16}{27}\delta^3)^{-1/6}$$

$$\kappa = -0.5C/h\overset{o}{\omega}_o$$

$$\mu = 2D/C$$

$$\eta = \frac{\delta}{\kappa}\frac{\omega_o(\delta)}{\overset{o}{\omega}_o} \qquad (3\text{-}4)$$

where C and D are the strength of spin-orbit interaction and the well flattening parameter, respectively. These are referred to Ref. (Ni55).

In order to obtain Eqs. (3-1), (3-2), (3-3) and (3-4), it is assumed that the nuclear volume remains constant during the deformation and the $l*s$ and l^2 terms are

independent of the volume condition. When the axially symmetric oscillator potential V(x,y,z) can be written in Cartesian coordinates,

$$V(x,y,z) = \frac{1}{2} M[\omega_\perp^2(x^2 + y^2) + \omega_z^2 z^2] \qquad (3\text{-}5)$$

where

$$\omega_z^2 = \omega_o^2(1 - \tfrac{4}{3}\delta)$$
$$\omega_\perp^2 = \omega_o^2(1 + \tfrac{2}{3}\delta),$$

and the volume condition lead to

$$\omega_\perp^2\omega_z = \omega_o^3(1 - \tfrac{4}{3}\delta)^{\frac{1}{2}}(1 + \tfrac{2}{3}\delta) = \overset{o}{\omega}_o^3 = \text{const.} \qquad (3\text{-}6)$$

The energy eigenvalues ε_ν of the total Hamiltonian H are then given by

$$\varepsilon_\nu = (N + \tfrac{3}{2})\hbar\omega_o(\delta) + \kappa\hbar\overset{o}{\omega}_o r_\nu^{N\Omega} \qquad (3\text{-}7)$$

where $r_\nu^{N\Omega}$ are eigenvalues of an operator R and N is the number of harmonic oscillator quantum. Since the potential is axially symmetric, the states can be labelled by Ω, that is, the projection of the angular momentum along the symmetry axis (j_3). As the states $j_3 = \pm\Omega$ degenerate, two like particles can occupy the states of equal energy.

The normalized intrinsic wave functions $|\nu\rangle$ are expanded in terms of the spherical harmonic oscillator eigenfunctions specified by N, l, $l_z = \Lambda$ and $s_z = \Sigma$, as in the form

$$|\nu\rangle = \sum_{l\Lambda\Sigma} a_{l\Lambda}|Nl\Lambda\Sigma\rangle \qquad (l - \Lambda \text{ representation}). \qquad (3\text{-}8)$$

All operators of l^2, l_z and s_z commute with $\overset{o}{H}_o$ and corresponding quantum numbers are denoted as l, Λ and Σ.

It is impossible to solve Eq. (3-1) exactly, but the good approximate solutions can be obtained by diagonalizing the finite matrices composed of above basic vectors. In the neighbourhood of spherical shape, the state can be labelled by the l and j quantum numbers. Using eigenfunctions specified by these quantum numbers, the intrinsic wave function $|\nu\rangle$ can be also expanded as follows:

$$|\nu\rangle = \sum_j c_j |Nlj\Omega\rangle \qquad (j - \Omega \text{ representation}). \qquad (3\text{-}9)$$

The coefficients c_j are simply connected with the coefficients $a_{l\Lambda}$ by the angular momentum additional relations and are given by

$$c_j = \sum_{l\Lambda} (l\Lambda \tfrac{1}{2}\Sigma | j\Omega) a_{l\Lambda}. \qquad (3\text{-}10)$$

The illustrative correspondence of the basic vectors in two representations is shown in Table 3-1.

Table 3-1. $l\Lambda - j\Omega$ representation of basic vectors

N		l	j
3	1/2	|330 1/2 +> |310 1/2 +> |331 1/2 -> |311 1/2 ->	|33 7/2 1/2> |31 3/2 1/2> |33 5/2 1/2> |31 1/2 1/2>
3	3/2	|331 1/2 +> |311 1/2 +> |332 1/2 ->	|33 7/2 3/2> |31 3/2 3/2> |33 5/2 3/2>
3	5/2	|332 1/2 +> |333 1/2 ->	|33 7/2 5/2> |31 5/2 5/2>
3	7/2	|333 1/2 +>	|33 7/2 7/2>

3-2. Determination of Parameters

As has been mentioned in the preceding section, Nilsson Hamiltonian has four parameters $\mathring{\omega}_0$, κ, μ and η. The $\mathring{\omega}_0$ is closely connected with the standard nuclear radius. The parameters κ and μ are related to the spin-orbit strength and the flattness of potential well, while η is well known as a deformation parameter. The determination of these parameters is the most important procedure in the present model.

i) $\mathring{\omega}_0$

A reasonable value for $\mathring{\omega}_0$ has been proposed by Nilsson (Ni55), by taking the root mean square radius for each nucleus to be equal to $\frac{3}{5}\cdot 1.2\cdot A^{1/3}$ fm, which gives $\hbar\mathring{\omega}_0 = 41\cdot A^{-1/3}$ MeV for all nuclei. This value is reasonable and is adopted in this report.

ii) κ and μ

These two parameters have been reasonably fixed for the $N > 3$. However, in the case of $N = 3$, there remains arbitrariness in a choice of them. For odd-mass nuclei with $31 < Z < 37$ and $21 < Z < 25$, the unpaired proton or hole is situated mainly in the No. 10, 12, 13, 14, 15, 16, 17, 19, 20 or 26 Nilsson orbital, which all belong to $N = 3$ shell. Therefore in order to investigate the nuclei of the above Z

regions, it is necessary to predetermine accurately the level energies and the wave functions for the N = 3 shell.

First, we determine κ and μ by referring to the observed single particle level spectrum of the nucleus which is composed of a doubly magic core plus one nucleon. As pointed out previously, a nucleus of closed or nearly closed shell would have a spherical shape, the shape parameter δ being equal to zero. In addition to this, the energy gap Δ would disappear at a closed shell. If a single particle (or hole) outside (or inside) closed shell moves in the non-deformed well, the energy spectrum attributed to the single particle (or hole) would be found. Such spectra would be expected in ^{69}Cu and ^{57}Ni nuclei, and are represented by $1f_{7/2}$, $2p_{3/2}$, $1f_{5/2}$ and $2p_{1/2}$ states. The nucleus ^{69}Cu is composed of a doubly magic core (Z = 28, N = 40) plus one proton and is quite close to the present A region of 70 $\sim$ 90. Unfortunately, since the level spectrum of this nucleus has not been reported at all, and we can not obtain any significant information about κ and μ.

The nucleus ^{57}Ni is also composed of a doubly magic core (Z = 28, N = 28) plus one neutron, and the level energy spectrum has been well investigated. Fig. 3-1 summarizes the ^{57}Ni excitation energies determined by the ^{56}Ni(p,d) and ^{58}Ni(p,t) reaction experiments (Co67). The neutron pick up transitions with the angular momentum transfer Δl = 1 have been assigned for the ground and 1.08

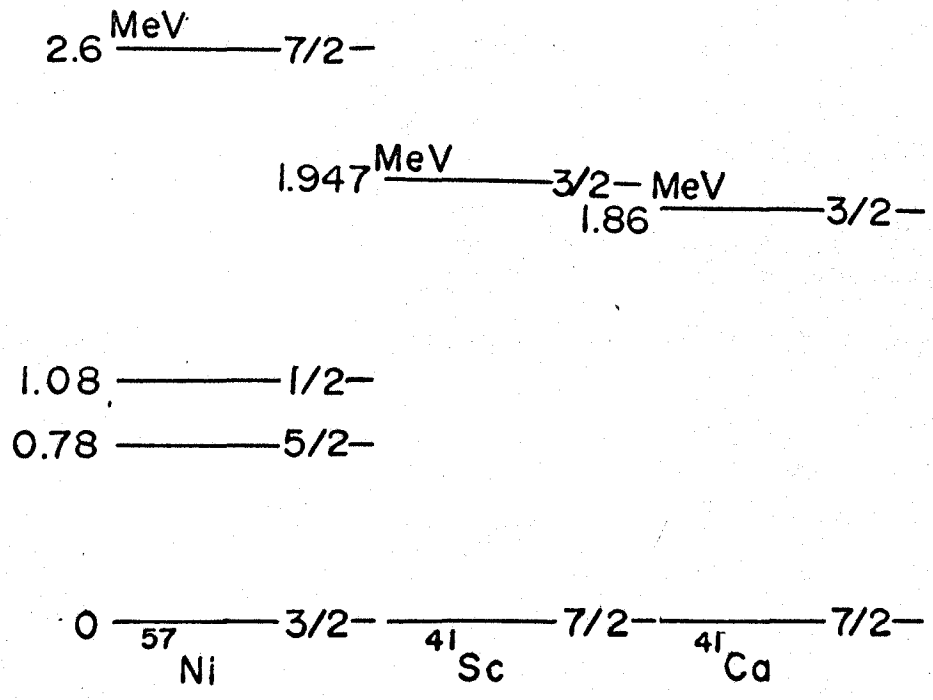

Fig. 3-1. Observed low-lying states in ^{57}Ni, ^{41}Sc and ^{41}Ca.

MeV excited states, while $\Delta l = 3$ transitions have been reported for the 0.78 and 2.6 MeV states. No other level has been found up to 3 MeV excitation energy. From these facts, S.Cohen et al. (Co67) have interpreted the ground, 0.78 and 1.08 MeV states of ^{57}Ni as $2p_{3/2}$, $1f_{5/2}$ and $2p_{1/2}$ single particle states, respectively, and the 2.6 MeV level as a $1f_{7/2}$ single hole state. These typical level energies are quite important and we decide κ and μ values by the following procedure:

When a nucleus is spherical or nearly spherical, $\delta \simeq 0$ and the first term in Eq. (3-1) vanishes. Then we obtain

$$R = -2\bar{l}\bar{s} - \mu\bar{l}^2. \qquad (3\text{-}11)$$

Since the states with same l and j but with different Ω degenerate, we can determine κ and μ by solving the eigenvalue equation only for $N = 3$ and $\Omega = 1/2$ in $|Nl\Lambda\Sigma\rangle$ representation. Using these eigenvectors, we obtain the following equation:

$$\begin{vmatrix} -12\mu - r & 0 & -\sqrt{3} & 0 \\ 0 & -2\mu - r & 0 & -\sqrt{2} \\ -2\sqrt{3} & 0 & -12\mu + 1 - r & 0 \\ 0 & -\sqrt{2} & 0 & -2\mu + 1 - r \end{vmatrix} = 0 \qquad (3\text{-}12)$$

which leads to the equations of

$$r_{f_{7/2}} = -3 - 12\mu$$
$$r_{f_{5/2}} = 4 - 12\mu$$

$$r_{p_{3/2}} = -1 - 2\mu$$

$$r_{p_{1/2}} = 2 - 2\mu. \qquad (3\text{-}13)$$

By combining Eqs. (3-7) and (3-13) with the experimental level spacing of ^{57}Ni, we find

$$\begin{aligned} \varepsilon_{p_{3/2}} - \varepsilon_{p_{1/2}} &= 1.08 \text{ MeV (exp.)} \\ &= 3 \times 41 \cdot (57)^{-1/3} \kappa \text{ (theory)} \\ \varepsilon_{f_{5/2}} - \varepsilon_{p_{3/2}} &= 0.78 \text{ MeV (exp.)} \\ &= 5(1 - 2\mu) \cdot \kappa \cdot 41 \cdot (57)^{-1/3} \text{ (theory)}. \end{aligned} \qquad (3\text{-}14)$$

Thus finally from the above two equations, we obtain

$$\kappa = 0.034, \qquad \mu = 0.284,$$

and the corresponding values of the parameters C and D are

$$C = -0.068\hbar\omega_o^o, \qquad D = 0.0096\hbar\omega_o^o.$$

It is quite interesting that these values also account well for the observed $2p_{3/2} - 1f_{7/2}$ level spacing in ^{41}Ca and ^{41}Sc, whose energy spectra are shown in Fig. 3-1. Though Ni, Ca and Sc nuclei locate in the A = 40 $\sim$ 60 region, the above κ and μ values would be well applicable to the present A = 70 $\sim$ 90 region, because any significant change of these parameters cannot be expected in the same N region.

Under the present choice of κ and μ, we try to obtain the eigenvalues and eigenfunctions for the Hamiltonian (3-1).

In this calculation, we have coded a program named NILSR in the language of FORTRAN IV, the program being shown in Appendix. We first calculate the matrix elements of the operator R in the $l\Lambda$ representation, and we diagonalize the matrix by the Jacobi diagonalization procedure, and we finally obtain the eigenvalues $r_\nu^{N\Omega}$ and $a_{l\Lambda}$ (and $c_{j\Omega}$) presented in Table 3-2 for different deformation parameter η. The Nilsson diagram for N = 3 shell is also shown in Fig. 3-2 as a function of η.

iii) η

The independent determination of this parameter is quite difficult, since there remains other important parameters of Δ and λ, the gap parameter and chemical potential respectively, both being functions of η. Therefore it is reasonable for us to remain η as a final parameter. The determination of η will be discussed in Chap. 5.

Table 3-2. Eigenvalues and eigenfunctions for Nilsson deformed field.
(In 1Λ representation)

Deformation	1	2	3	4	5	6	7	8	
N = 3, Ω = 1/2									
$r_\nu^{N\Omega}$	-7.2886	-8.4685	-9.8822	-11.4639	-13.1616	-14.9383	-16.7691	-18.6380	No.14
|330+⟩	0.7567	0.7477	0.7360	0.7246	0.7144	0.7057	0.6982	0.6920	
|310+⟩	0.1566	0.3007	0.4157	0.5006	0.5614	0.6047	0.6360	0.6590	
|331-⟩	0.6287	0.5768	0.5128	0.4493	0.3927	0.3449	0.3052	0.2725	
|311-⟩	0.0871	0.1335	0.1501	0.1501	0.1425	0.1323	0.1219	0.1121	
$r_\nu^{N\Omega}$	-0.3542	-1.060	-1.4506	-1.6735	-1.8123	-1.9050	-1.9703	-2.0182	No.20
|330+⟩	-0.6127	-0.6238	-0.6423	-0.6607	-0.6768	-0.6900	-0.7007	-0.7093	
|310+⟩	0.0169	0.2875	0.4613	0.5476	0.5913	0.6153	0.6290	0.6372	
|331-⟩	0.6768	0.5484	0.4165	0.3215	0.2567	0.2113	0.1782	0.1533	
|311-⟩	0.4078	0.4769	0.4486	0.4003	0.3553	0.3174	0.2859	0.2596	
$r_\nu^{N\Omega}$	-2.2581	-3.1650	-4.2237	-5.3197	-6.4073	-7.4779	-8.5331	-9.5761	No.17
|330+⟩	0.0237	-0.0238	-0.0531	-0.0576	-0.0524	-0.0450	-0.0379	-0.0319	
|310+⟩	-0.9108	-0.8613	-0.7468	-0.6395	-0.5519	-0.4818	-0.4254	-0.3797	
|331-⟩	0.2443	0.5001	0.6580	0.7449	0.7956	0.8271	0.8476	0.8613	
|311-⟩	-0.3320	-0.0870	0.0810	0.1815	0.2441	0.2857	0.3148	0.3360	
$r_\nu^{N\Omega}$	1.9489	2.7412	3.6045	4.5051	5.4292	6.3692	7.3205	8.2803	No.26
|330+⟩	0.2267	0.2263	0.2074	0.1876	0.1700	0.1568	0.1418	0.1306	
|310+⟩	-0.3817	-0.2918	-0.2380	-0.2013	-0.1744	-0.1538	-0.1376	-0.1243	
|331-⟩	0.2950	-0.3413	-0.3614	-0.3741	-0.3832	-0.3902	-0.3958	-0.4004	
|311-⟩	0.8461	0.8644	0.8773	0.8856	0.8910	0.8945	0.8968	0.8984	

(continued)

Deformation	1	2	3	4	5	6	7	8	
N = 3, Ω = 3/2									
$r_\nu^{N\Omega}$	-6.9272	-7.5824	-8.3264	-9.1307	-9.9773	-10.8545	-11.7544	-12.6714	No.13
|331+⟩	0.8618	0.8732	0.8813	0.8871	0.8912	0.8941	0.8962	0.8977	
|311+⟩	0.1157	0.1937	0.2471	0.2849	0.3124	0.3331	0.3489	0.3613	
|332-⟩	0.4938	0.4472	0.4028	0.3632	0.3289	0.2993	0.2739	0.2520	
$r_\nu^{N\Omega}$	0.5425	0.8656	1.5487	2.3913	3.2969	4.2329	5.1862	6.1503	No.19
|331+⟩	-0.5058	-0.4654	-0.4277	-0.4115	-0.4065	-0.4059	-0.4070	-0.4088	
|311+⟩	0.2679	0.6036	0.7796	0.8446	0.8719	0.8852	0.8923	0.8964	
|332-⟩	0.8200	0.6473	0.4575	0.3425	0.2732	0.2275	0.1952	0.1711	
$r_\nu^{N\Omega}$	-0.9993	-0.6672	-0.6063	-0.6446	-0.7036	-0.7624	-0.8159	-0.8630	No.16
|331+⟩	0.0374	0.1446	0.2010	0.2092	0.2014	0.1892	0.1763	0.1641	
|311+⟩	0.9565	0.7734	0.5754	0.4533	0.3772	0.3249	0.2864	0.2567	
|332-⟩	-0.2894	-0.6172	-0.7928	-0.8664	-0.9040	-0.9266	-0.9417	-0.9525	
N = 3, Ω = 5/2									
$r_\nu^{N\Omega}$	-6.2810	-6.1800	-6.0984	-6.0315	-5.9758	-5.9288	-5.8887	-5.8542	No.12
|332+⟩	0.9420	0.9538	0.9625	0.9691	0.9742	0.9781	0.9813	0.9838	
|333-⟩	0.3357	0.3006	0.2713	0.2467	0.2258	0.2080	0.1926	0.1792	
$r_\nu^{N\Omega}$	1.4650	2.3640	3.2824	4.2155	5.1598	6.1128	7.0727	8.0382	No.15
|332+⟩	-0.3357	-0.3006	-0.2713	-0.2467	-0.2258	-0.2080	-0.1926	-0.1792	
|333-⟩	0.9420	0.9538	0.9625	0.9691	0.9742	0.9781	0.9813	0.9838	
N = 3, Ω = 7/2									
$r_\nu^{N\Omega}$	-5.4080	-4.4080	-3.4080	-2.4080	-1.4080	-0.4080	0.5920	1.5920	No.10
|333+⟩	1.0000	1.0000	1.0000	1.0000	1.0000	1.0000	1.0000	1.0000	

(continued)
(In jΩ representation)

Deformation	1	2	3	4	5	6	7	8	
N = 3, Ω = 1/2									
$r_\nu^{N\Omega}$	-7.2886	-8.4685	-9.8822	-11.4639	-13.1616	-14.9383	-16.7691	-18.6380	No.14
$\|3,7/2,1/2\rangle$	0.9836	0.9428	0.8921	0.8418	0.7971	0.7592	0.7276	0.7015	
$\|3,5/2,1/2\rangle$	-0.0202	-0.0535	-0.0942	-0.1347	-0.1708	-0.2013	-.02264	-0.2470	
$\|3,3/2,1/2\rangle$	0.1781	0.3226	0.4261	0.4954	0.5406	0.5701	0.5896	0.6028	
$\|3,1/2,1/2\rangle$	-0.0193	-0.0646	-0.1174	-0.1665	-0.2077	-0.2410	-0.2677	-0.2890	
$r_\nu^{N\Omega}$	-0.3542	-1.060	-1.4506	-1.6735	-1.8123	-1.9050	-1.9703	-2.0182	No.20
$\|3,7/2,1/2\rangle$	-0.0201	-0.1126	-0.2129	-0.2889	-0.3435	-0.3833	-0.4130	-0.4358	
$\|3,5/2,1/2\rangle$	0.9127	0.8230	0.7353	0.6756	0.6371	0.6114	0.5934	0.5802	
$\|3,3/2,1/2\rangle$	0.2493	0.5101	0.6356	0.6782	0.6881	0.6856	0.6786	0.6702	
$\|3,1/2,1/2\rangle$	0.3232	0.2234	0.0999	0.0106	-0.0514	-0.0961	-0.1297	-0.1559	
$r_\nu^{N\Omega}$	-2.2581	-3.1650	-4.2237	-5.3197	-6.4073	-7.4779	-8.5331	-9.5761	No.17
$\|3,7/2,1/2\rangle$	-0.1779	-0.3094	-0.3906	-0.4441	-0.4813	-0.5075	-0.5262	-0.5397	
$\|3,5/2,1/2\rangle$	-0.1692	-0.3936	-0.5322	-0.6008	-0.6357	-0.6547	-0.6656	-0.6720	
$\|3,3/2,1/2\rangle$	0.9353	0.7535	0.5630	0.4173	0.3097	0.2284	0.1656	0.1160	
$\|3,1/2,1/2\rangle$	-0.2547	-0.4262	-0.4973	-0.5174	-0.5180	-0.5115	-0.5027	-0.4936	
$r_\nu^{N\Omega}$	1.9489	2.7412	3.6045	4.5051	5.4292	6.3692	7.3205	8.2803	No.26
$\|3,7/2,1/2\rangle$	-0.0217	-0.0523	-0.0799	-0.1031	-0.1224	-0.1385	-0.1520	-0.1634	
$\|3,5/2,1/2\rangle$	-0.3714	-0.4061	-0.4090	-0.4056	-0.4009	-0.3963	-0.3920	-0.3882	
$\|3,3/2,1/2\rangle$	0.1768	0.2608	0.3122	0.3469	0.3720	0.3908	0.4055	0.4172	
$\|3,1/2,1/2\rangle$	0.9112	0.8742	0.8538	0.8393	0.8282	0.8192	0.8117	0.8053	

(continued)

Deformation	1	2	3	4	5	6	7	8	
N = 3, Ω = 3/2									
$r_\nu^{N\Omega}$	-6.9272	-7.5824	-8.3264	-9.1307	-9.9773	-1o.8545	-11.7544	-12.6714	No.13
|33,7/2,3/2⟩	0.9923	0.9770	0.9601	0.9439	0.9290	0.9157	0.9039	0.8935	
|33,5/2,3/2⟩	-0.0433	-0.0888	-0.1306	-0.1672	-0.1984	-0.2250	-0.2475	-0.2668	
|33,3/2,3/2⟩	0.1157	0.1937	0.2471	0.2849	0.3124	0.3331	0.3489	0.3613	
$r_\nu^{N\Omega}$	0.5425	0.8656	1.5487	2.3913	3.2969	4.2329	5.1862	6.1503	No.19
|33,7/2,3/2⟩	0.0108	-0.0473	-0.1170	-0.1647	-0.1975	-0.2214	-0.2397	-0.2540	
|33,5/2,3/2⟩	0.9634	0.7958	0.6152	0.5095	0.4482	0.4092	0.3825	0.3632	
|33,3/2,3/2⟩	0.2679	0.6036	0.7796	0.8446	0.8719	0.8852	0.8923	0.8964	
$r_\nu^{N\Omega}$	-0.9993	-0.6672	-0.6063	-0.6446	-0.7036	-0.7624	-0.8159	-0.8630	No.16
|33,7/2,3/2⟩	-0.1231	-0.2077	-0.2539	-0.2863	-0.3130	-0.3354	-0.3543	-0.3704	
|33,5/2,3/2⟩	-0.2646	-0.5989	-0.7774	-0.8441	-0.8716	-0.8843	-0.8902	-0.8923	
|33,3/2,3/2⟩	0.9565	0.7734	0.5754	0.4533	0.3772	0.3249	0.2864	0.2567	
N = 3, Ω = 5/2									
$r_\nu^{N\Omega}$	-6.2810	-6.1800	-6.0984	-6.0315	-5.9758	-5.9288	-5.8887	-5.8542	No.12
|33,7/2,5/2⟩	0.9990	0.9966	0.9936	0.9904	0.9873	0.9842	0.9813	0.9786	
|33,5/2,5/2⟩	-0.0452	-0.0822	-0.1126	-0.1379	-0.1592	-0.1772	-0.1926	-0.2059	
$r_\nu^{N\Omega}$	1.4650	2.3640	3.2824	4.2155	5.1598	6.1128	7.0727	8.0382	No.15
|33,7/2,5/2⟩	0.0452	0.0822	0.1126	0.1379	0.1592	0.1772	0.1926	0.2059	
|33,5/2,5/2⟩	0.9990	0.9966	0.9936	0.9904	0.9873	0.9842	0.9813	0.9786	
N = 3, Ω = 7/2									
$r_\nu^{N\Omega}$	-5.4080	-4.4080	-3.4080	-2.4080	-1.4080	-0.4080	0.5920	1.5920	No.10
|33,7/2,7/2⟩	1.0000	1.0000	1.0000	1.0000	1.0000	1.0000	1.0000	1.0000	

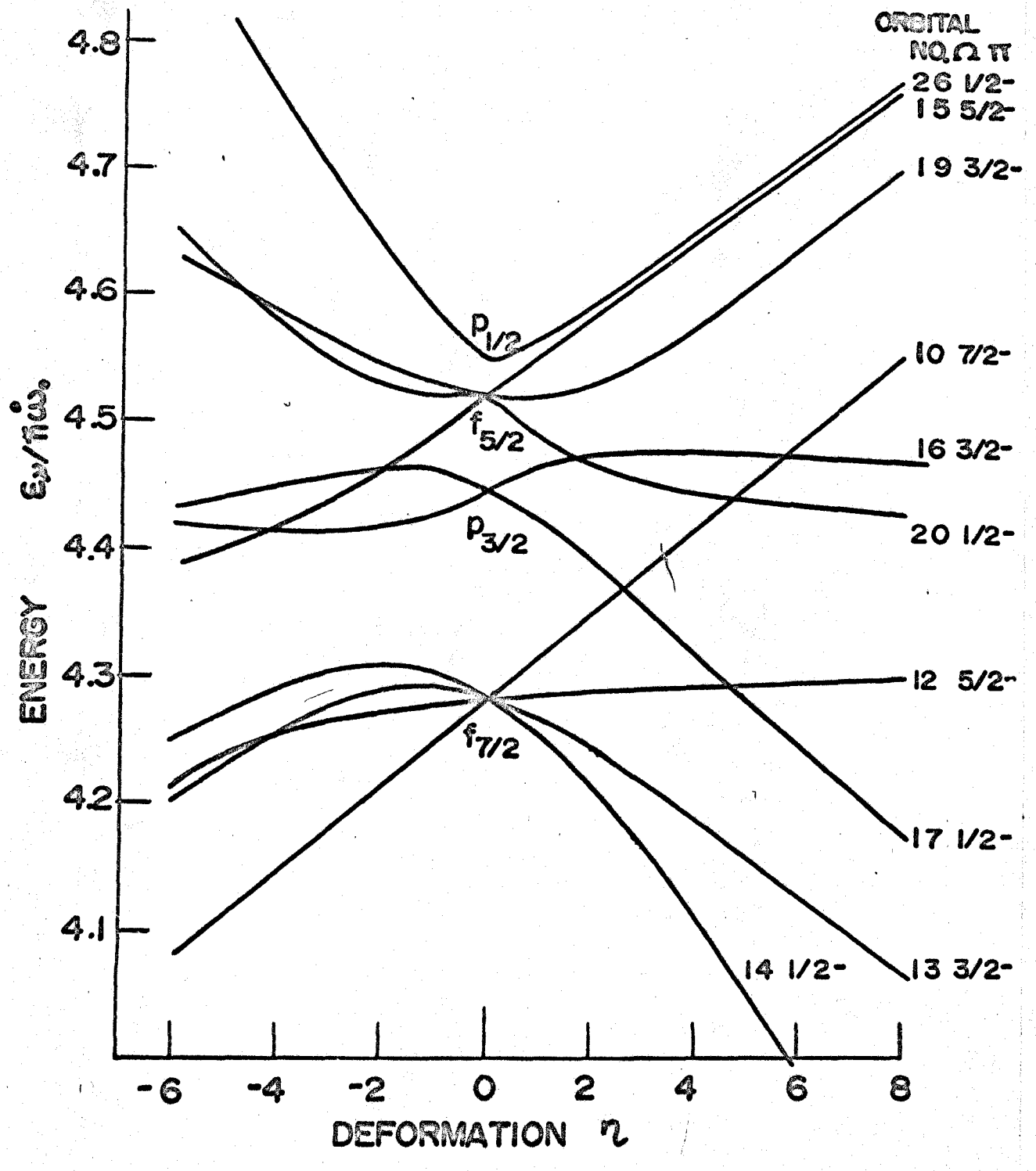

Fig. 3-2. Modified Nilsson diagram calculated for $\mu = 0.284$ and $\kappa = 0.034$.

CHAPTER 4. DETERMINATION OF GAP PARAMETER AND CHEMICAL POTENTIAL

4-1. General

In the preceding chapter, we determined the single particle energy ε_ν as a function of deformation η. Since the quasiparticle energy E_ν is connected with ε_ν, λ and Δ by Eq. (2-6), the determination of chemical potential and gap parameter is necessary, these being functions of η. We describe in this chapter, a method how to obtain these parameters and present the results in the form of figure.

The two parameters λ and Δ are determined from the non-linear equations (2-7) and (2-8) through a pairing strength G and a true particle number n. According to Belyaev (Be59), it is reasonable to assume that G for the same A is constant. Therefore we first try to know the value of G.

4-2. Determination of G

There are several methods in determining the value of G. The first method has been proposed by Bohr and Mottelson (Bo62). Since G would correspond to a short range part of the real nucleon-nucleon force, it could be decided from the experimental S wave nucleon-nucleon phase shift. An estimate of $G \approx 25/A$ MeV has been given.

The second value is obtained from the compiled data on the experimental binding energies. Since the binding

energy differences between odd- and doubly-even-mass nuclei depend highly on G, Kisslinger and Sorensen (Ki60) have determined the value according to the following procedures:

The ground state energy differences between the above nuclei are given by

$$P_n(Z,N) = E(Z,N) + E(Z,N-2) - 2E(Z,N-1)$$
$$P_p(Z,N) = E(Z,N) + E(Z-2,N) - 2E(Z-1,N), \qquad (4\text{-}1)$$

where E(Z,N) is the total binding energy of the (Z,N) nucleus, while P_n and P_p correspond to those of Z closed and N closed nucleus, respectively. On the otherhand, the theoretical odd-even mass difference should be just equal to $2E_\nu$, twice the energy of odd-mass quasiparticle. Referring to the data on the experimental binding energies, Kisslinger and Sorensen have calculated the odd-mass quasiparticle energy and deduced the G values. Their results are shown in Fig. 4-1, where P_n (or P_p) and the theoretical value are given for each single closed shell. In the Z = 28 and N = 28 region, G = 19/A MeV seems appropriate.

The third method is an application of a systematics of one quasiparticle state. Since we are interested in the regions of Z = 21 $\sim$ 25 and 33 $\sim$ 37, we could refer to the result of Ni isotopes. In Fig. 4-2, a systematic trend of the energy levels of odd-mass Ni isotopes is shown. The theoretical values are calculated for G = 19/A MeV.

Kisslinger and Sorensen (Ki60) have carried out the

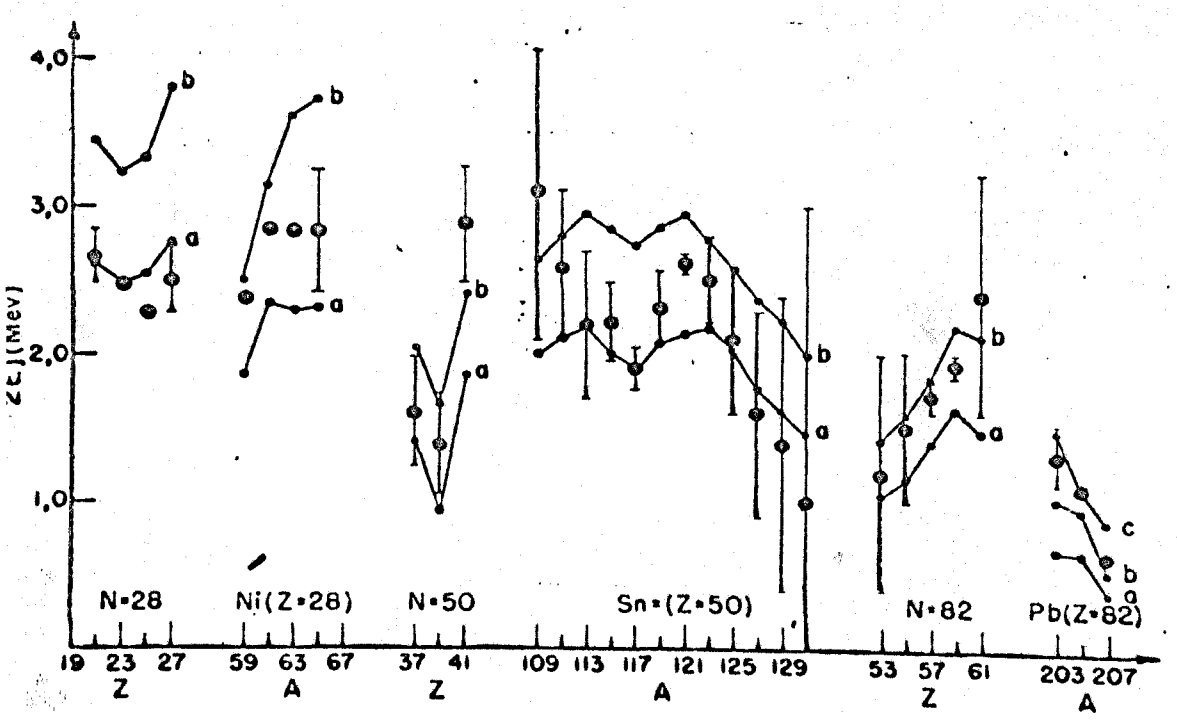

Fig. 4-1. Even-odd-A mass difference. The $P_n(Z,N)$ and $P_p(Z,N)$ are experimental quantities. The theoretical curves are simply $2E_\nu$, twice the energy of the lowest lying quasiparticle for the odd-mass isotope. Curves a and b correspond to G = 19/A and 23/A, respectively. Curve c corresponds to G = 30/A. (Cited from ref.(Ki60).)

calculation by using some single particle energies. However, we somewhat modify the energies according to the discussion in Chap. 3, which appear partly in Fig. 3-1. The comparison is shown in Table 4-1. Fig. 4-3 shows the energy levels of even-mass Ni isotopes given by Kisslinger and Sorensen (Ki60) for G = 19/A MeV.

Referring to these rerults, we reach a conclusion that it is appropreate to use the strength parameter for the pairing force of G = 19/A MeV, especially in the present Z regions.

Table 4-1. Single particle level energies in MeV.

State	Kisslinger & Sorensen	Present
$p_{3/2}$	0	0
$f_{5/2}$	0.75	0.78
$p_{1/2}$	1.56	1.08
$g_{9/2}$	4.25	4.25

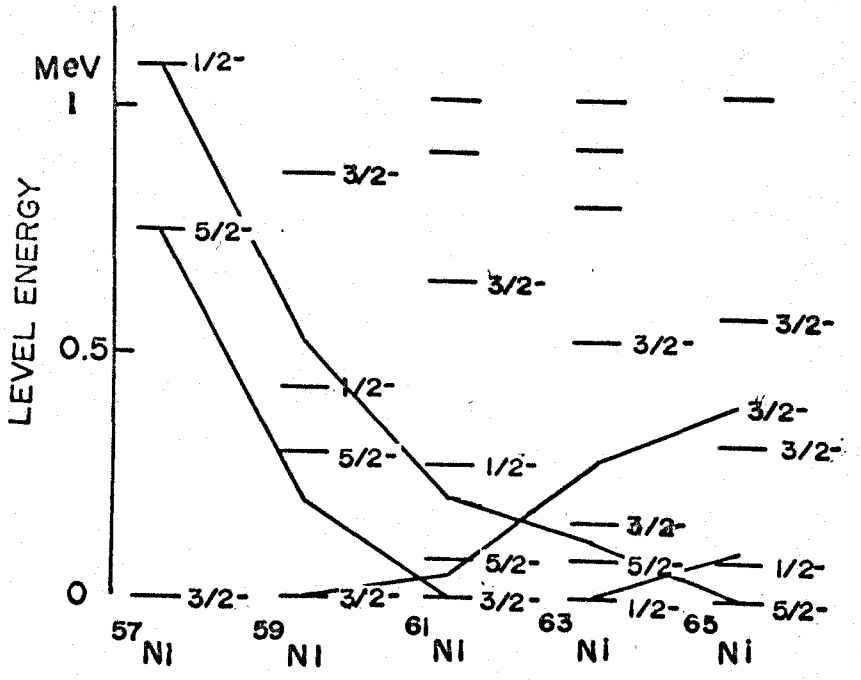

Fig. 4-2. Energy levels of odd-mass Ni isotopes. Horizontal lines are the experimental levels and solid lines join the theoretical ones calculated for G = 19/A MeV.

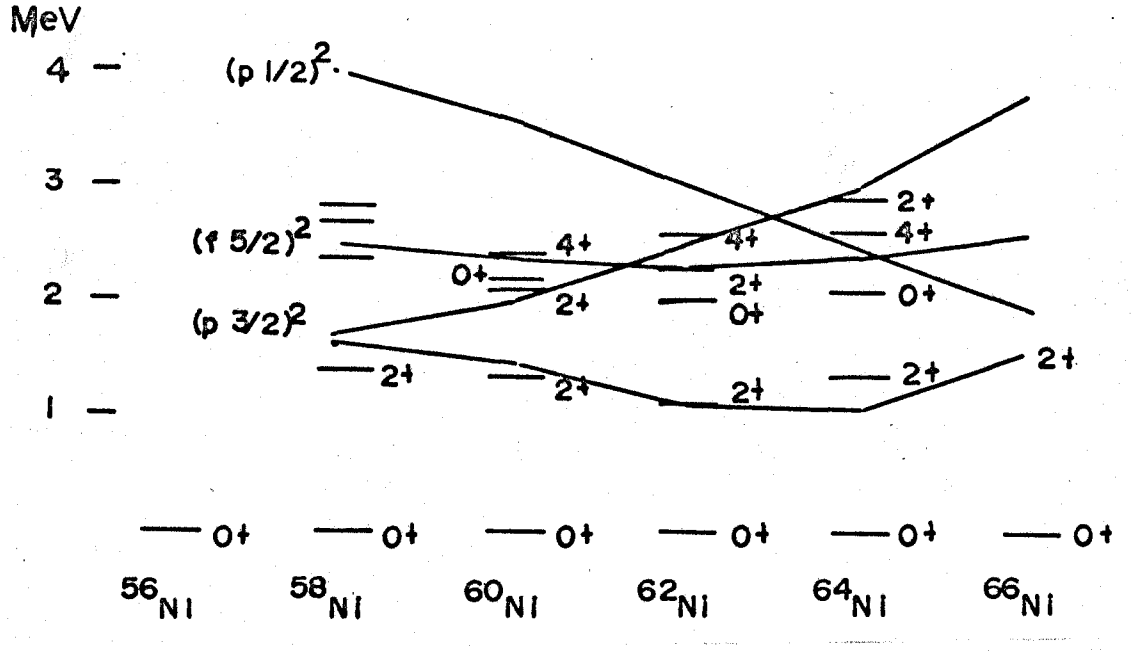

Fig. 4-3. Energy levels of doubly-even-mass Ni isotopes. Horizontal lines are the experimental levels and solid lines join the theoretical ones calculated for G = 19/A MeV.

4-3. Determination of λ and Δ

Now we proceed in determining the values of λ and Δ, inserting the obtained G = 19/A MeV and the true particle number n into Eqs. (2-7) and (2-8). In this calculation, we sum thirty consecutive Nilsson states for protons, the level energies being presented in Table 4-2 for positive values.

Since Eqs. (2-7) and (2-8) are non-linear simultaneous equations and we cannot solve analytically, we carry out the summation for a large number of λ and Δ sets and search a set which fits best to the given G and n. This procedure is coded in FORTRAN IV language and named QPFEEG. The details are shown in Appendix.

Fig. 4-4 shows the representative example. In Fig. 4-4-a, the n values for several Δ's are shown as a function of λ, while in Fig. 4-4-b, the values of G for several λ's are given as a function of Δ. Both are the cases for η = 6 in ^{75}As nucleus. From this figure, we can deduce that n is more sensitive to λ than Δ, whereas G is more dependent on Δ than λ.

The determined values of λ and Δ are presented in the form of figures in Fig. (4-5) for arsenic, bromine, rubidium and scandium isotopes.

Table 4-2. The Nilsson level energy (MeV) used to calculate the energy gap and the chemical potential.

orbital number	N	deformation 1	2	3	4	5	6	7	8
1	0								
2	1	-0.7333	-0.5467	-0.3200	-0.0933	0.1333	0.3600	0.5867	0.8133
3	1	-1.2582	-1.5685	-1.9161	-2.2899	-2.6820	-3.0872	-3.5018	-3.9235
4	1	2.0315	2.1152	2.2361	2.3832	2.5487	2.7272	2.9152	3.1102
5	2	-1.5466	-1.0933	-0.6400	-0.1867	0.2667	0.7200	1.1733	1.6267
6	2	-2.4698	-3.0891	-3.7937	-4.5505	-5.3421	-6.1578	-6.9910	-7.8373
7	2	-2.1043	-2.2318	-2.3772	-2.5366	-2.7069	-2.8859	-3.0718	-3.2633
8	2	3.3310	3.6851	4.0572	4.4433	4.8403	5.2459	5.6585	6.0766
9	2	0.0469	0.1110	0.1184	0.0485	-0.0847	-0.2592	-0.4581	-0.6710
10	3	-5.4080	-4.4080	-3.4080	-2.4080	-1.4080	-0.4080	0.5920	1.5920
11	2	2.7429	2.6180	2.6352	2.7821	3.0268	3.3370	3.6892	4.0683
12	3	-6.2810	-6.1800	-6.0984	-6.0315	-5.9758	-5.9288	-5.8887	-5.8542
13	3	-6.9272	-7.5824	-8.3264	-9.1307	-9.9773	-10.8545	-11.7544	-12.6714
14	3	-7.2886	-8.4685	-9.8822	-11.4639	-13.1616	-14.9383	-16.7691	-18.6380
15	3	1.4650	2.3640	3.2824	4.2155	5.1598	6.1128	7.0727	8.0382
16	3	-0.9993	-0.6672	-0.6063	-0.6446	-0.7036	-0.7624	-0.8159	-0.8630
17	3	-2.2581	-3.1650	-4.2237	-5.3197	-6.4073	-7.4779	-8.5331	-9.5761
18	4	-12.0933	-11.1867	-10.2800	-9.3733	-8.4667	-7.5600	-6.6530	-5.7467
19	3	0.5425	0.8656	1.5487	2.3913	3.2969	4.2329	5.1862	6.1503
20	3	-0.3342	-1.0598	-1.4506	-1.6735	-1.8123	-1.9050	-1.9703	-2.0182
21	4	-12.7026	-12.4137	-12.1320	-11.8565	-11.5861	-11.3203	-11.0582	-10.7996
22	4	-13.1751	-13.3921	-13.6431	-13.9221	-14.3341	-14.5451	-14.8822	-15.2328
23	4	-13.4995	-14.0852	-14.7472	-15.4756	-16.2609	-17.0947	-17.9693	-18.8785
24	4	-13.6651	-14.4505	-15.3526	-16.3674	-17.4881	-18.7065	-20.0128	-21.3965
26	3	1.9489	2.7412	3.6045	4.5051	5.4292	6.3692	7.3205	8.2803
27	4	-4.1421	-3.9668	-3.8485	-3.7264	-3.5946	-3.4530	-3.3025	-3.1440
29	4	-4.9111	-5.3365	-5.8792	-6.4707	-7.0239	-7.5900	-8.1461	-8.6916
30	4	-5.3670	-6.2525	-7.3631	-8.6048	-9.8965	-11.1972	-12.4878	-13.7605
33	4	-4.3230	-4.4551	-4.4546	-4.3959	-4.3027	-4.1851	-4.0489	-3.8981
34	4	-4.6884	-5.4685	-6.2043	-6.8820	-7.5197	-8.1264	-8.7076	-9.2675

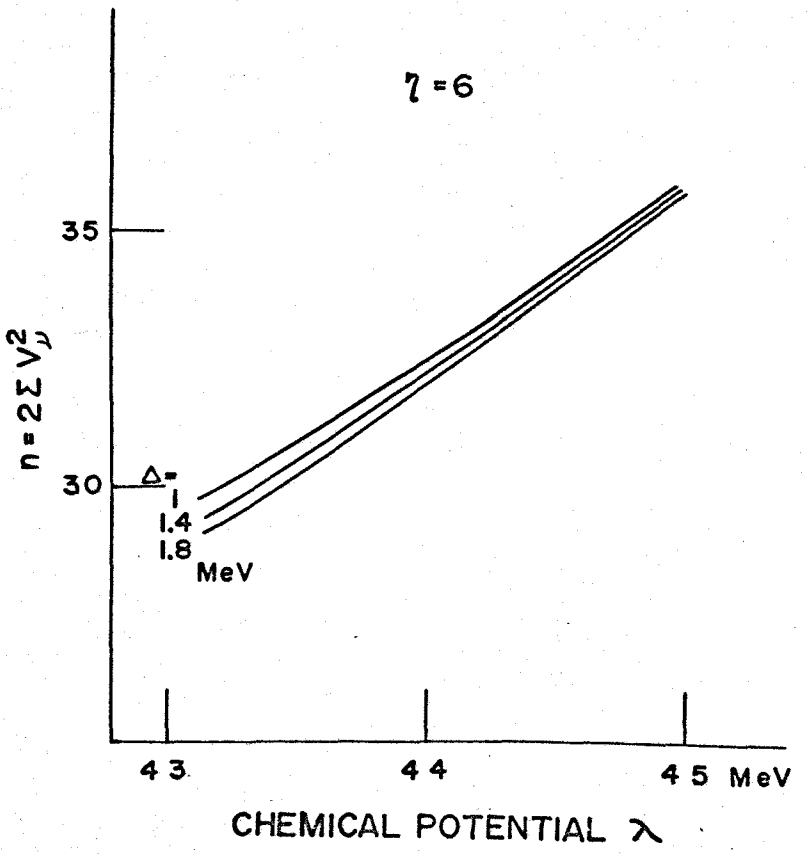

Fig. 4-4-a. The value of number of particles as a function of chemical potential for several values of energy gap.

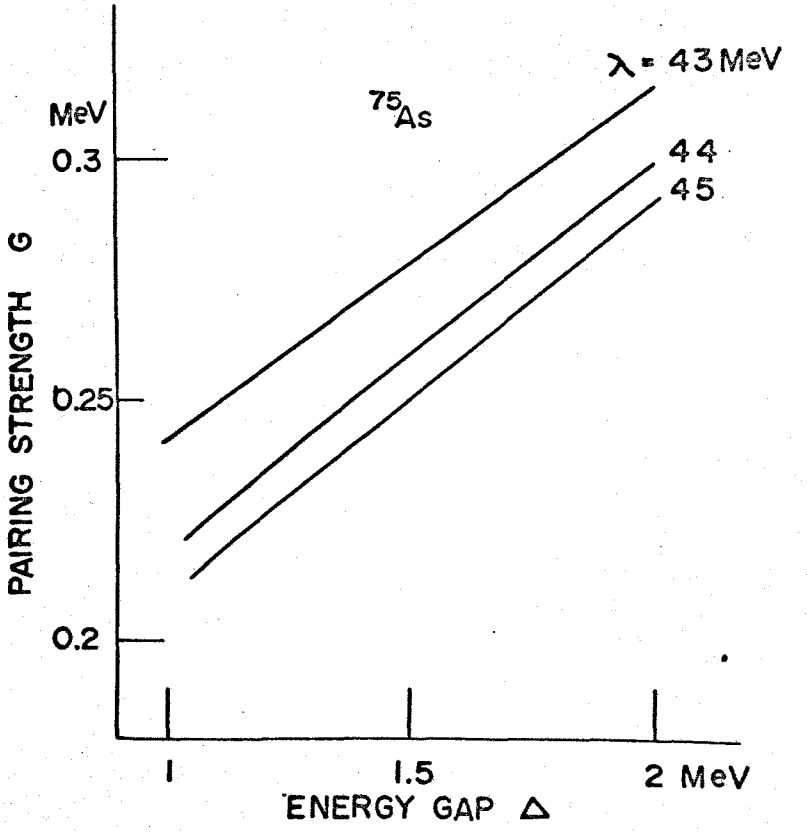

Fig. 4-4-b. The value of pairing strength as a function of energy gap for several values of chemical potential.

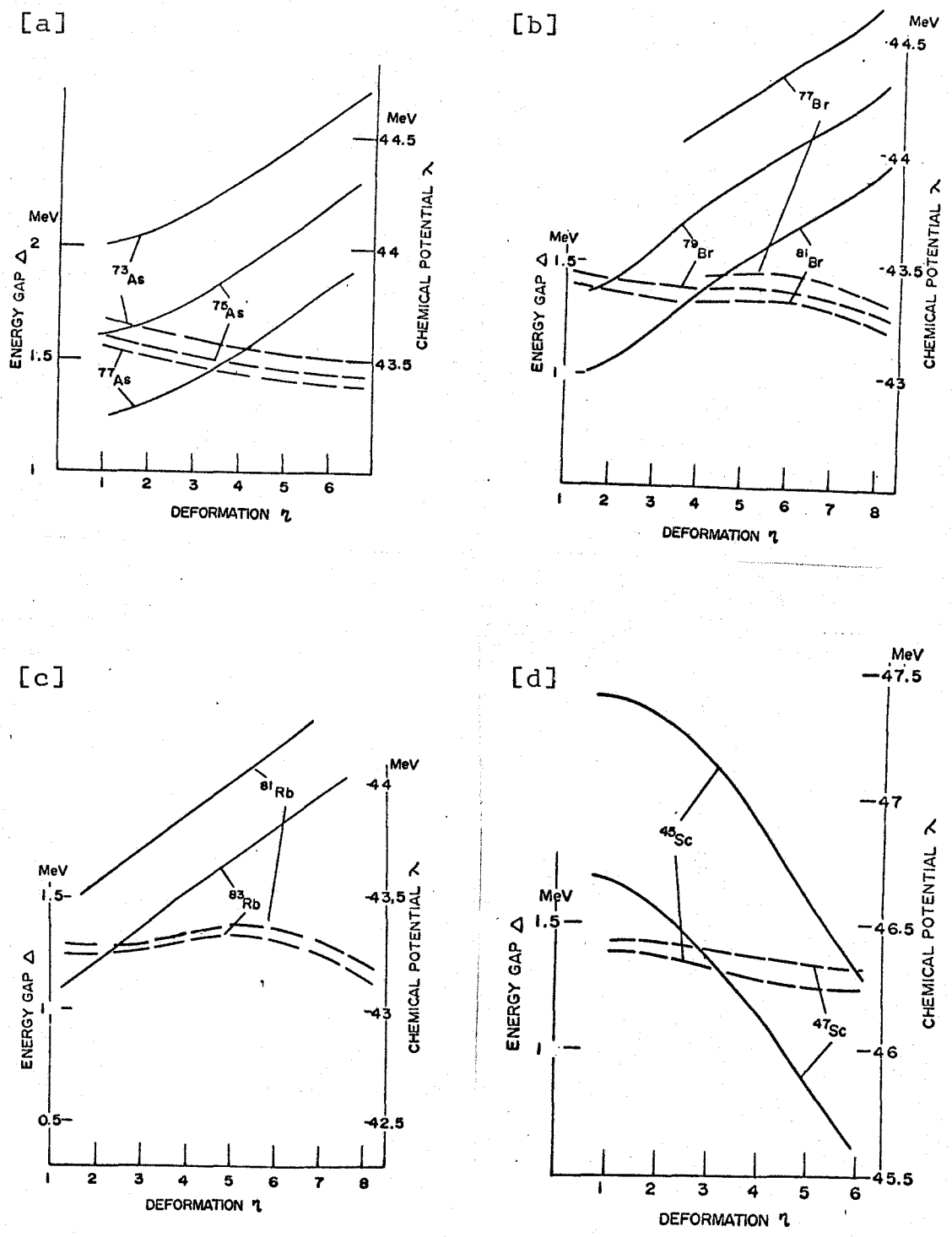

Fig. 4-5. The values of chemical potential and energy gap as a function of deformation for arsenic [a], bromine [b], rubidium [c] and scandium [d] isotopes.

CHAPTER 5. LEVEL ENERGY AND WAVE FUNCTION

5-1. General

The present level spectra are obtained by diagonalizing the Coriolis interaction with the rotational wave functions, which are built on a number of intrinsic states. These states are attributed to the motion of single "quasi-proton" in No. 15, 16, 17, 19, 20 or 26 orbital for so called $p_{3/2}$ or $f_{5/2}$ shell nuclei, and in No. 10, 12, 13 or 14 orbital for $f_{7/2}$ shell nuclei. In these calculations, we omit the neutron states, because all neutrons form pairs in the ground states of the present nuclei and their excitation energies are so high that they do not contribute to the low-lying states below 1 MeV.

In the well known deformed region, the rotational constants $\frac{\hbar^2}{2\mathcal{J}}$ of odd-mass nuclei are ordinarily smaller than those of neighbouring even nuclei. The differences between them vary rather randomly as shown in Fig. 5-1. In the level calculation, therefore, the rotational constant $\frac{\hbar^2}{2\mathcal{J}}$ is used as a parameter, which is chosen the same value for all bands and for the strength of the Coriolis coupling in each nucleus.

Again, Nilsson wave functions and level energies depend on η. The band head energies computed from Eq. (2-6) are also a function of η. Therefore, we finally calculate the model energy spectra as functions of η and $\frac{\hbar^2}{2\mathcal{J}}$ by the FORTRAN IV program CORIOJ , and then search the best fit with

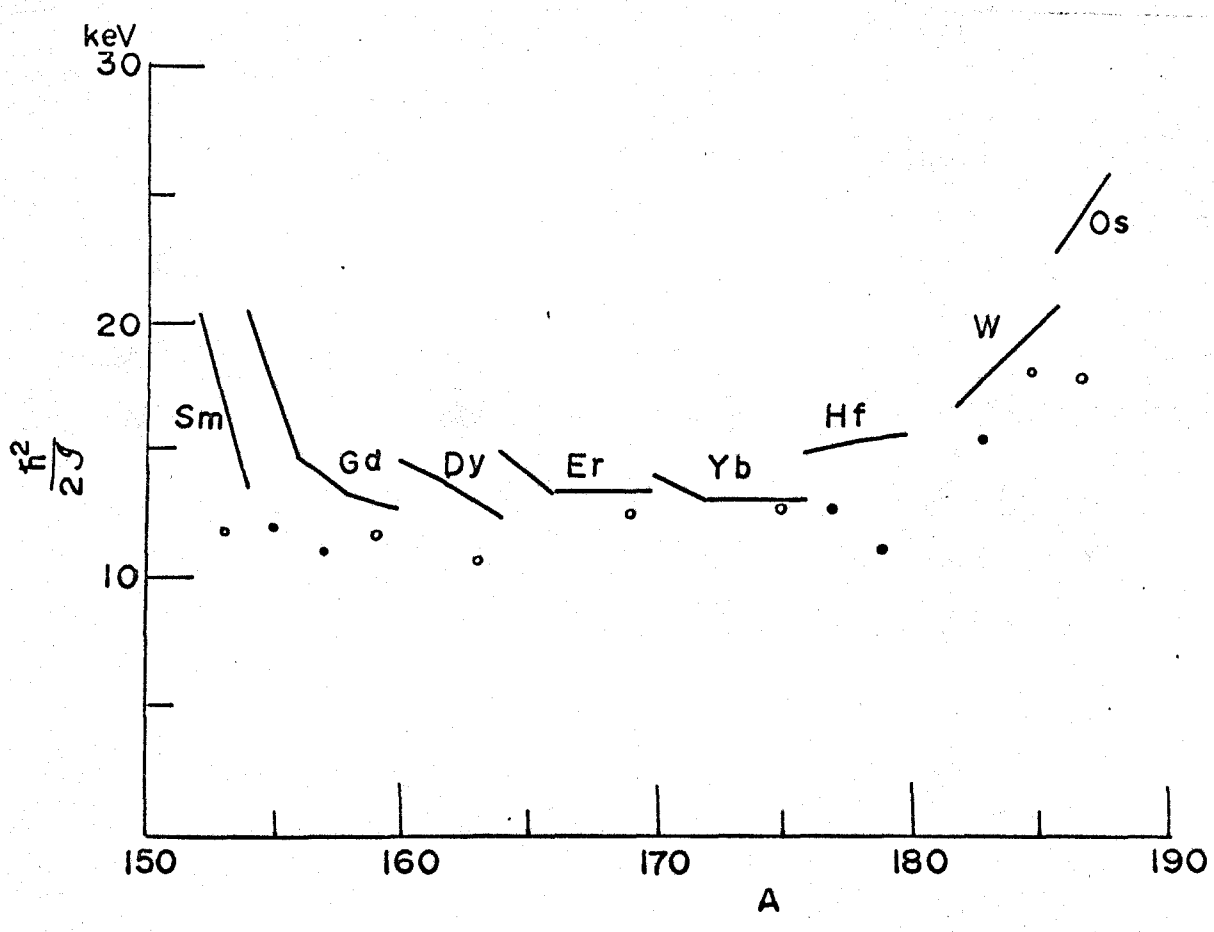

Fig. 5-1. The rotational constants for nuclei in the well known deformed region.

the experimental levels. We can obtain simultaneously the mixing amplitudes $C^{I}_{K\xi}$ in Eq. (2-18), that is the total wave functions for the levels considered.

In the following sections, we first summarize the level energies and gamma ray properties which have been confirmed until now, and then compare these with the theoretical level spectra based on the present model and on the other previous models. The experimental data are greatly indebted to Nuclear Data Sheets (N.D.S.).

5-2. Arsenic Isotopes

5-2-1. Compilation of experimental data

i) ^{71}As nucleus

This nucleus has not been observed in detail and many ambiguities still exist.

a) Ground state.....Since the transition to the 5/2 - level in ^{71}Ge is allowed, the ground state I^{π} is 3/2 -, 5/2 - or 7/2 -. The transition to the 9/2 + level in ^{71}Ge has log ft = 7.8, and 3/2 - is excluded. I^{π} of this state is probably 5/2 -.

ii) ^{73}As nucleus

The level spectrum of ^{73}As was investigated by several authors through the studies of ^{73m,g}Se decays. As is pointed in N.D.S. (ND66), the 66.9, 75.7 and 427 keV levels presumably exist. Ricci, van Lieshout and van ven Bold (Ri60) observed the 66.9 keV gamma rays with NaI(Tl) counter, while in addition, Rao and Fink (Ra66) reported the relatively strong 75.1 keV gamma rays by using a Ge(Li) detector. The levels and decay schemes are presented in Fig. 5-2.

a) Ground state.....The spin and parity of this state is inferred to have I^{π} = 3/2 -. This is based on the analogy with ^{75}As and ^{77}As. Similar result is given from the log ft (= 5.2) for the electron decay to 1/2 - ^{73}Ge isomeric state.

b) 66.9 KeV level.....I^{π} = 5/2 - is assigned from the

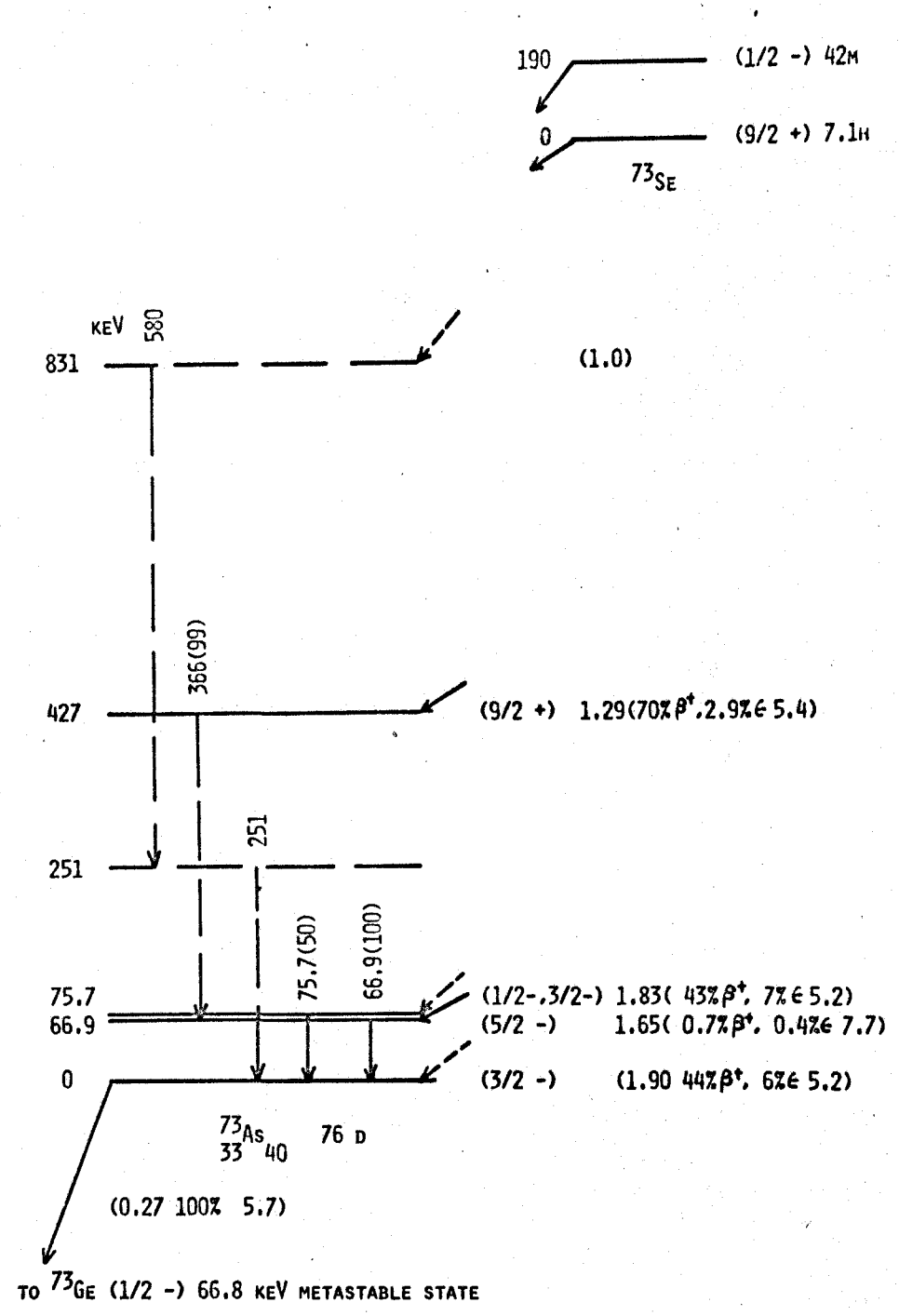

Fig. 5-2. The experimental level spectrum in ^{73}As (ND66).

angular correlation experiment of 360 - 66.9 keV gamma rays. The spin and parity are also consistent with the M1 nature of the 66.9 keV transition.

c) 75.7 keV level.....The total internal conversion coefficient for the 75.7 keV transition is observed as 0.22, which is consistent with the theoretical estimate of 0.18 for the M1 transition. The log ft value for the positon decay of ^{73}Se to this level is 4.9 and this supports the transition is an allowed type. These facts indicate I^{π} = 1/2 or 3/2 - for this level.

iii) ^{75}As nucleus

The low-lying states of ^{75}As have been extensively investigated through the studies of ^{75}Ge negaton decay, ^{75}Se electron capture decay and ^{75}As Coulomb excitation. The level spectrum is cited from N.D.S. (ND66a) as shown in Fig. 5-3. The ^{75}Ge decay has been studied by Schardt and Welker (Sc55) and by van den Bold, Geijn and Endt (Bo58a) and the 199, 265, 470 and 618 keV levels were identified. The study of ^{75}Se decay has been carried out by de Croes and Backstrom (Cr60), Grigoriev and Zolotain (Gr61), Edward and Gallogher (Ed61), Rao, McDaniels and Crasemann (Ra66a) and Speidel et al. (Sp68). The levels of 198.6, 264.7, 303.7, 400.5 and 572.3 keV are in general agreement. An additional level at 617.7 keV has been reported both by Varma and Eswaran (Va62) and by Rao, McDaniels and Crasemann

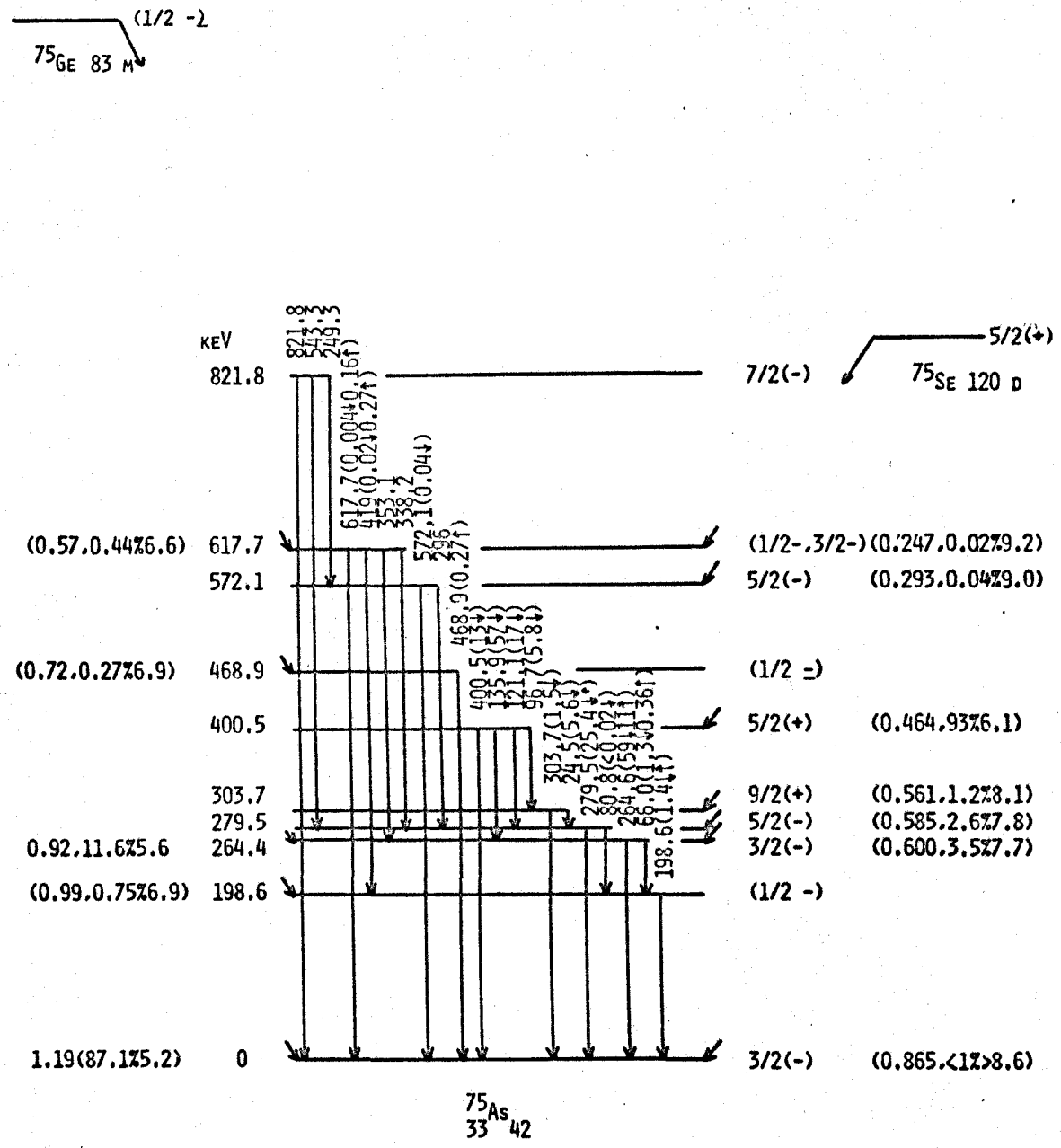

Fig. 5-3. The experimental level spectrum in ^{75}As (ND66a).

(Ra66a). Coulomb excitation studies of ^{75}As were done by Temmer and Heydenberg (Te56), Kamitsubo with proton (Ka62), Ritter, Stelson, McGowan and Robinson with Ne ions (Ri62), Imanishi, Fukuzawa and Sakisaka with N ions (Im67) and most recently Robinson, McGowan, Stelson and Milner with alpha and O ions (Ro67).

a) Ground state.....I = 3/2 has been assigned by a microwave measurement. π = - is reasonable from the analogy with ^{77}As and ^{79}As.

b) 198.6 keV level.....I^{π} = 1/2 - is reasonable. The average α_K given by many workers (Gr61,Ed61) shows the M1 + E2 character for the 198.6 keV transition, which leads to I = 1/2, 3/2 or 5/2. The value of the radiative admixture δ^2, which is deduced from the life time (Sh59), B(E2) measurement with Coulomb excitation and the conversion data, indicates the spin to be 1/2 or 3/2. Since the negaton transition from the ground ^{75}Ge (I^{π} = 1/2 -) to this state is allowed or first forbidden, I = 5/2 is excluded. On the other hand, I = 1/2 is preferable from the angular distribution for 66 and 198.6 keV gammas in Coulomb excitation experiment. π = - is deduced from the Coulomb excitation cross section.

c) 264.7 keV level.....The 264.7 keV gamma is predominantly M1 radiation, because $\alpha_K = 0.36 \pm 0.05$ has been given by Edward et al.(Ed61). The 66 keV gamma transition to the 198.6 keV level has a M1 type, and then the possible spin

is restricted to 1/2 or 3/2. The angular distribution study by Metzger (Me62) and Langhoff and Schumacher (La67) rejects out the spin 1/2. The parity is deduced from the Coulomb excitation experiment. Therefore, $I^{\pi} = 3/2 -$ is very probable.

d) 279.6 keV level.....Coulomb excitation of this level and the angular correlation of 121.1 - 279.6 keV gamma rays are only consistent with the assignment $I^{\pi} = 5/2 -$.

e) 468.9 keV level.....This level is fed by the 0.72 MeV negaton decay (log ft = 6.9) from ^{75}Ge ground state (1/2 -), but is hardly fed by the electron capture decay from ^{75}Se ground state (5/2 +). The gamma transitions from the 468.9 keV level to the 279.6 and 264.7 keV levels are less than 1 %. Coulomb excitation of this level is found. These suggest $I^{\pi} = 1/2 -$.

f) 572.3 keV level.....The angular distribution of the 572.3 keV gamma rays and Coulomb excitation lead to an assignment $I^{\pi} = 5/2 -$.

g) 617.7 keV level.....Since this is fed by the 0.57 MeV negaton decay (log ft = 6.3) from ^{75}Ge ground state, I = 1/2 or 3/2.

h) 821.8 keV level.....The angular distribution of the 821.8 keV gamma rays following Coulomb excitation establishes that $I^{\pi} = 7/2 -$.

In Fig.5-3, the observed level spectrum of ^{75}As is presented.

iv) ^{77}As nucleus

The level spectrum of ^{77}As has been investigated by several authors through the studies of ^{77g}Ge (11.3h) and ^{77m}Ge (55.5s) (Ko65,Do68,Ng68,Im69,Im70). The result is shown in Fig. (5-4). The level spins and parities have been assigned mainly by the analogy of the levels between ^{75}As and ^{77}As and by the gamma - gamma angular correlation experiments. We summarize these results as follows:

a) Ground state.....The nucleus ^{77}As decays to the 1/2 - ground and 5/2 - 247.4 keV states in ^{77}Se with log ft = 5.7 and 7.2, respectively. These two facts determine I^{π} = 3/2 - for this state.

b) 194.5 keV level.....Since this level is fed by the negaton decay from ^{77m}Ge (1/2 -) with log ft 6.7, it is supposed to have I^{π} = 1/2 - analogously with ^{75}As and ^{79}Br.

c) 215.5 keV level.....Since this level is fed by negaton decay from 1/2 - ^{77m}Ge state with log ft = 5.3, then I^{π} = 1/2 - or 3/2 -. However, the angular correlation measurements of the 563 - 368 and 563 - 417 keV cascades leave the possible assignment of only I^{π} = 3/2 -.

d) 264.4 keV level.....I^{π} = 5/2 - is deduced from the analogy with ^{73}As and ^{75}As isomeric states. The M2 transition probabilities from these states are about 1/20 times the Weisskopf estimate, which is just the same as the 210 keV isomeric transition of probable M2 type in ^{77}As. The 475 keV isomeric state of ^{77}As is assigned I^{π} = 9/2 +

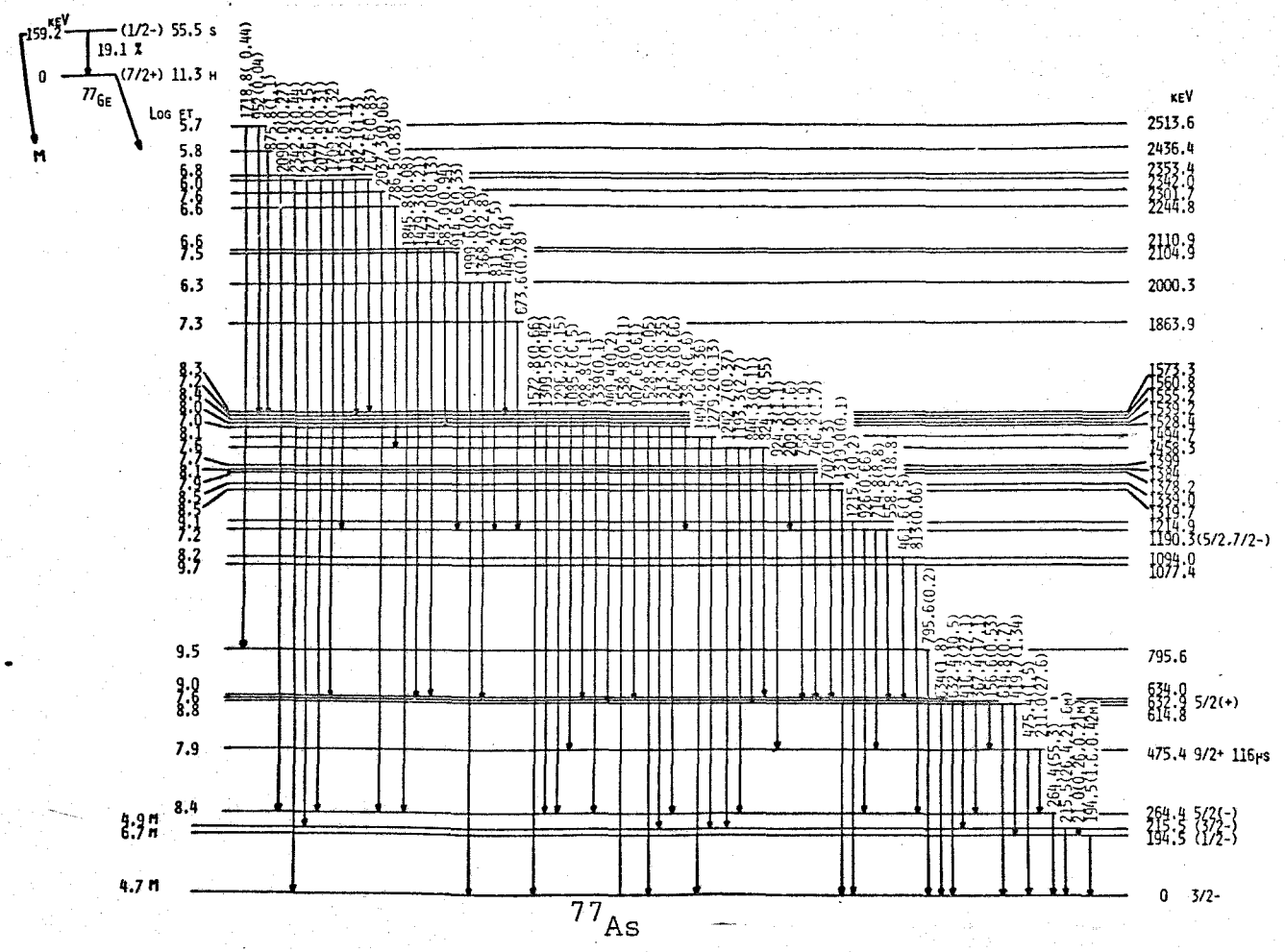

Fig. 5-4. The experimental level spectrum in ^{77}As.

from the above analogy. Therefore $I^{\pi} = 5/2^-$ seems reasonable for this state. This is also supported by the 210 - 264 keV angular correlation study.

e) 1195 keV level.....This level has either $I = 5/2$ or $7/2$, since it decays both to the $3/2^-$ ground state and to the $9/2^+$ level at 475 keV.

5-2-2. Theoretical calculations of level spectra (Im69a)

In the previous subsection, the level energies, spins and parities of odd-mass arsenic nuclei are presented. Among them, the ^{75}As level scheme is well established. Therefore we first apply a least-squares fitting procedure to this isotope. Similar treatment are done for ^{77}As, ^{73}As and ^{71}As isotopes, but since the confirmed odd-parity levels are not many, the theoretical levels presented may be representative proposals.

i) ^{75}As nucleus

The levels based on our model are the function of deformation η and rotational constant $\frac{\hbar^2}{2\mathcal{I}}$. In Fig. 5-5-a, the level spectra without Coriolis coupling are presented against η for $\frac{\hbar^2}{2\mathcal{I}} = 80$ and 60 keV. The level energies are modified by Coriolis coupling, as seen in Fig. 5-5-b. Fig. 5-6 shows the example how the wave functions and level energies with Coriolis coupling vary against η.

As seen from these figures, for small value of η the $5/2^-$ state is most lowered and as the value of η becomes

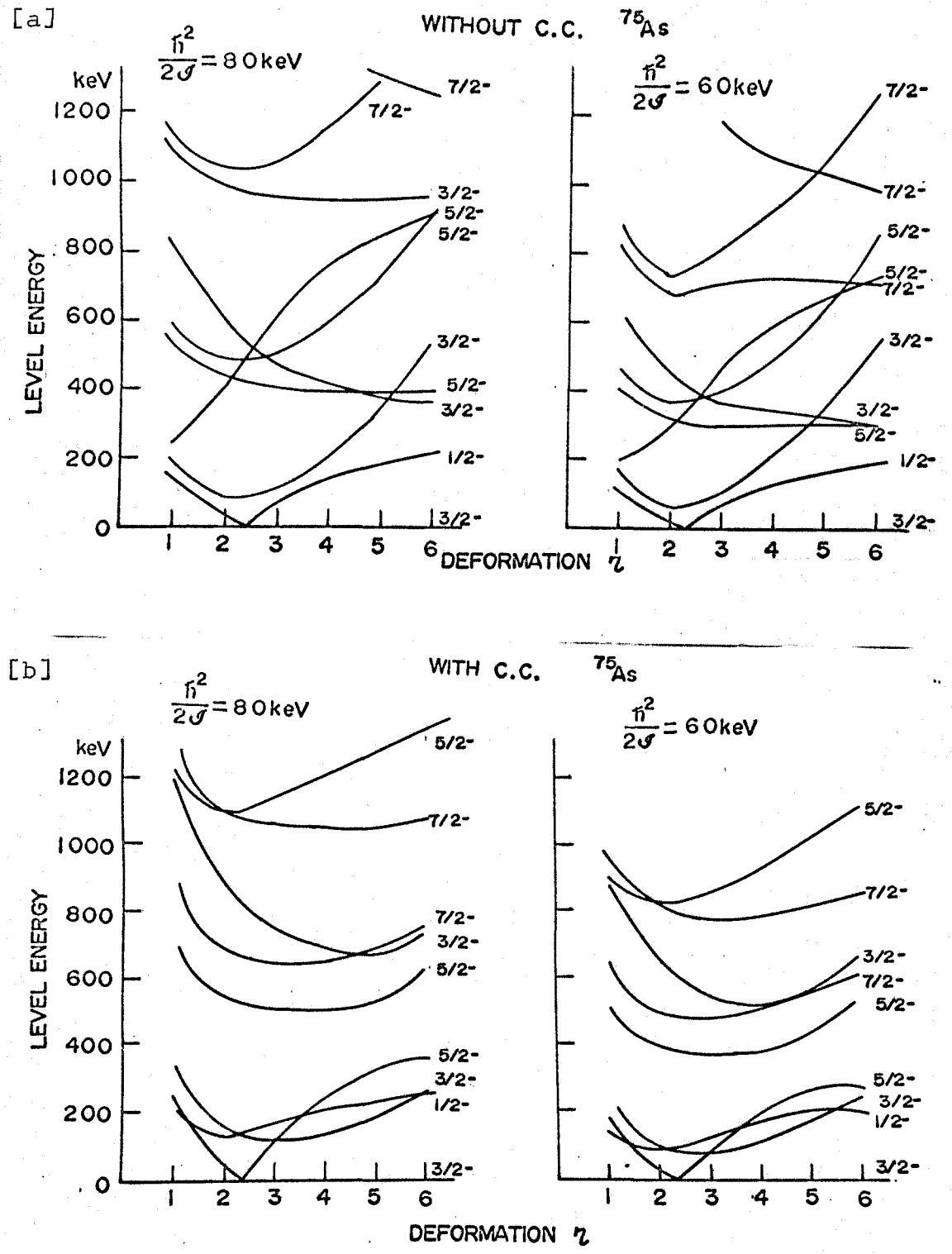

Fig. 5-5. The calculated odd-parity level spectra in ^{75}As as a function of deformation for different rotational constants. These spectra are calculated without [a] and with [b] Coriolis interaction.

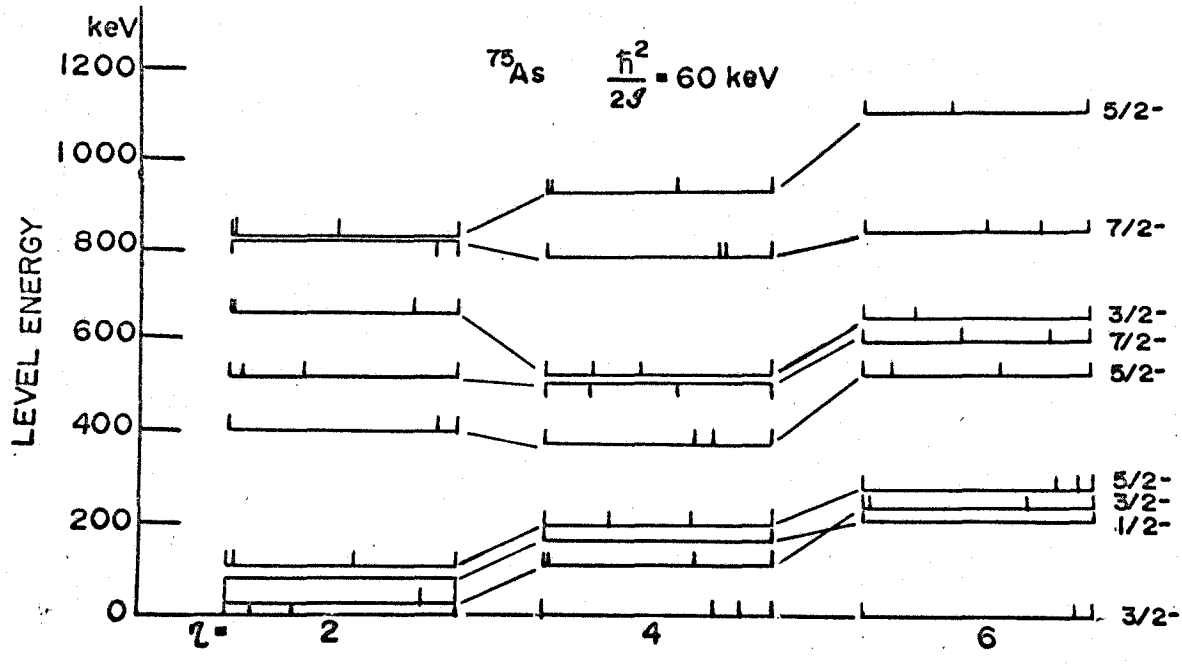

Fig. 5-6. The wave functions for levels in ^{75}As for some combinations of deformation and rotational constant. The width between two adjacent verticals denotes the amplitude of each K band. The order of K bands is as follows:

No. 16 20 19 for I = 3/2, 5/2 and 7/2,

and

No. 20 for I = 1/2.

large , the 3/2 state is abruptly lowered and for $\eta > 2.5$ the ground state has the spin and parity 3/2-in this calculation.

A characteristic feature appeared in this calculation is that several levels locate nearby one another and form apparent groups. For example, four levels of 3/2 - (ground), 3/2 -, 1/2-and 5/2-make a lower excitation group, while three levels of 5/2 -, 3/2 - and 7/2 - appear at a little higher excitation energy. This feature is also seen in the experimental level scheme. The lower grouping depends strongly on the deformation and slightly on the rotational constant.

Fig. 5-7 shows the level spectra as a function of $\frac{\hbar^2}{2\mathcal{J}}$ for different η's without and with Coriolis coupling. It is seen that the level locations change monotonically with the rotational constant. Fig. 5-8 gives the wave functions and level energies with Coriolis coupling for $\eta = 6$.

Since the core and the unpaired outside-particle in ^{75}As are subject to a pairing effect, the level spectra calculated without the pairing effect would be quite different from the complete spectra. An example is presented in Fig. 5-9 and any level grouping is not seen. Therefore the theory without pairing effect cannot explain the experimental level spectra.

The best agreement with experiment is obtained for $\eta = 6$ and $\frac{\hbar^2}{2\mathcal{J}} = 60$ keV. The experimental and the calculated energy

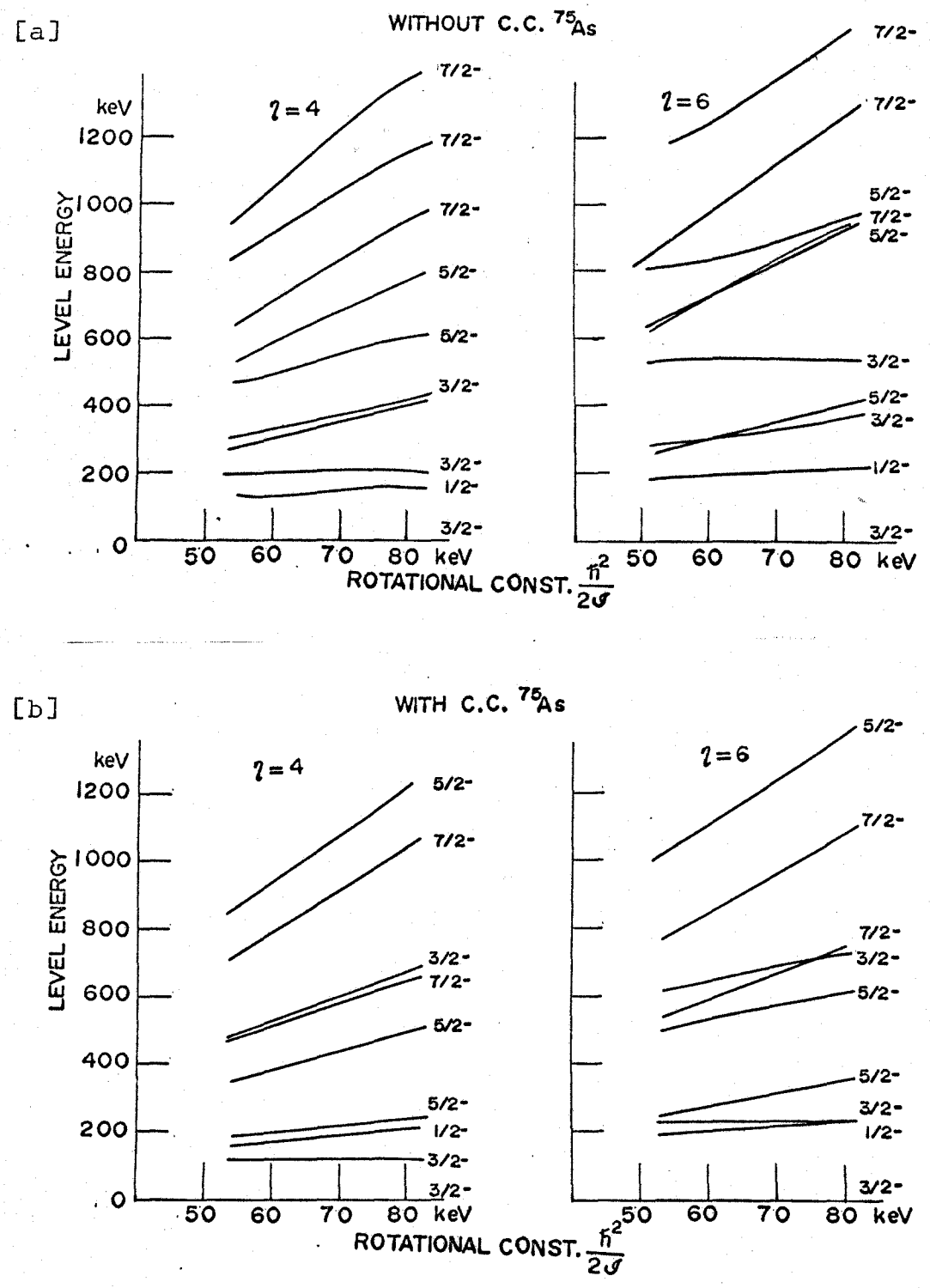

Fig. 5-7. The calculated odd-parity level spectra in ^{75}As as a function of rotational constant for different deformations. These spectra are calculated without [a] and with [b] Coriolis interaction.

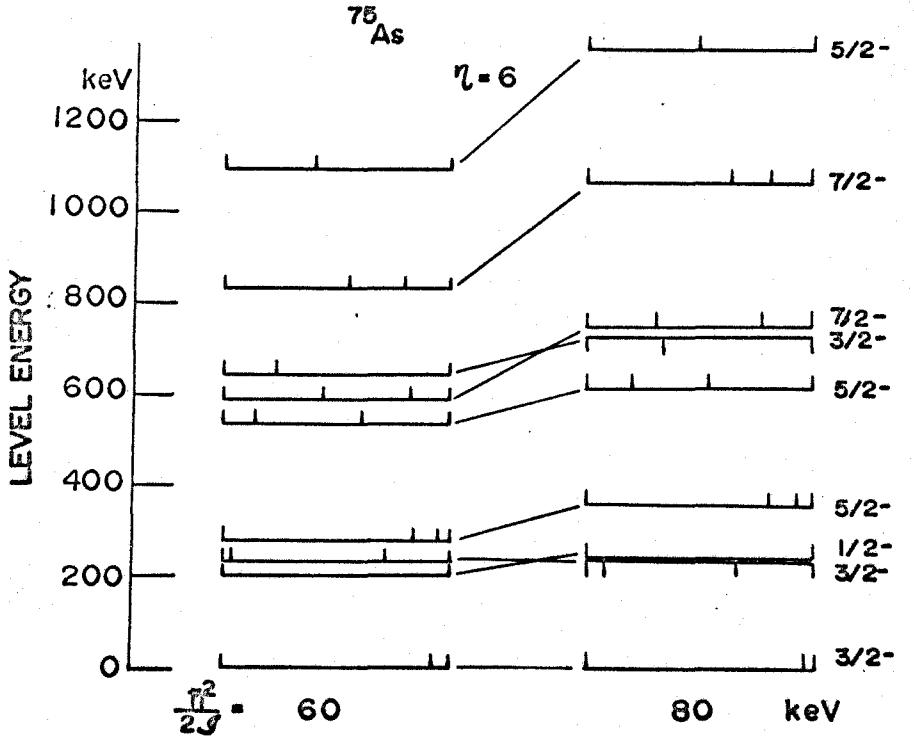

Fig. 5-8. Same as Fig. 5-6.

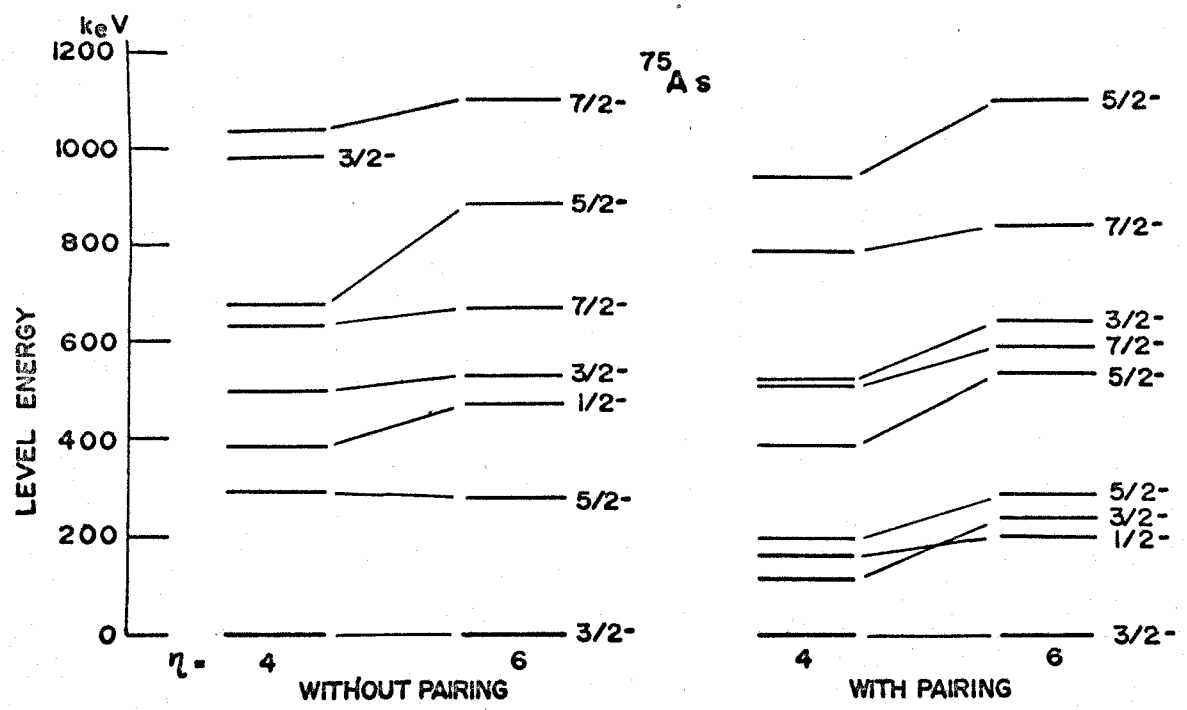

Fig. 5-9. Comparison between the results calculated with and without pairing effect.

levels are shown in Fig. 5-10. The theoretical levels proposed by Kisslinger and Sorensen (Ki63), Scholz and Malik (Sc67) and Kisslinger and Kumar (Ki67) are also presented in the figure.

Kisslinger and Sorensen have studied systematically the various nuclear properties, using the pairing plus quadrupole forces as residual interaction, and obtained overall agreement for many nuclei. But they have pointed out that their model seems inadequate for the nuclei with $32 \leq Z \leq 36$. In ^{75}As nucleus, for example, they predict only four levels below 1 MeV and the ground state to be 1/2, as shown in Fig. 5-10. The modification of this model has been done by Kisslinger and Kumar, considering the anharmonisity of the doubly-even system. They obtained the improved level spectra for the nuclei around Z (and N) $\sim$ 28 closed shell, and the ground spin of ^{75}As was correctly predicted and also many other levels were depressed below 1 MeV excitation. However, the calculated spectra do not always explain the experimental ones. The theoretical levels proposed by Scholz and Malik is not satisfactory.

The present theory reproduces rather well the spins and locations of the low-lying odd-parity levels except the 468.8 keV 1/2 - state. In the least-squares fitting procedure, we fitted the theoretical 651 keV state to the experimental 617.7 keV level. The overall agreement of the present model with the experiment means that both pairing

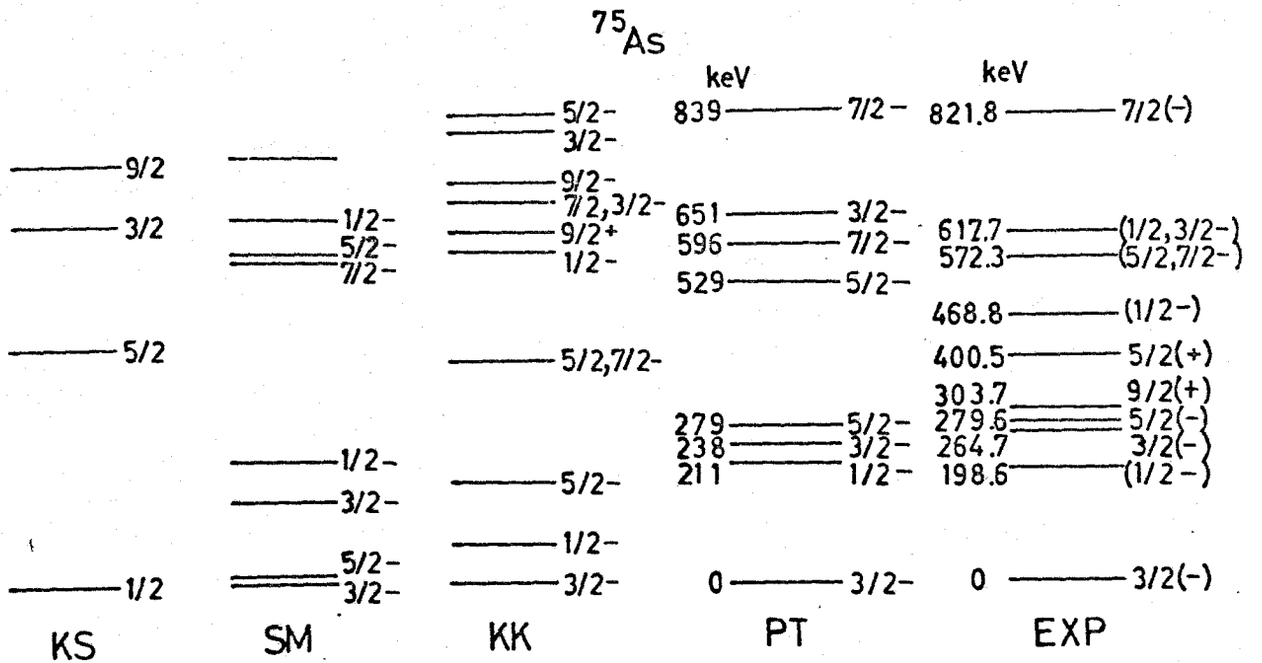

Fig. 5-10. Comparison of the theoretical level energies in ^{75}As with those obtained by experiment (marked EXP). Present theoretical level energies (marked PT) are obtained for $\eta = 6$ and $\frac{\hbar^2}{2\mathcal{I}} = 60$ keV. Previous theoretical works done by Kisslinger and Sorensen, Scholz and Malik and Kisslinger and Kumar are marked KS, SM and KK, respectively.

and Coriolis forces seem essential as residual interactions, but other small interactions still remain. This must be studied in future.

Table 5-1 gives the wave functions of the calculated energy levels for the optimum η and $\frac{\hbar^2}{2\mathcal{J}}$ values. The wave functions will be used in Chap. 6 to calculate the reduced transition probability in the ^{75}As Coulomb excitation experiment.

ii) ^{77}As nucleus

As described previously, the spin assignment has been done for the ground, 194.5, 215.5 and 264.4 keV states as 3/2 -, (1/2 -), (3/2 -) and 5/2 (-), respectively. Therefore we present here only the level positions as functions of η and $\frac{\hbar^2}{2\mathcal{J}}$, instead of trying a least-squares fit. The calculated level spectra are shown in Fig. 5-11 and the comparison of the various theoretical results with experiment is done in Fig. 5-12. Our proposed levels in this figure are given for η = 6 and $\frac{\hbar^2}{2\mathcal{J}}$ = 60 keV. This model predicts the possible exsistence of 5/2 - 529, 7/2 - 597, 3/2 - 646 and 7/2 - 838 keV levels.

iii) ^{73}As nucleus

Among the odd-parity levels in ^{73}As, only three of them have been assigned, that is, the ground, 66.7 and 75.7 keV states as (3/2 -), (5/2 -) and (1/2 - or 3/2 -), respectively.

Table 5-1. Energies, spins and amplitudes of ^{75}As odd-parity levels calculated for $\eta = 6$ and $\frac{\hbar^2}{2\mathcal{J}} = 60$ keV.

Energy (keV)	Spin Parity	Eigenfunction |3 3/2 1 2⟩	|3 1/2 1 0⟩	|3 3/2 0 1⟩
0	3/2 -	0.97	-0.25	0.08
211	1/2 -		1	
238	3/2 -	0.26	0.84	-0.48
279	5/2 -	0.93	0.33	0.17
529	5/2 -	-0.36	0.69	0.63
596	7/2 -	-0.67	0.64	-0.38
651	3/2 -	0.05	0.48	0.88
839	7/2 -	0.73	0.50	-0.46

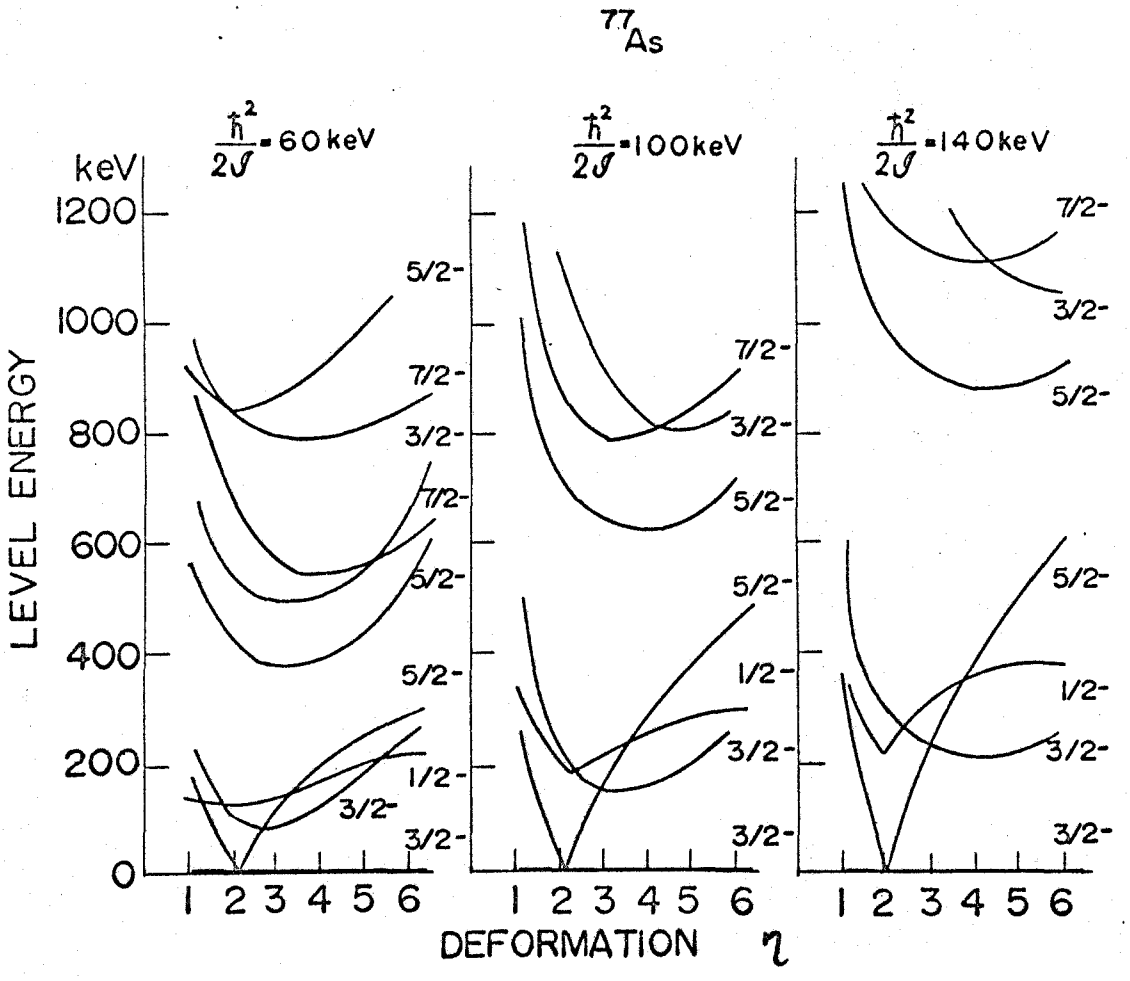

Fig. 5-11. Theoretical odd-parity level spectra in ^{77}As as a function of deformation for different rotational constants.

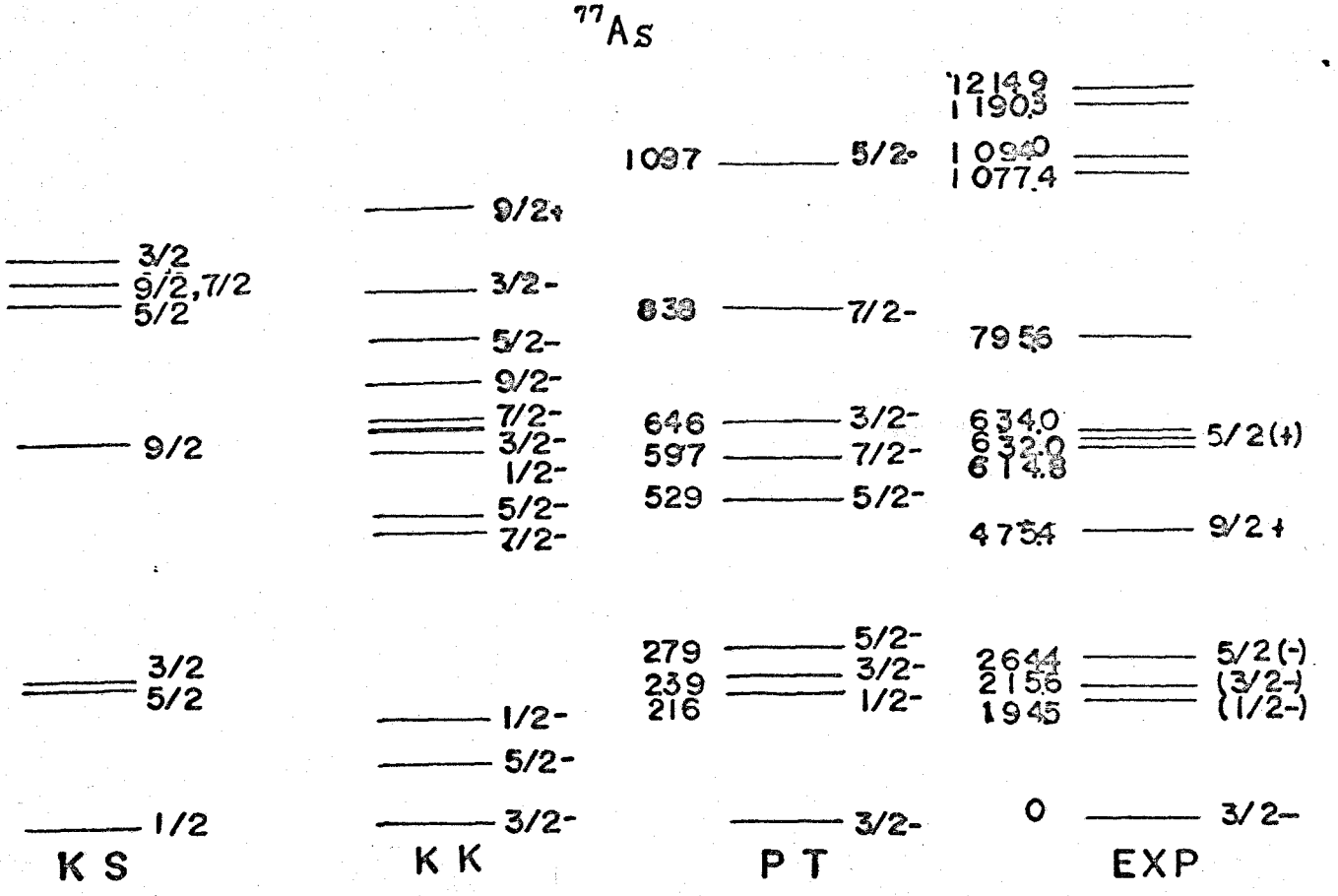

Fig. 5-12. Comparison of the theoretical level energies in ^{77}As with those obtained by experiment (marked EXP). Present theoretical level energies (marked PT) are obtained for $\eta = 6$ and $\frac{\hbar^2}{2\vartheta} = 60$ keV. Previous theoretical works done by Kisslinger and Sorensen and by Kisslinger and Kumar are marked KS and KK, respectively.

Therefore the theoretical treatment is done similarly to ^{77}As. These are shown in Figs. 5-13 and 5-14. However, η = 2.7 and $\frac{\hbar^2}{2\mathcal{J}}$ = 60 keV are temporarily adopted in order to reproduce the closely observed levels near 70 keV excitation energy.

iv) ^{71}As nucleus

The ground state is known to be (5/2 -), which suggests η smaller than 2.5 according to the present model. Further information cannot be derived because the experimental data are scanty.

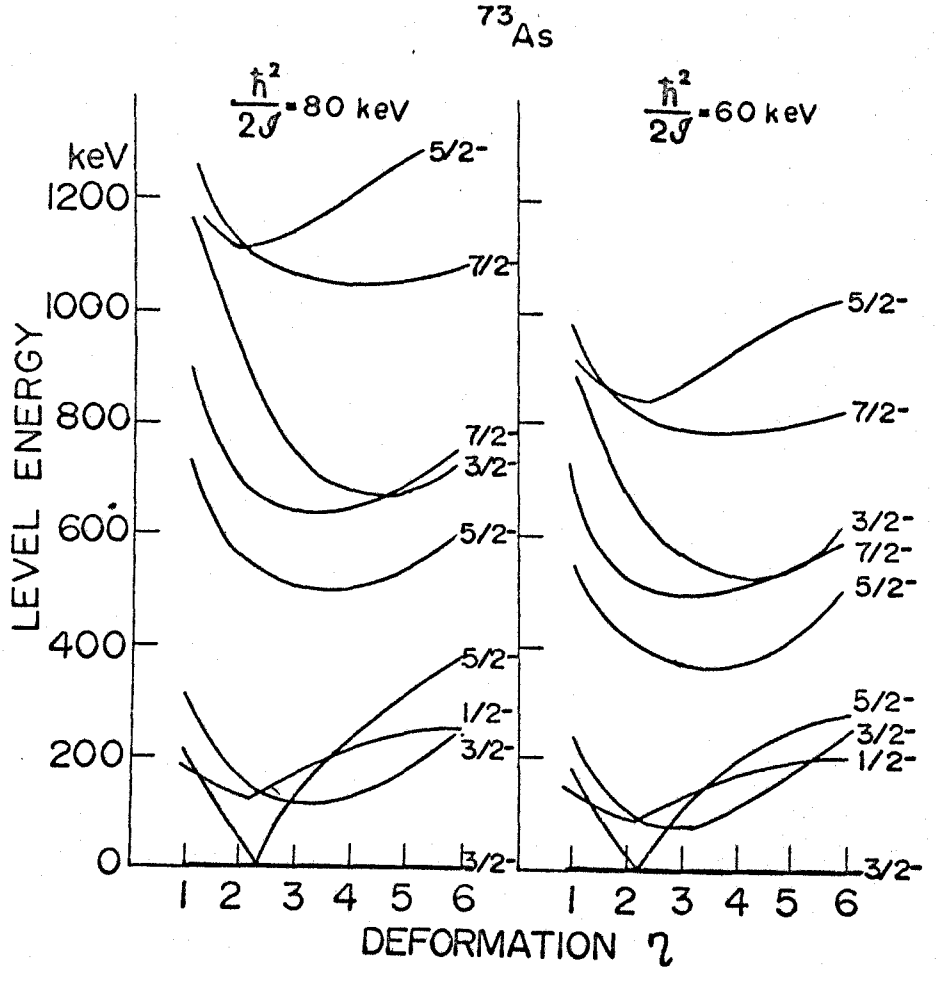

Fig. 5-13. The calculated odd-parity level spectra in ^{73}As as a function of deformation for different rotational constants.

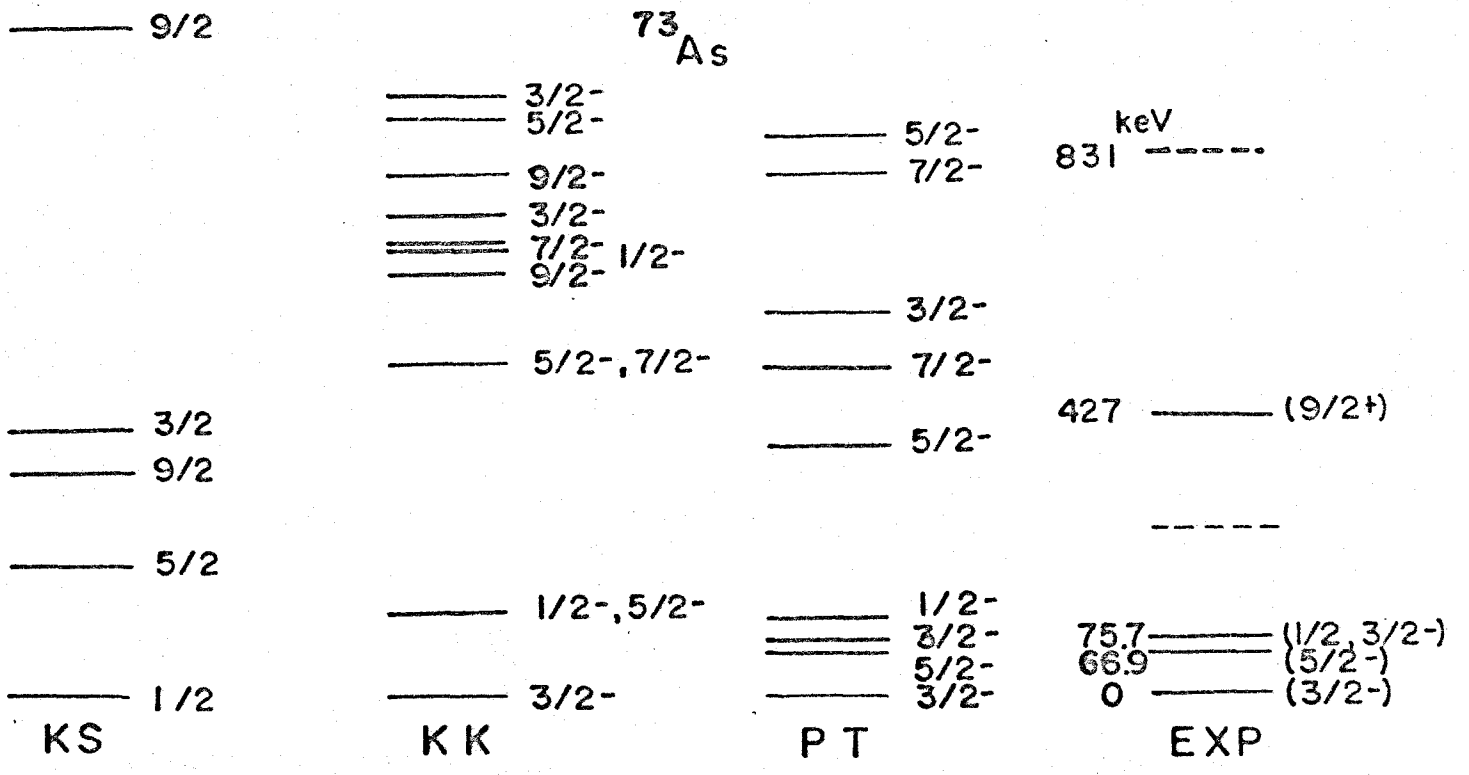

Fig. 5-14. Same as Fig. 5-12 but in ^{73}As for η = 2.7 and $\frac{\hbar^2}{2\mathcal{J}}$ = 60 keV.

5-3. Bromine Isotopes

5-3-1. Compilation of experimental data

i) ^{79}Br nucleus

The level scheme of this nucleus has been investigated precisely by various methods. Thulin (Th55) and Bonacalza (Bo64) have studied $\overset{it}{\wedge}$ using the decay of ^{79}Kr, and Robinson, McGowan, Stelson and Milner (Ro67a) through the Coulomb excitation experiment. The resonance fluorescence method has been applied by Langhoff, Frevert, Schott and Flammersfeld (La66). Referring to these works, we summarize the low-lying odd-parity levels. The level spectrum of the ^{79}Br nucleus are shown in Fig. 5-15.

a) Ground state.....I^{π} = 3/2 - is determined by the atomic beam method (ND66b).

b) 217.2 keV level.....The angular distribution of the 217.2 keV gamma ray following Coulomb excitation establishes I^{π} = 5/2 -.

c) 261.4 keV level.....The log ft value of 6.1 from the 1/2 - ground state of ^{79}Kr to this level indicates I = 1/2 or 3/2. The intensity ratios of the K, L and M conversion electrons observed by Thulin lead to the fact that the 43 keV transition (261.4 → 217.2 keV) has a M1 character. Thus the spin and parity of 3/2 - are concluded.

d) 306.7 keV level.....The positon decay of ^{79}Kr to this level which has log ft = 7.3 and the angular distribution of the 307.7 keV gamma ray following Coulomb excitation are consistent with I^{π} = 1/2 - or 3/2 -.

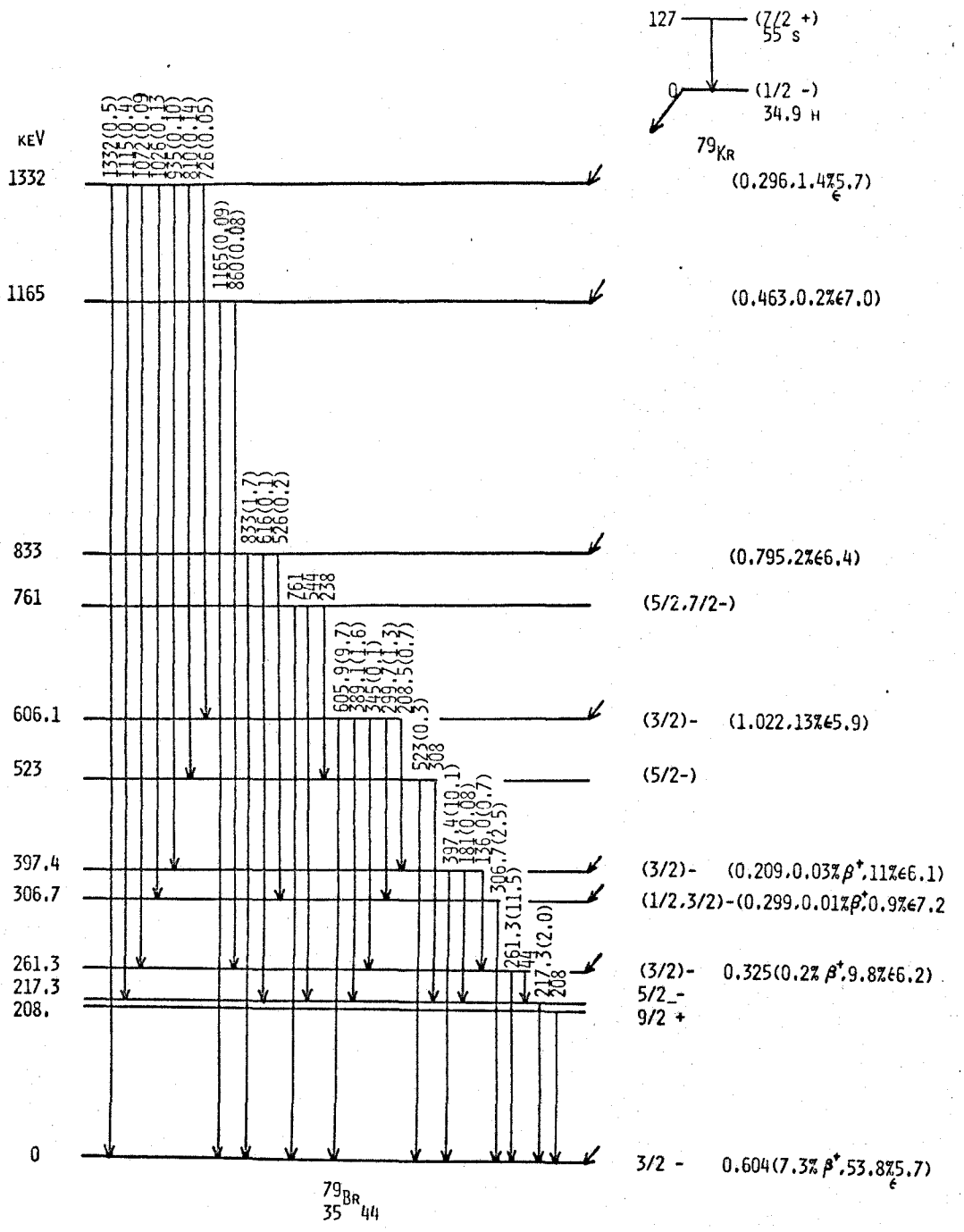

Fig. 5-15. The experimental level spectrum in ^{79}Br (ND66b).

e) 397.4 keV level.....From the similar positon decay observation M1 character of the 135.7 and 181 keV transitions and Coulomb excitation are consistent with $I^{\pi} = 3/2 -$.

f) 605.9 keV level.....The M1 character of the 389.1 keV (605.9 $\rightarrow$ 217.2 keV) radiation, the log ft value of 5.9 for the electron capture decay to this level and the angular anisotropy of the 605.9 keV gammas are all consistent with $I^{\pi} = 3/2 -$.

g) 761.2 keV level.....This level is not observed in the decay of ^{79}Kr and the 761 keV radiation following Coulomb excitation has a large anisotropy. These facts indicate the spin of this level 5/2 or 7/2 and parity odd.

h) 831.6 keV level.....From the log ft value of 6.3, it is considered I = 1/2 or 3/2. The transition characters from this level prefer the spin 3/2.

ii) ^{81}Br nucleus

The level spectrum of ^{81}Br has been investigated by several authors, through the studies of ^{81}Se negaton decay, Coulomb excitation of ^{81}Br and the nuclear reactions of (γ, γ') and (^{3}He,d). However, there exist considerable discrepancies in the determination of the level positions, as seen in Table 5-2.

5-3-2. Theoretical calculations of level spectra

i) ^{79}Br nucleus

Table 5-2. Observed levels in ^{81}Br.

keV

Evans (Ev67)	Ythier et.al. (Yt60)	Kuroyanagi (Ku60)	Rao et.al. (Ra67)	Prawirosoehardjo (Pr67)
		170		
283	282	275	276 (5/2 -)	276 (5/2 -)
		410		
	450	480		
546	545		539 (5/2-,7/2-)	
		550		
	565		566 (3/2 -)	566. (3/2 -)
665	653	650		650
		690		
804	820			815
841		840	829 (1/2-,3/2-)	829 (1/2-,3/2-)
1122				1146
1203				
			gnd 3/2 -	

Among bromine isotopes the level scheme of this nucleus is well established, as described in the previous subsection. Therefore, we can carry out a least-squares fit to ^{79}Br, just similarly to ^{75}As. Figs. 5-16-a and b give the level spectra as a function of deformation for different rotational constants, the former being treated without Coriolis interaction and the latter with that interaction, respectively.

The wave functions obtained simultaneously are also shown schematically in Fig. 5-17. In this calculation, five Nilsson orbitals of No. 15, 16, 19, 20 and 26 are taken into consideration. As known from these figures, for smaller values of η the ground state spin is predicted to be 5/2 -, and generally for $\eta > 6$ the 3/2 - state is most lowered in this calculation. For smaller value of rotational constant, however, this feature is a little more complicated.

In ^{79}Br, there does not exist as clear grouping of levels as do in ^{75}As, which is quite consistent with the experimental level scheme. The level order changes rapidly with the deformation and slightly with the rotational constant, but the level spacing depends strongly on both of them. Figs. 5-18-a, b and 5-19 show the level spectra rewritten from Figs. 5-16-a, b and 5-17.

The best agreement with the experiment is obtained by choosing $\eta = 7.5$ and $\frac{\hbar^2}{2\vartheta} = 60$ keV. The calculated level scheme as well as the experimental levels are presented in Fig. 5-20. The predicted levels by Kisslinger and Sorensen

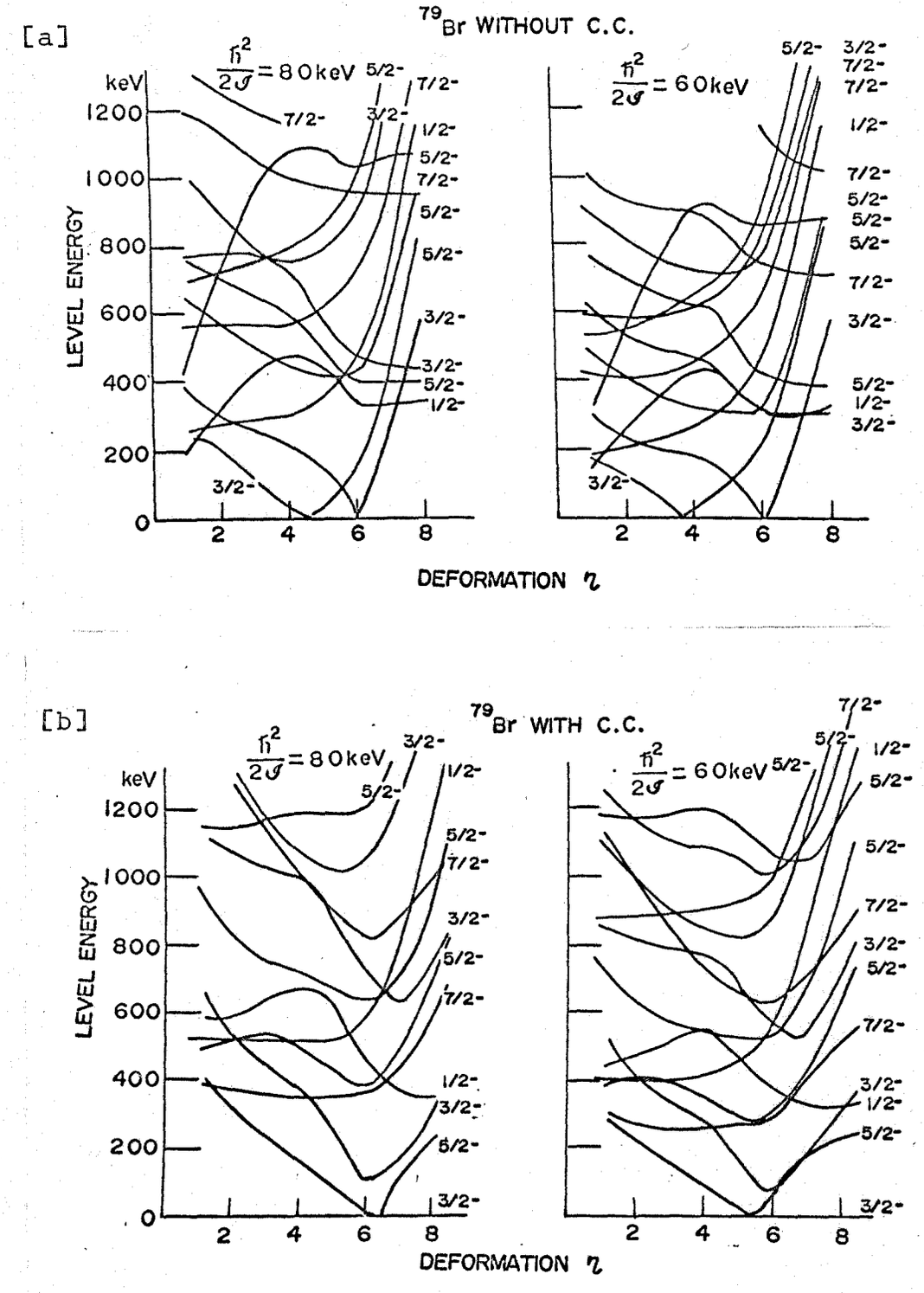

Fig. 5-16. The calculated odd-parity level spectra in ^{79}Br as a function of deformation for different rotational constants. These spectra are calculated without [a] and with [b] Coriolis interaction.

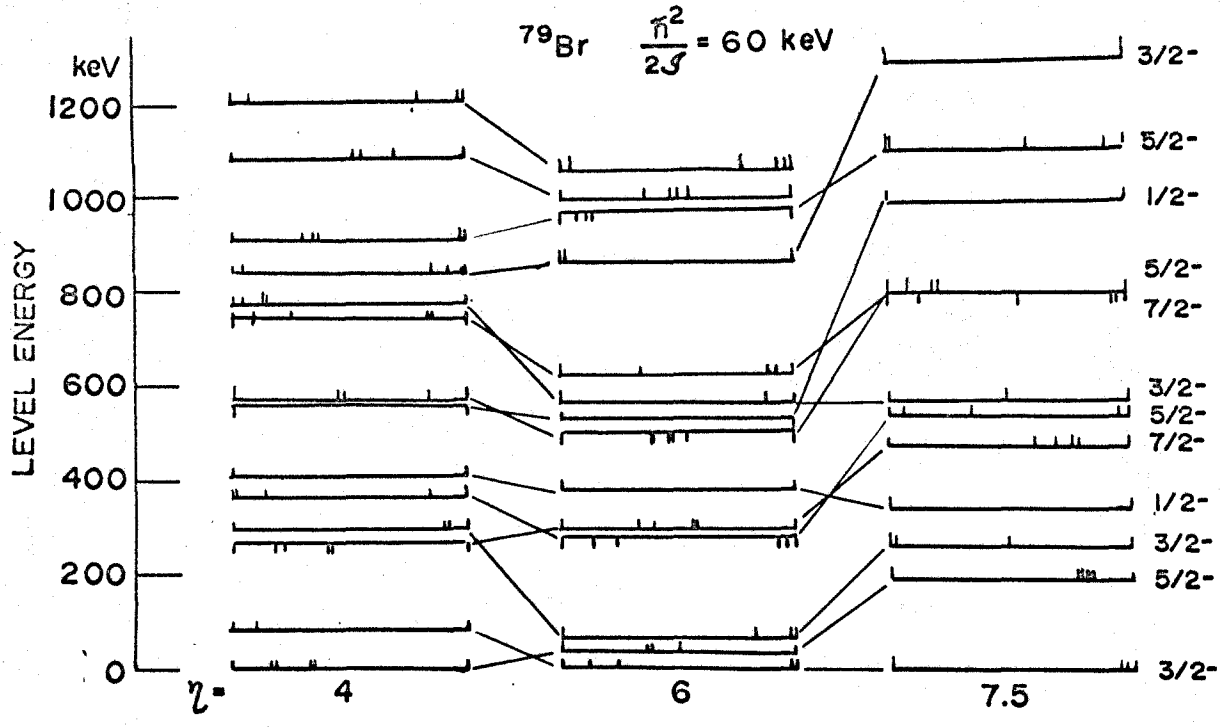

Fig. 5-17. The wave functions for levels in ^{79}Br for some combinations of deformation and rotational constant. The width between two adjacent verticals denotes the amplitude of each K band. The order of K bands is as follows:

No. 16 20 19 26 15 for I = 5/2 and 7/2,

No. 16 20 19 26 for I = 3/2

and

No. 20 26 for I = 1/2.

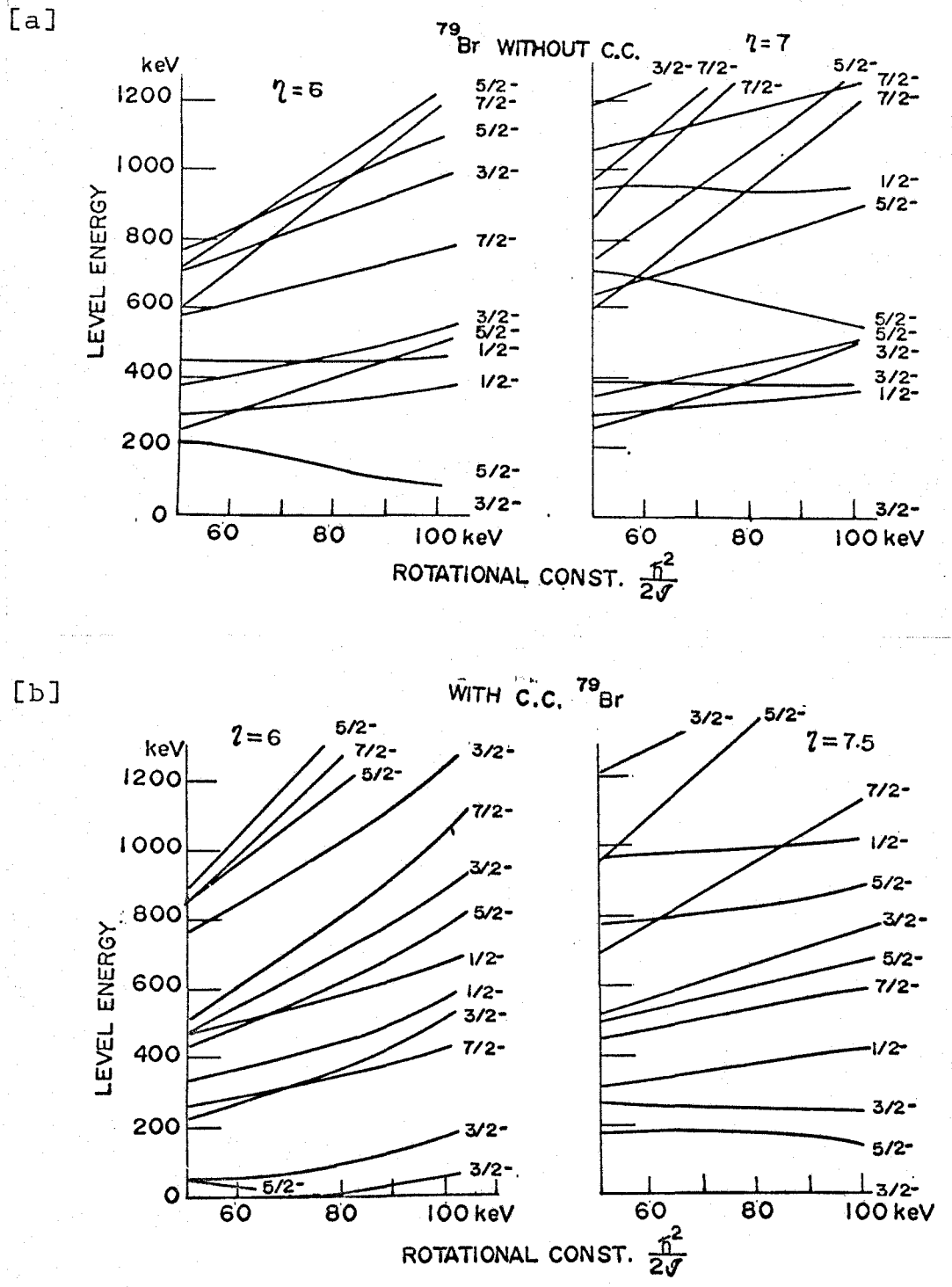

Fig. 5-18. The calculated odd-parity level spectra in ^{79}Br as a function of rotational constant for different deformations. These spectra are calculated without [a] and with [b] Coriolis interaction.

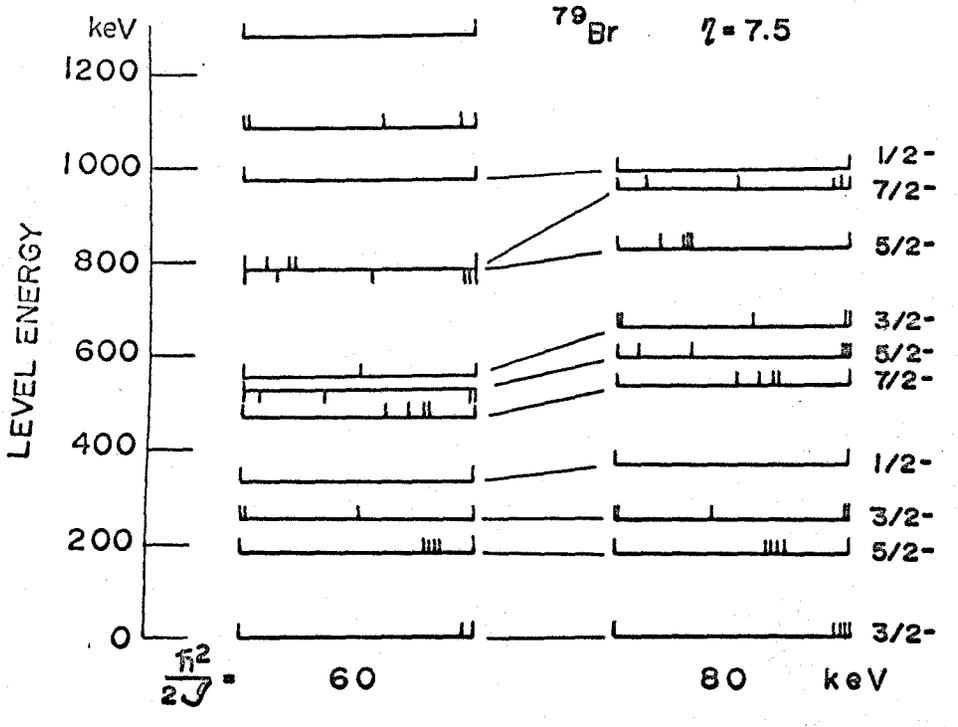

Fig. 5-19. Same as Fig. 5-17.

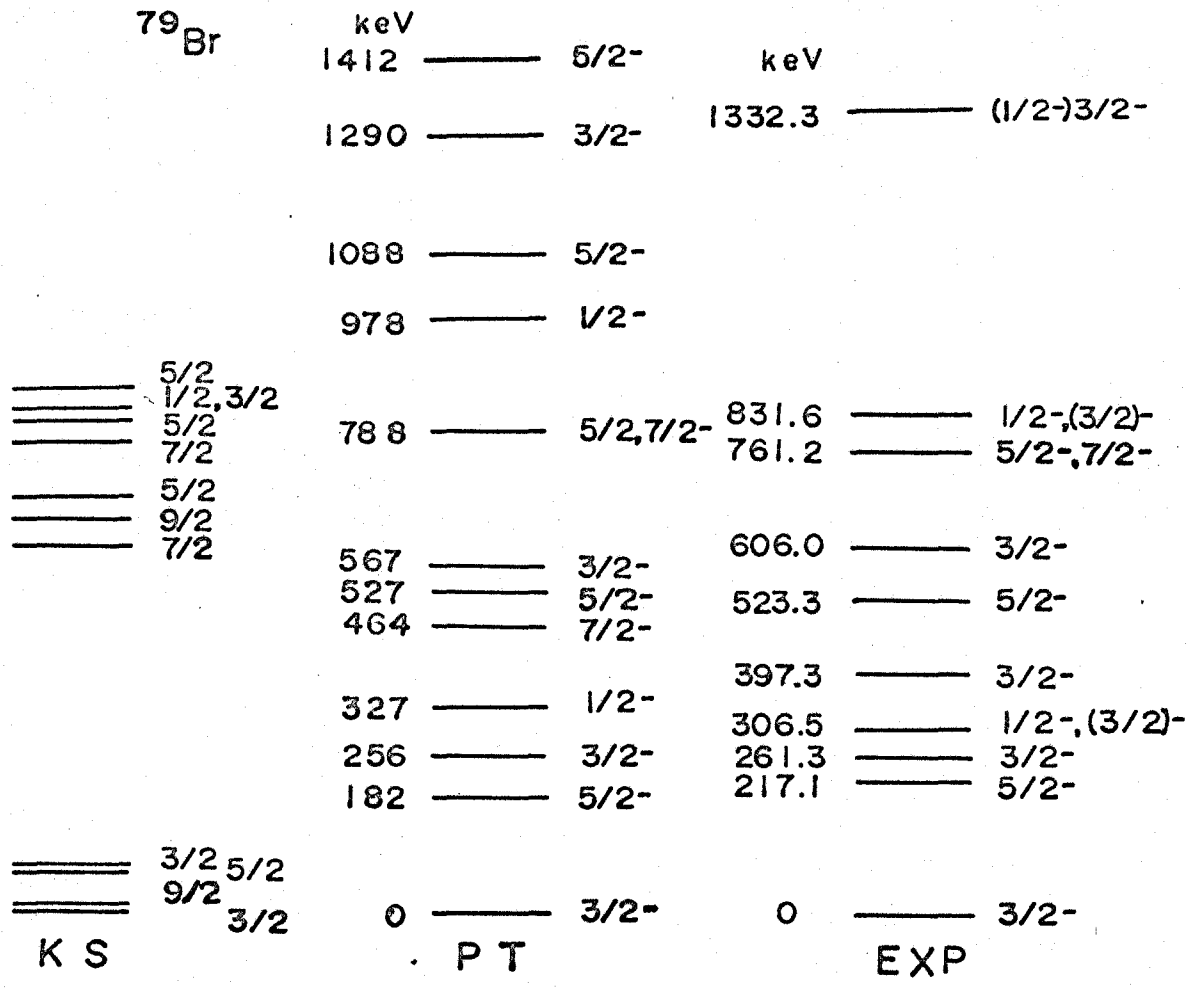

Fig. 5-20. Comparison of the theoretical level energies in ^{79}Br with those obtained by experiment (marked EXP). Present theoretical level energies (marked PT) are obtained for η = 7.5 and $\frac{\hbar^2}{2\vartheta}$ = 60 keV. Previous theoretical work done by Kisslinger and Sorensen is marked KS.

(Ki63) are also shown in the figure, but seems inadequate as already pointed out by them. According to the simple shell model, the ground state spin of ^{79}Br is 5/2, which is inconsistent with the experiment.

The present theory predicts the correct ground state spin and explains rather well the locations and the order of the excited states. In ^{75}As, the low-lying 1/2 -, 3/2 - and 5/2 - states seem to compose an apparent triplet. The similar feature is also seen in the same spin levels of ^{79}Br, but not so clear as in ^{75}As and the spin order are reversed. This feature is clearly reproduced by the present theory. Other higher states are fitted well as follows:

experimental		theoretical	
606 keV	(1/2-) or 3/2-	567 keV	3/2-
834	1/2- or (3/2-)	978	1/2-
1332	3/2- or (1/2-)	1290	3/2-.

The fitness between the experimental and the theoretical level locations is about 20 keV in the root mean square deviation.

The selected rotational constant $\frac{\hbar^2}{2\mathcal{J}}$ = 60 keV is equal to the value of ^{75}As. The nearest doubly-even nuclei, i.e. ^{78}Se and ^{80}Kr, have values of about 100 keV. In the well known deformed regions, the constants for odd-mass nuclei are generally smaller than those for the nearest doubly-even nuclei, with which the present model value is compatible.

The ground state is mainly composed of 96 % $|312\rangle$ and 3 % $|310\rangle$. The wave functions of other states are presented in Table 5-3, and these are used in Chap. 6 for explaining the electric properties. The ground state electric quadrupole moment is also calculated in the same chapter, using the obtained value of deformation η.

ii) ^{81}Br nucleus

As is pointed out in the previous subsection, the level scheme of ^{81}Br nucleus has not been established. Therefore we present only the level positions as a function of η for the most probable rotational constant, instead of trying a least-squares fitting procedure. This is given in Fig. 5-21.

iii) ^{77}Br nucleus

The calculated level spectrum for $\eta = 7.5$ and $\frac{\hbar^2}{2\mathcal{J}} = 60$ keV is presented in Fig. 5-22.

Table 5-3. Energies, spins and amplitudes of ^{79}Br odd-parity levels calculated for $\eta = 6$ and $\frac{\hbar^2}{2\vartheta} = 60$ keV.

Energy (keV)	Spin Parity	Eigenfunction $\|3\frac{3}{2}12\rangle$	$\|3\frac{1}{2}10\rangle$	$\|3\frac{3}{2}01\rangle$	$\|3\frac{1}{2}01\rangle$	$\|3\frac{5}{2}03\rangle$
0	3/2 -	0.98	-0.16	0.05	-0.08	0.
182	5/2 -	0.89	0.17	0.13	0.12	0.39
256	3/2 -	0.15	0.69	-0.70	-0.04	0.
327	1/2 -	0.	1.	0.	0.	0.
464	7/2 -	0.72	-0.32	0.24	-0.10	-0.45
527	5/2 -	-0.24	0.53	0.80	-0.11	0.09
567	3/2 -	0.08	0.70	0.71	0.03	0.
785	7/2 -	0.38	0.65	-0.64	-0.11	-0.12
788	5/2 -	-0.31	-0.32	0.	-0.09	0.89
978	1/2 -	0.	0.	0.	1.	0.
1088	5/2 -	-0.17	0.77	-0.57	0.03	0.23
1290	3/2 -	0.08	-0.	-0.05	0.996	0.

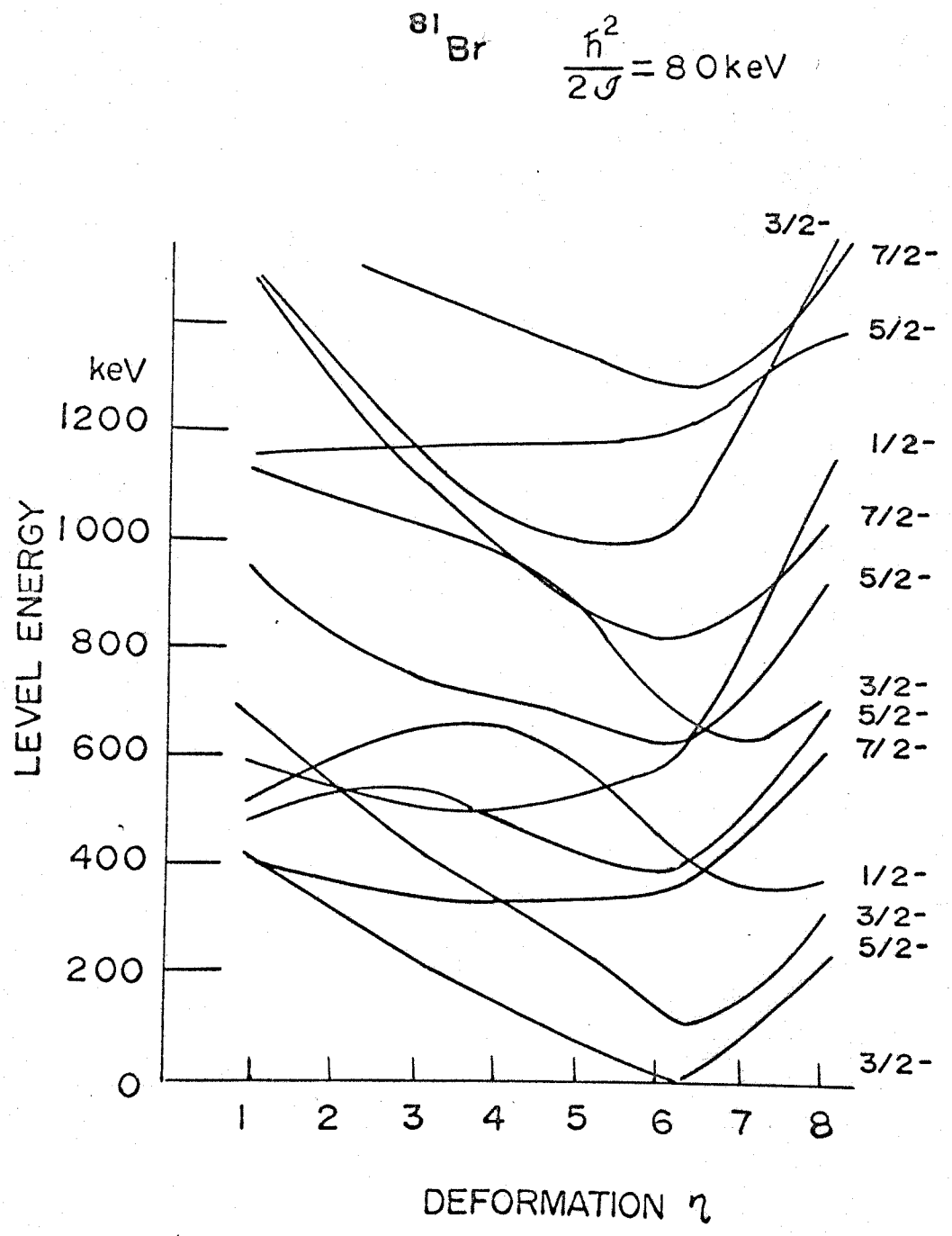

Fig. 5-21. The calculated odd-parity level energies in ^{81}Br as a function of deformation for $\frac{\hbar^2}{2\mathcal{I}}$ = 80 keV. These are calculated with Coriolis interaction.

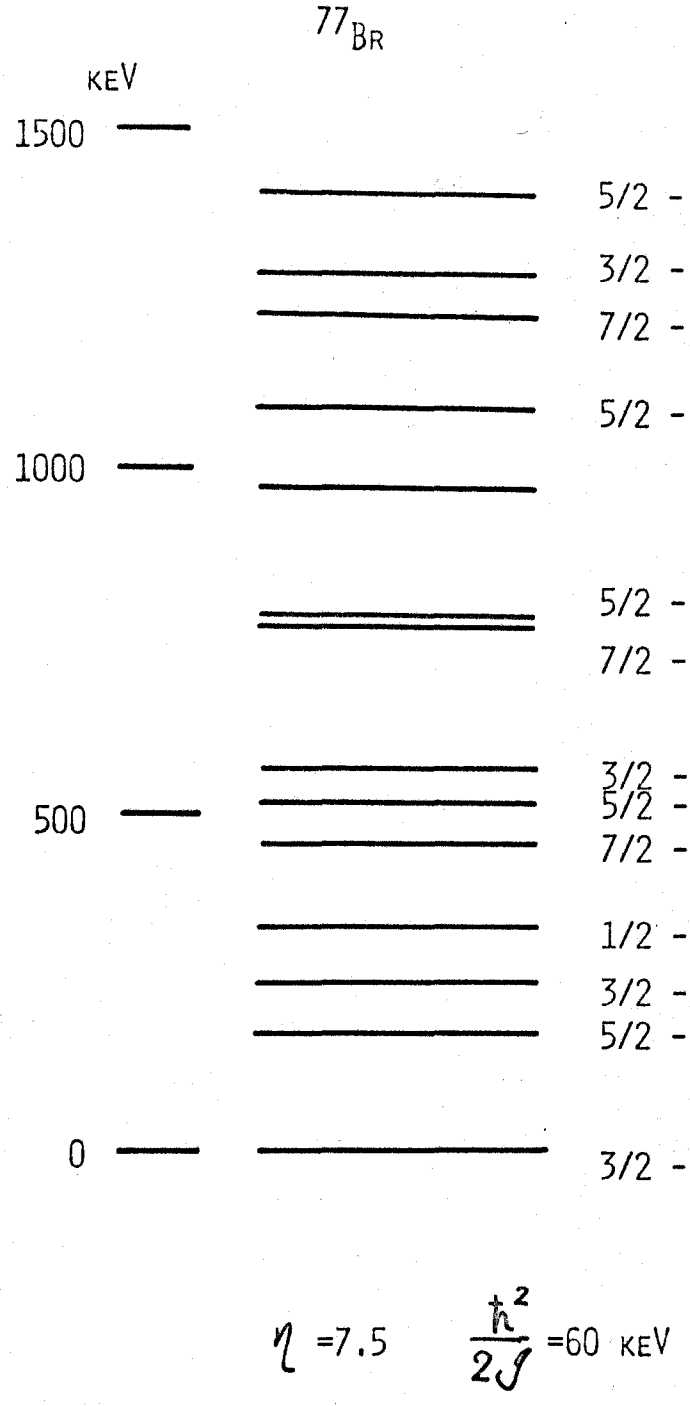

Fig. 5-22. The tentatively calculated spectrum in ^{77}Br nucleus (η = 7.5 and $\frac{\hbar^2}{2\mathcal{J}}$ = 60 keV).

5-4. Rubidium Isotopes

5-4-1. Compilation of experimental data

i) ^{83}Rb nucleus

The nuclear structure of this isotopes has been scantly investigated experimentally and theoretically. Very recently however, the level structure of the ^{83}Rb nucleus has been proposed by Etherton, Beyer, Kelley and Horen (Et68)through the study of ^{83}Sr decay as shown in Fig. 5-23. They used a Ge(Li) detector and a magnetic spectrometer. By that time only the preliminary investigations were done by several authors (Ku61,Ma62,Re64). We reproduce here the level properties mainly according to Etherton et al.

a) Ground state.....The spin has been determined as 5/2 by an atomic beam method (ND66c). The odd-parity is compatible with the magnetic moment.

b) 5 keV level.....Neither photons nor conversion electrons are not detected directly in the transition to the ground state. However, without this level, the decay scheme consistent with the experimental data would not be constructed. The E1 character of the 418.6 keV transition (423.5 $\longrightarrow$ 5.0 keV) implies that the 5.0 keV has negative parity with spin 3/2 or greater, but less than 9/2. From the relative intensities between the 37.3 keV photons and the 42.3 keV photons, I^{π} = 3/2 - is very plausible for the 5.0 keV level.

c) 295.2 keV level.....The M1 + E2 mixing nature of the 290.2 keV radiation (295.2 $\longrightarrow$ 5.0 keV), the high log ft (>9)

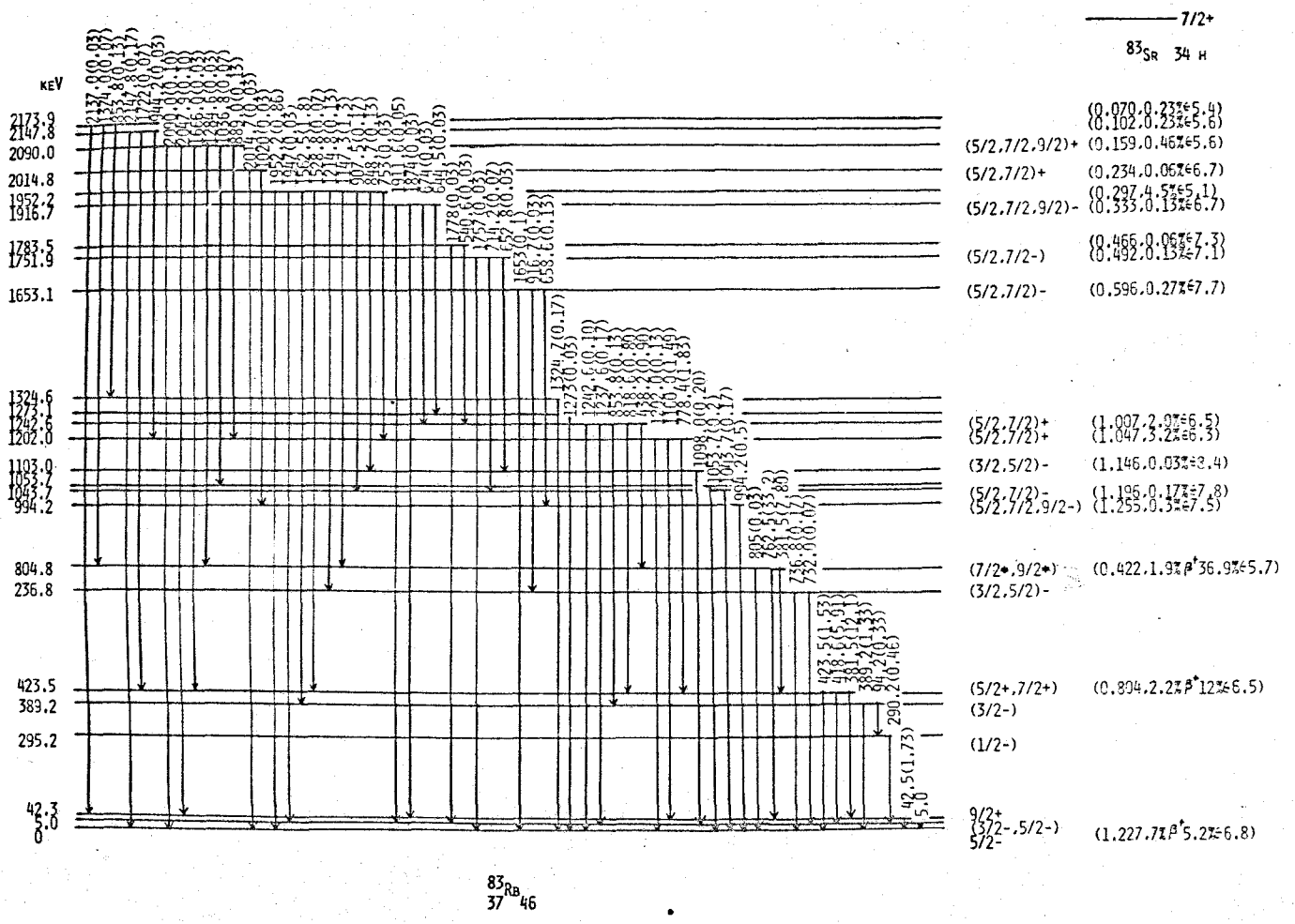

Fig. 5-23. The experimental level spectrum in ^{83}Rb (Et68).

value for the positon decay to this level, and the absence of a direct transition to the ground state and other transition to this level suggest the spin and parity of this level is 1/2 -.

d) 389.2 keV level.....Since the 389.2 keV radiation has a E2 character and the 94.0 keV radiation (389.2 $\rightarrow$ 295.2 keV) has M1 + E2 character, $I^{\pi} = 3/2$ - is reasonable for this level.

e) higher levels.....The suggested locations, spins and parities for the higher levels are presented in Fig. 5-23.

5-4-2. Theoretical calculations of level spectra

i) ^{83}Rb nucleus

As the isotope masses increase the neutron number in the rubidium isotopes approaches to the magic number 50, and the deformation would probably decrease. Then among the rubidium isotopes, ^{81}Rb and ^{83}Rb would be profitable in testing the present theory. Unfortunately the nuclei other than ^{83}Rb have been scantly investigated experimentally and the calculation is applied only to the ^{83}Rb nucleus. In this calculation, five Nilsson orbitals of Nos. 15, 16, 19, 20 and 26 are considered in order to reproduce the low-lying states.

Similarly to the previous nuclei, Fig. 5-24-a gives an example of the calculated level spectra when the deformation changes for the fixed rotational constant of $\frac{\hbar^2}{2\mathcal{J}}$ = 60 keV. As seen from this figure, the ground state spin is predicted

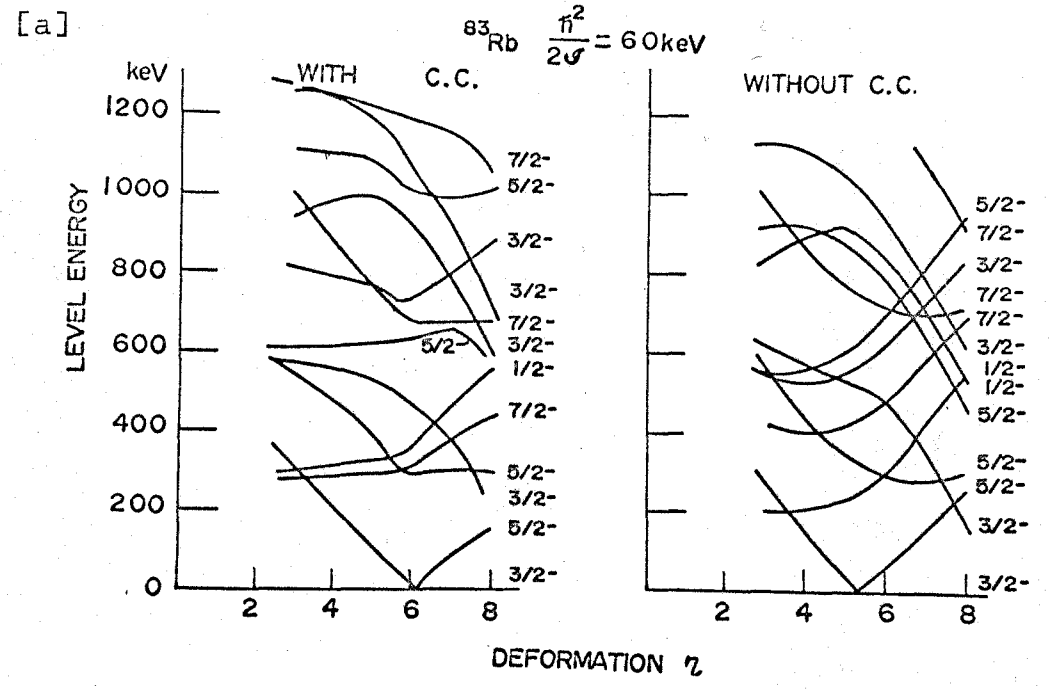

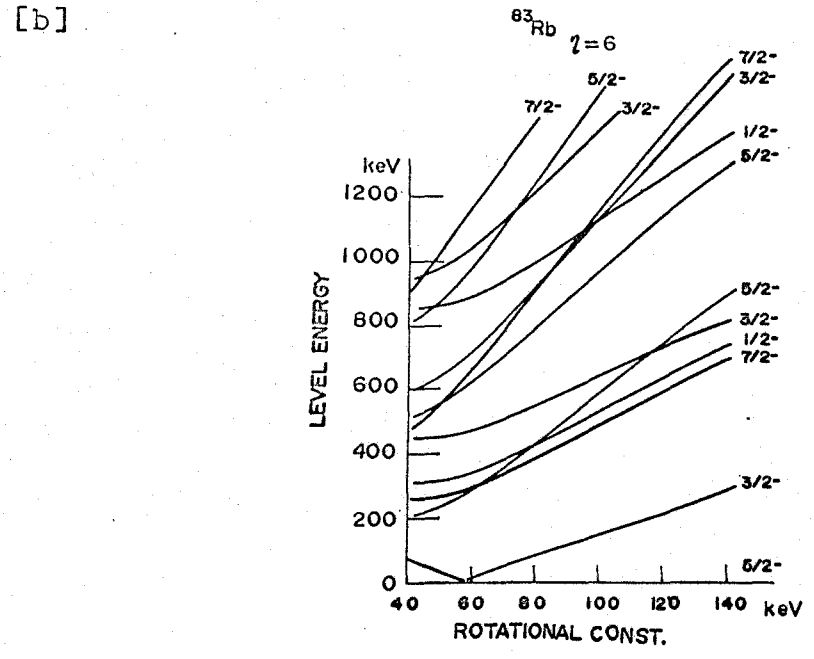

Fig. 5-24. The calculated odd-parity level spectra in ^{83}Rb as a function of deformation for $\frac{\hbar^2}{2\mathcal{J}}$ = 60 keV [a] and a function of rotational constant for η = 6 [b].

to be 5/2 - for the smaller value of η, and the 3/2 - state is greatly lowered when $\eta > 6$. The simple shell model predicts only $f_{5/2}$ for the ground state. Fig. 5-24-b shows the level spectra for $\eta = 6$ as a function of a rotational constant. The 3/2 - and 5/2 - states cross at about $\frac{\hbar^2}{2\mathcal{I}}$ = 60 keV.

One of the clearest nature of the experimental level scheme is that the 3/2 - level locates at only 5 keV above the 5/2 - ground state. This is distinctly reproduced by the present theory for a set of parameters, $\eta = 6$ and $\frac{\hbar^2}{2\mathcal{I}} = 60$ keV. Using these parameters, the odd-parity levels are calculated and compared with the experimental ones, as shown in Fig. 5-25. The calculated levels with lower spin values are fitted very well to the observed ones within about 40 keV deviation, but the levels with higher spin (7/2) are not found in the lower energy part of the experimental level scheme.

ii) ^{81}Rb nucleus

The calculated spectrum for $\eta = 7$ and $\frac{\hbar^2}{2\mathcal{I}} = 60$ keV is presented in Fig. 5-26.

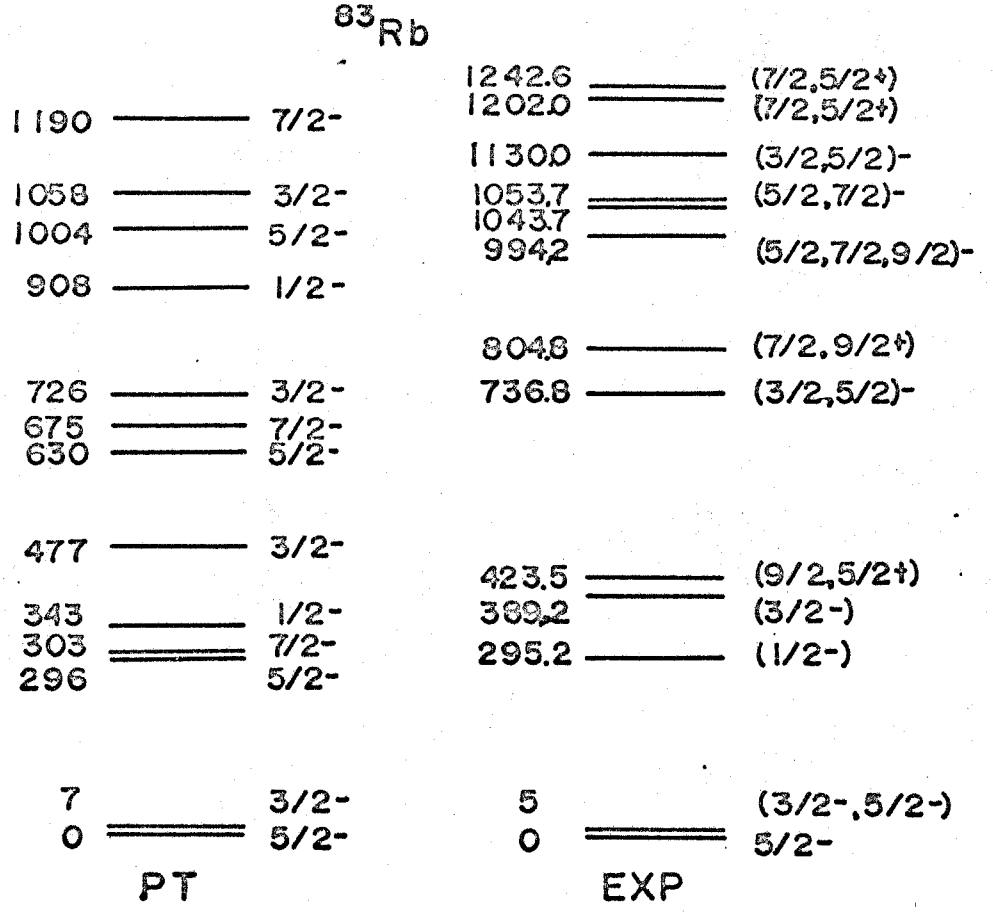

Fig. 5-25. Comparison of the theoretical level energies in ^{83}Rb with those obtained by experiment (marked EXP). Present theoretical level energies (marked PT) are obtained for $\eta = 6$ and $\frac{\hbar^2}{2\mathcal{J}} = 60$ keV.

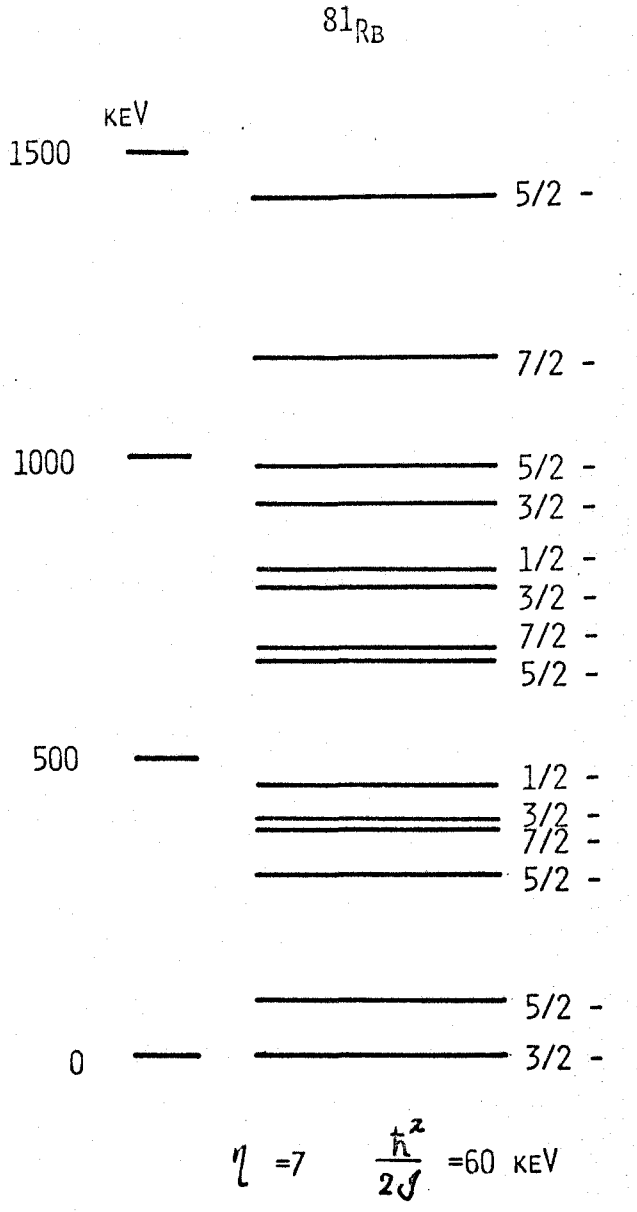

Fig. 5-26. The tentatively calculated spectrum in ^{81}Rb nucleus (η = 7 and $\frac{\hbar^2}{2\mathcal{J}}$ = 60 keV).

5-5. Scandium Isotopes

In the previous sections, we have shown that the level locations of odd-mass nuclei in the $1f_{5/2}$-$2p_{3/2}$ shell are well interpreted by the present model. In this section, we apply this model to other shell nuclei whose level structures have been hardly predicted from the theoretical point of view. As examples, we calculate the energy levels of ^{45}Sc and ^{47}Sc nuclei.

5-5-1. Compilation of experimental data

i) ^{45}Sc nucleus

The locations and other properties of levels of this nucleus have been investigated by many authors, mainly using the nuclear reactions. The informations are given by Schwartz and Alford (Sc66) with ^{44}Ca(^{3}He,d)^{45}Sc, by Yntema and Sachler (Yn64) with ^{45}Ti(p,α)^{45}Sc, by Buechner, Mazari and Revista (Bu58) with ^{45}Sc(p,p')^{45}Sc and by Bjerregaard, Hansen and Sidenius (Bj64) with ^{47}Ti(d,α)^{45}Sc reactions. Quite recently, Clikeman, Roger and Beghian (Cl69) studied the gamma rays from ^{45}Sc(n,n')^{45}Sc reaction. On the other-hand, Porter, Freedman, Wagner and Orlandini (Po66) investigated ^{45}Ti(β^{+},EC)^{45}Sc decay. In the following subsection, we compile the level natures referring to the above observations. The experimental level spectrum of ^{45}Sc is presented in Fig. 5-27.

a) Ground state.....A DWBA analysis of the ^{44}Ca(^{3}He,d)^{45}Sc

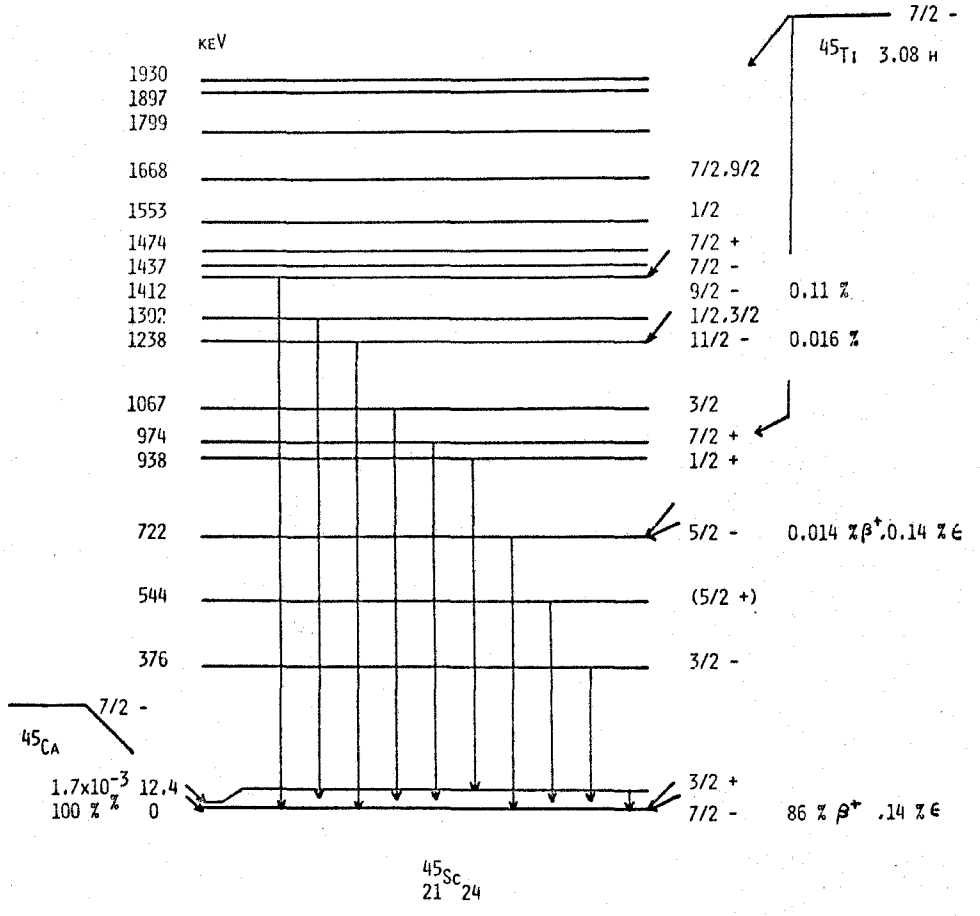

Fig. 5-27. The experimental level spectrum in ^{45}Sc.

reaction indicates the ground spin and parity to be 7/2 -.

b) 376 keV level.....This level is found by a p-wave transition in the $^{44}Ca(^{3}He,d)^{45}Sc$ reaction and by the Coulomb excitation with Nitrogen ions. These facts show that this level has the spin and parity of 3/2 -.

c) 725.1 keV level.....This level is fed by the positon decay of ^{45}Ti with log ft = 6.3, and the spin and parity of this level is 5/2 -, 7/2 - or 9/2 -. From the (n,n') reaction, this level is confirmed as I^{π} = 5/2 -.

d) 1238 keV level.....The spin and parity of 11/2 - is assigned through the studies of the EC decay of ^{45}Ti and the (n,n') experiment.

e) 1411 keV level.....From the similar investigations to the 1238 keV level, I^{π} = 9/2 - is concluded.

f) 1437 keV level.....The spin and parity of 7/2 - is supported by the study of the (n,n') reaction.

ii) ^{47}Sc nucleus

The level energies and other properties of the nucleus have been investigated using the nuclear reactions and the ^{47}Ca negaton decay. Schwartz, Alford and Marinor (Sc67b) observed the $^{46}Ca(^{3}He,d)^{47}Sc$ reaction and Yntema and Sachler (Yn64) the $^{48}Ca(d,^{3}He)^{47}Sc$ reaction. The reactions ^{48}Ti (t,α), $^{49}Ti(d,\alpha)$ and $^{50}Ti(p,\alpha)$ have been reported by Schwartz (Sc67a), Bjerregaard et al. (Bj64) and Plendl, Defelice and Sheline (Pl65), respectively. They were also invest-

gated by $^{47}Ca(\beta^-)^{47}Sc$ decay (Fr63). These results are presented in Fig. 5-28.

a) Ground state.....From the angular momentum transfer in the (^{3}He,d) and (d,^{3}He) reactions and from the spectroscopic studies, I^π of this state may be assigned 7/2 -.

b) 807.6 keV level.....The above two reactions, the gamma-gamma angular correlation and the polarization-correlation experiments support I^π = 3/2 -.

c) 1296.6 keV level.....The spin and parity of 5/2 - is obtained through the gamma-gamma and polarization measurements. The beta-gamma circular polarization-correlation experiment also supports this conclusion.

5-5-2. Theoretical calculations of level spectra

i) ^{45}Sc nucleus

Six levels of odd-parity have been established below 1.5 MeV excitation, as summarized in subsection 5-5-1. In this section we carry out a least-squares fitting procedure to this isotope. Fig. 5-29-a gives the level spectra as a function of deformation η for different rotational constants $\frac{\hbar^2}{2\mathcal{J}}$. These are the spectra calculated with Coriolis coupling.

The lower 7/2 state belonging mainly to K = 1/2 band is greatly depressed for small η value, and this is caused by the Coriolis interaction. For a large value of deformation, the 3/2 state is the lowest. Therefore,

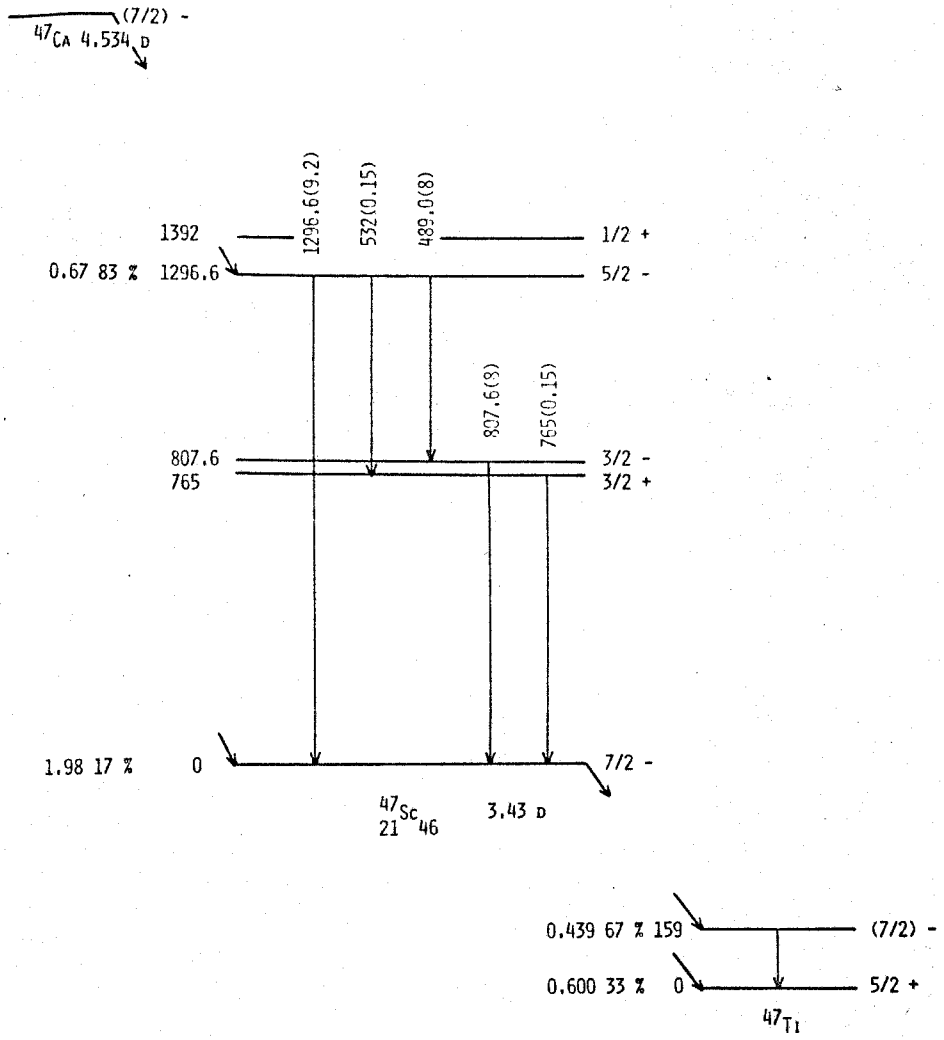

Fig. 5-28. The experimental level spectrum in ^{47}Sc (En67).

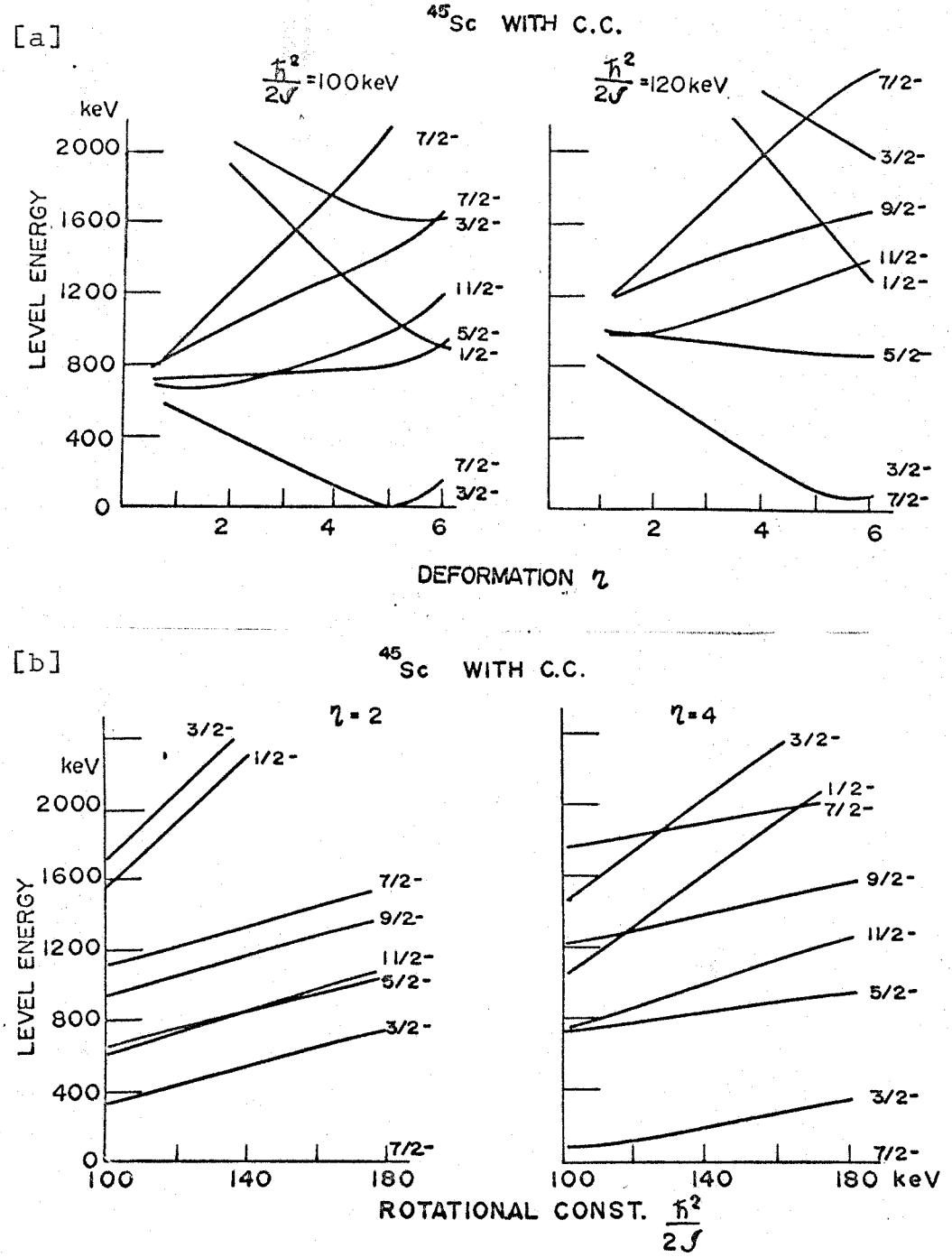

Fig. 5-29. The calculated odd-parity level spectra in ^{45}Sc as functions of deformation for different rotational constants [a] and of rotational constant for different deformations.

contrary to the nuclei of As and Br, the ground state of 7/2 - is predicted for rather small deformation. Fig. 5-29-b means that under the fixed η the level locations change monotonically with the rotational constant.

The best agreement with the experiment is obtained for $\eta = 4$ and $\frac{\hbar^2}{2\mathcal{I}} = 170$ keV. The experimental and theoretical energy levels are shown in Fig. 5-30, where the proposed spectra by other groups are also presented. One was calculated by McCullen, Bayman and Zamik (Mc64) and the other by Malik and Scholz (Ma66). McCullen et al. applied a shell model calculation to the $1f_{7/2}$ shell nuclei. They calculated the matrix of the residual interaction with respect to the states of pure $1f_{7/2}$ configuration and diagonalized it. However, they found in some cases the theoretical spectra do not always agree with the experiment. In ^{45}Sc, they predicted the first excited state at about 1.5 MeV, but experimentally many states are observed below 1.5 MeV.

Malik et al. introduced a Coriolis coupling to the $1f_{7/2}$ shell nuclei but did not consider a pairing interaction. According to their prediction, the ground and the first odd-parity excited states are well represented but the locations as well as the order of the higher excited states are not reproduced reasonably.

The present calculation reproduced better both the locations and the order of six low-lying states.

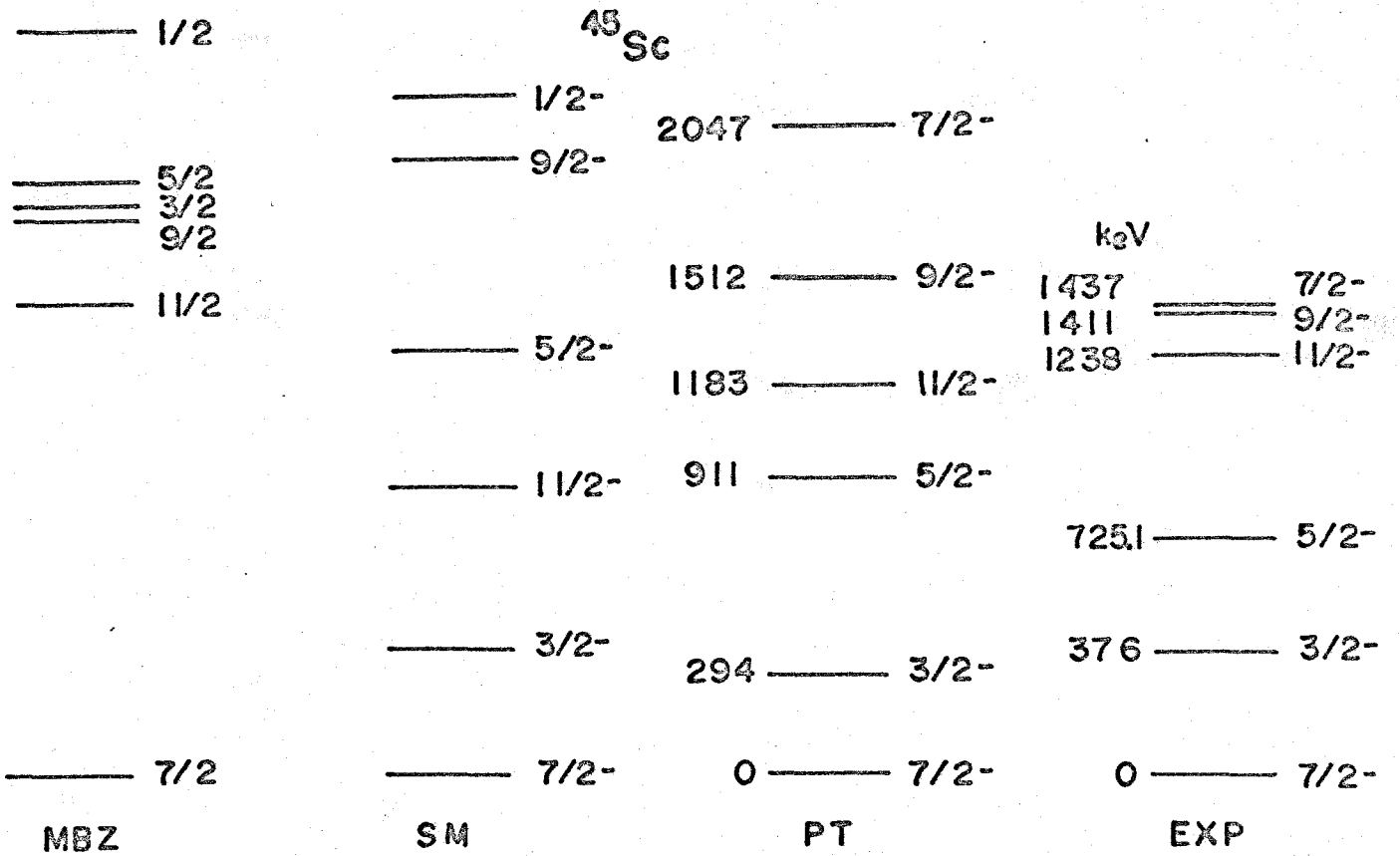

Fig. 5-30. Comparison of the theoretical level energies in ^{45}Sc with those obtained by experiment (marked EXP). Present theoretical level energies (marked PT) are obtained for $\eta = 4$ and $\frac{\hbar^2}{2\mathcal{J}} = 170$ keV. Previous theoretical works done by McCullen et al. and by Malik and Scholz are marked MBZ and SM, respectively.

The level spins of odd-parity above 0.5 MeV excitation have been recently established by the (n,n'γ) experiment. The results are consistent with our prediction. In ^{45}Sc, the level mixing due to the Coriolis interaction is quite significant, which lowers the level energies and produces a complicated arrangement of levels. These effects are predominant in our model, when compared with the original rotational bands.

ii) ^{47}Sc nucleus

Similar calculation to the ^{45}Sc nucleus is carried out for ^{47}Sc. General trend of the level energies as functions of η and $\frac{\hbar^2}{2\mathcal{J}}$ is shown in Figs. 5-31-a and b. The experimental level spacings are much larger than those for ^{45}Sc and only the three levels of odd-parity have been identified.

The best agreement is obtained for η = 3 and $\frac{\hbar^2}{2\mathcal{J}}$ = 240 keV. Considering these parameter values, the present η and $\frac{\hbar^2}{2\mathcal{J}}$ are a little less and larger than those for ^{45}Sc, respectively. This feature is reasonable, referring to the trend of both the first excited state (3/2 +) and the fitting of $1f_{7/2}$ neutron shells.

In Fig. 5-32, the theoretical level predictions by the present model, McCullen et al. (Mc64) and Malik et al. (Ma66) are presented with the experimental level scheme. The present model explains well the two excited levels of 807.6 keV 3/2 - and 1296.6 keV 5/2 -.

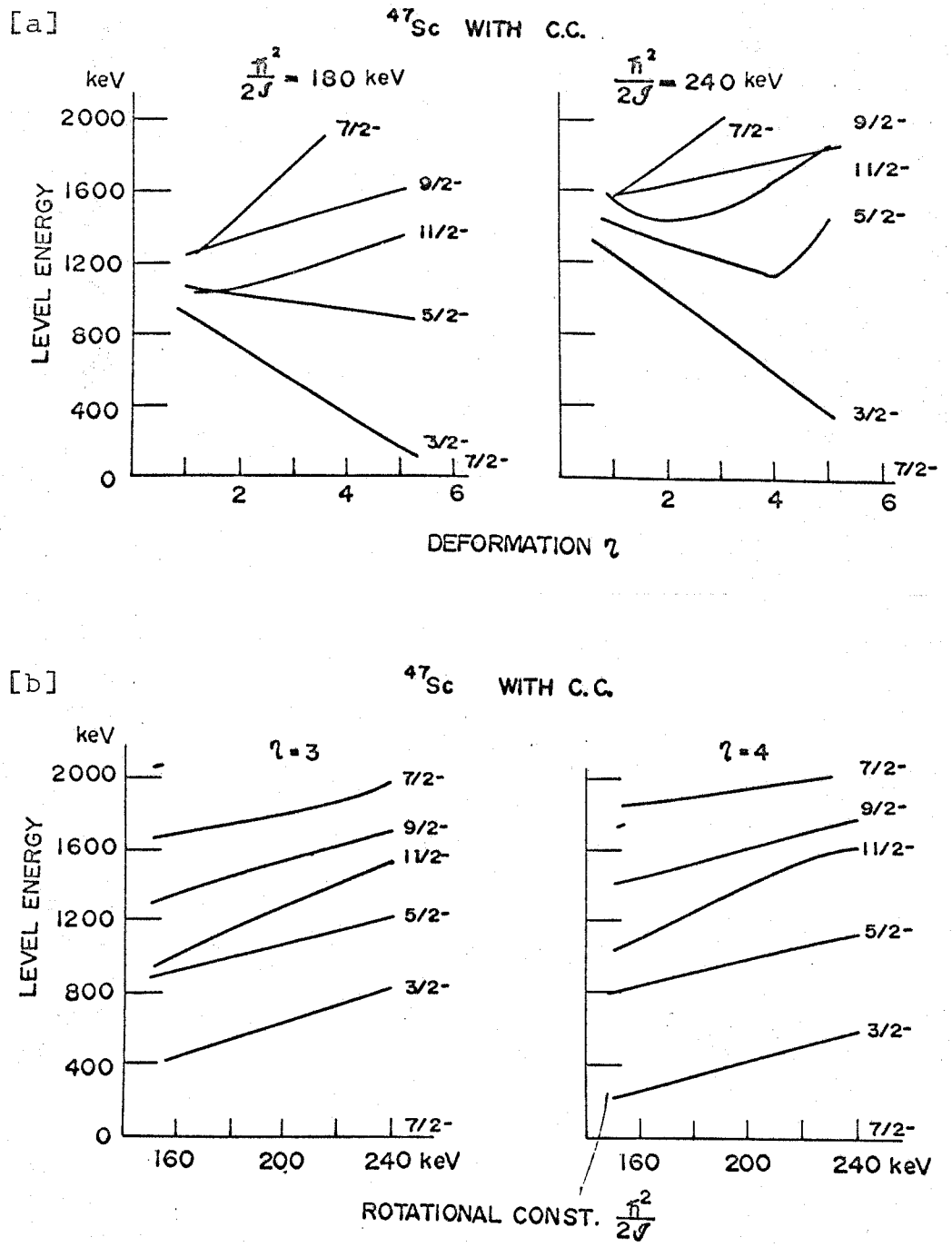

Fig. 5-31. The calculated odd-parity level spectra in ^{47}Sc as functions of deformation for different rotational constants [a] and of rotational constant for different deformations [b].

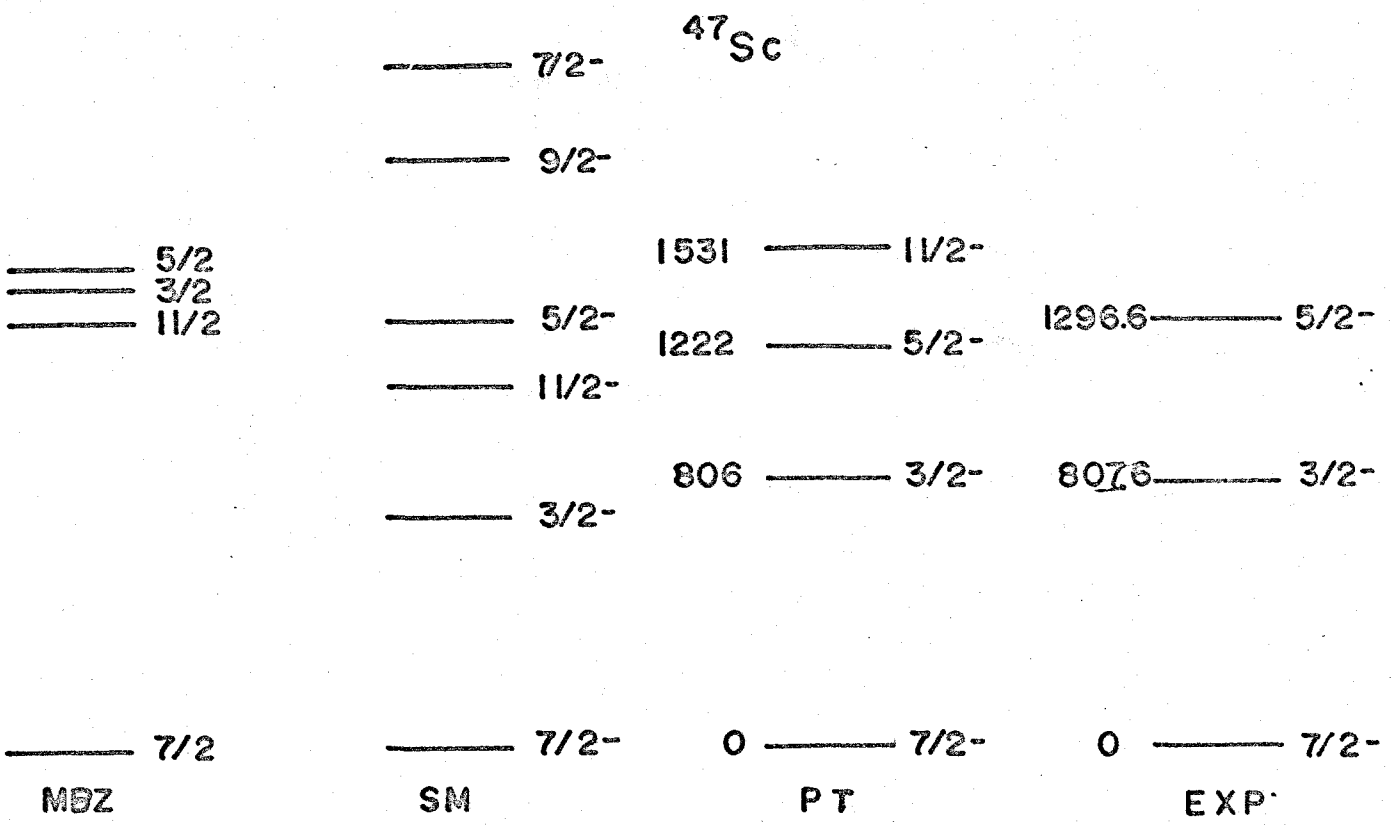

Fig. 5-32. Same as Fig. 5-30 but in ^{47}Sc for η = 3 and $\frac{\hbar^2}{2\mathcal{I}}$ = 240 keV.

5-6. Remarks on Parameters

The selected parameters of deformation η and rotational constant $\frac{\hbar^2}{2\mathcal{J}}$ are tabulated in Table 5-4. Since the rotational constant is inversely proportinal to the moment of inertia, which increases with increasing mass, the values of $\frac{\hbar^2}{2\mathcal{J}}$ for $A \sim 45$ must be far larger than those for $A \sim 75$. This feature is seen in Table 5-4.

The scandium isotopes are near to the magic number of 20 and the deformation values would be smaller than those for the other nuclei treated in this report. This is seen in the table.

The values of η for ^{73}As and ^{71}As are small when compared with those for ^{75}As and ^{77}As; this fact is easily expected, but the experimental informations about the level properties for those nuclei are very poor and so the precise measurements are expected.

Table 5-4. The selected parameters of deformation η and rotational constant $\frac{\hbar^2}{2\mathcal{J}}$.

Nucleus	^{45}Sc	^{47}Sc	^{71}As	^{73}As	^{75}As	^{77}As	^{79}Br	^{83}Rb
η	4	3	(2.5)	(2.7)	6	6	7.5	6
$\frac{\hbar^2}{2\mathcal{J}}$ keV	170	240		60	60	60	60	60

CHAPTER 6. ELECTRIC PROPERTIES

In this chapter, we discuss the electric properties of a nucleus. It is well known that the deformation of a nucleus leads to an enhancement of the electric quadrupole transition probability over a single particle rate. Therefore the comparison of this probability with the experimental data is another test of the nuclear wave functions obtained by the present model. Since Coulomb excitation is closely connected with both the transition probability and the wave function, we have carried out the excitation experiments for some of the present nuclei.

We present general formula to calculate electric transition probability in Sect. 6-1, and the Coulomb excitation experiments for ^{45}Sc and ^{75}As in the next section. We compare, in its subsection, the experimental results with the theory, and discuss the nuclear quadrupole moments in Sect. 6-3.

6-1. General Formula of the Reduced E2 Transition Probability

The E2 transition probability per unit time for the emission of a photon of energy $\hbar\omega=\hbar ck$ is (Ni55)

$$T(E2) = \frac{4}{3\cdot 25}\frac{1}{\hbar^2}(\omega/c)^5 B(E2;i \to f), \qquad (6\text{-}1)$$

where the reduced E2 matrix element $B(E2;i\to f)$ between the

initial state i with spin I_i and the final state f with spin I_f has the following form (Sc66):

$$B(E2;i \to f) = \frac{5e^2}{16\pi}\,[Q_c + \sum_{n=-2}^{2} q(n)]^2. \qquad (6\text{-}2)$$

The Q_c represents the quadrupole moment generated by the collective motion of a nucleus and is given by

$$Q_c = Q_o \sum \delta_{\nu_i \nu_f} (I_i K 20 | I_f K) C^I_{\nu_i} C^I_{\nu_f} . \qquad (6\text{-}3)$$

The intrinsic moment Q_o of the core is related to the well known parameter δ by a second order approximation as (Ni55)

$$Q_o = 0.8\ Z\ R_o^2 \delta (1 + \tfrac{2}{3}\delta), \qquad (6\text{-}5)$$

where R_o is the charge radius of the nucleus and

$$R_o = 1.2\ A^{1/3} \quad \text{fm}. \qquad (6\text{-}5)$$

The terms q(n) in Eq, (6-2), which are the contribution of quasiparticles to the quadrupole moment, are defined by

$$q(n) = (-1)^{n(I_f - \frac{1}{2})} (1+\tfrac{Z}{A}) \frac{2\hbar}{M_p \omega_o} \sum\!\!\!\!\!\!- \frac{}{K_i \xi_i \xi_f} (U_{\nu_i} U_{\nu_f} - V_{\nu_i} V_{\nu_f}) C^I_{\nu_i} C^I_{\nu_f}$$

$$\cdot [(I_i K_i 2n | I_f K_f) \sum\!\!\!\!\!\!- \frac{}{l_i l_f} \langle N_f l_f | r^2 | N_i l_i \rangle \left(\frac{2l_i+1}{2l_f+1}\right)^{\frac{1}{2}} (l_i 020 | l_f 0)$$

$$\cdot \sum\!\!\!\!\!\!- \frac{}{\Lambda_i \Lambda_f \Sigma_i \Sigma_f} \delta_{\Sigma_i \Sigma_f} a_{l_f \Lambda_f} a_{l_i \Lambda_i} (l_i \Lambda_i 2n | l_f \Lambda_f)] + q'(n) \qquad (6\text{-}6)$$

where

$$K_f = K_i + n \qquad \text{and} \qquad \Lambda_f = \Lambda_i + n.$$

The new terms q'(n) in the expression vanish for $K_i + K_f \geq 2$, and are given by

$$q'(n) = (-1)^{n(I_f - \frac{1}{2})}\left(1+\frac{Z}{A^2}\right)\frac{2\hbar}{M_p \omega_o}\sum_{K_i \xi_i \xi_f}(U_{\nu_i}U_{\nu_f} - V_{\nu_i}V_{\nu_f})C_{\nu_i}C_{\nu_f}$$

$$\cdot\left[(I_i K_i 2n | I_f K_f)\sum_{l_i l_f}\langle N_f l_f | r^2 | N_i l_i\rangle \left(\frac{2l_i+1}{2l_f+1}\right)^{\frac{1}{2}}(l_i 020 | l_f 0)\right.$$

$$\left.\cdot\sum_{\Lambda_i \Lambda_f \Sigma_i \Sigma_f}\delta_{-\Sigma_f \Sigma_i}\, a_{l_f \Lambda_f}\, a_{l_i \Lambda_i}(l_i \Lambda_i 2n | l_f \Lambda_f)\right] \qquad (6\text{-}7)$$

where

$$K_f = -K_i - n \qquad \text{and} \qquad \Lambda_f = -\Lambda_i - n.$$

The factor $(U_{\nu_i} U_{\nu_f} - V_{\nu_i} V_{\nu_f})$ in Eq. (6-7) results from the pairing effect and diminishes the contribution of quasi-particles.

6-2. Coulomb Excitation

6-2-1. Experimental method

Coulomb excitation (Al56) is a very precious and widely used tool to extract the reduced quadrupole transition probability. Many investigations have been done and much information about the transition probabilities, excited level properties and wave functions has been accumulated. We have also done the Coulomb excitation experiment and obtained the values of B(E2) for some nuclei. In this section we summarize the experimental method and the extraction of the B(E2) values for ^{45}Sc and ^{75}As nuclides.

The thick targets were bombarded with triply ionized nitrogen ions which were accelerated third subharmonically in the cyclotron in Kyoto University and extracted with energy of 11.5 MeV. The details have been reported elsewhere (Fu67). De-excitation gamma rays from the target nuclei were detected with a $1\frac{3}{4}$" x 2" NaI(Tl) crystal mounted on an RCA-6342A photomultiplier tube. The experimental arrangement is shown schematically in Fig. 6-1. Each target was thick enough to stop the insident particles and was arranged at the bottom of a cup. Eight cups were arranged on a rotatable disc in a vacuum chamber and the target assembly was covered with an electric shield. The beam current up to 10nA of N^{3+} ions was measured by using a vibrating reed electrometer.

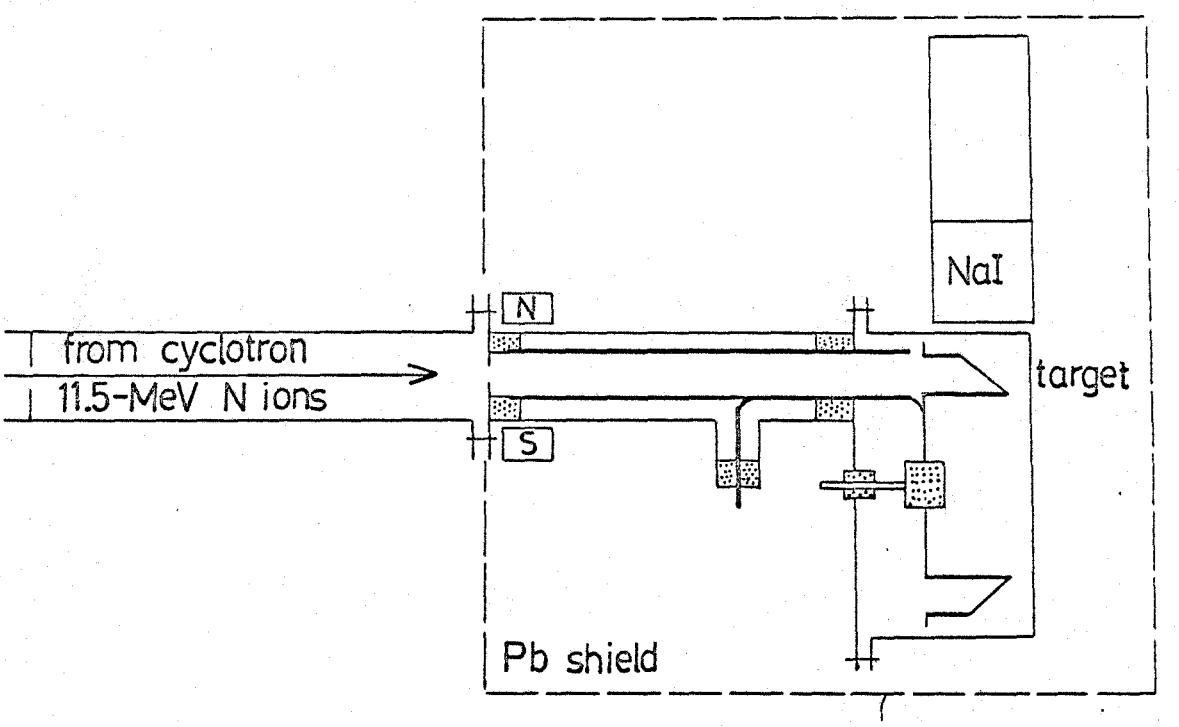

Fig. 6-1. Schematic drawing of the target chamber and detector arrangement.

A large gamma ray background resulting from the residual activities in the measuring room was found. This was reduced by a factor of 1000 with a lead shield of about 10 cm thick surrounding the detector. Since target materials were all in powder form, they were solidified with cellulose acetate. The transfer reactions, $^{12}C(^{14}N,^{15}N)^{11}C$ and $^{12}C(^{14}N,^{13}N)^{13}C$, were, therefore, caused by the nitrogen ion bombardment, and the gamma rays resulting from the positon annihilation of ^{11}C and ^{13}N produced a new background. This could be subtracted by using the gamma ray spectrum obtained with a pure cellulose acetate target. The background effect of bremsstrahlung due to the collision of the projectile and target nucleus was negligible.

6-2-2. Gamma ray spectra and yields

Examples of the gamma ray spectra which remained after subtracting the background are shown in Fig. 6-2. The target materials were Sc_2O_3 and As of powder form. The peeling procedure of each gamma ray spectrum was carried out, referring to the spectra of the following sources placed at the target position:

^{57}Co	123 keV	137 keV
^{114m}In	192 keV	
^{131}I	364 keV	
^{137}Cs	662 keV.	

The gamma ray spectra which were obtained by the Coulomb

[a]

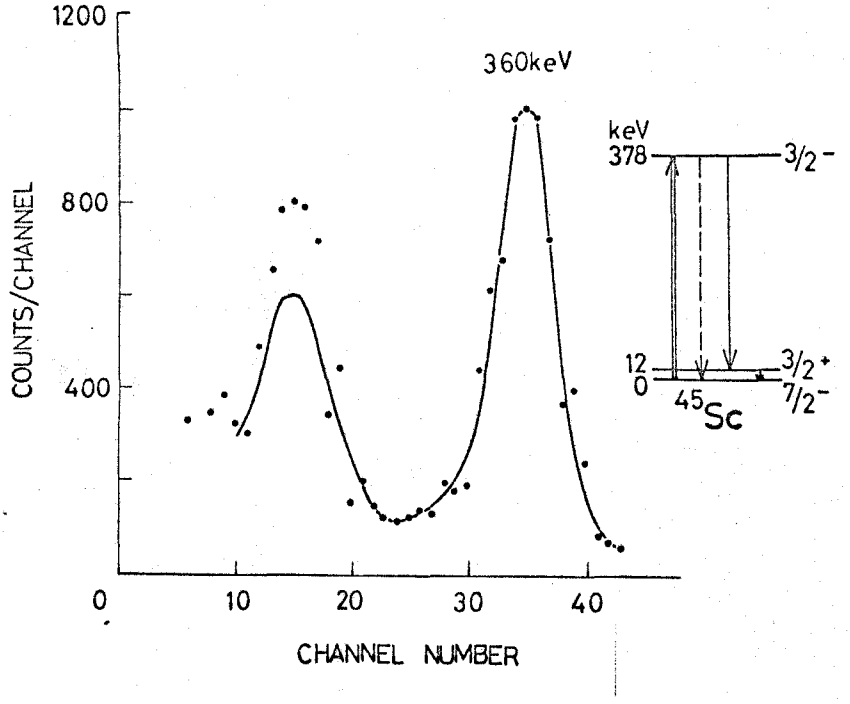

[b]

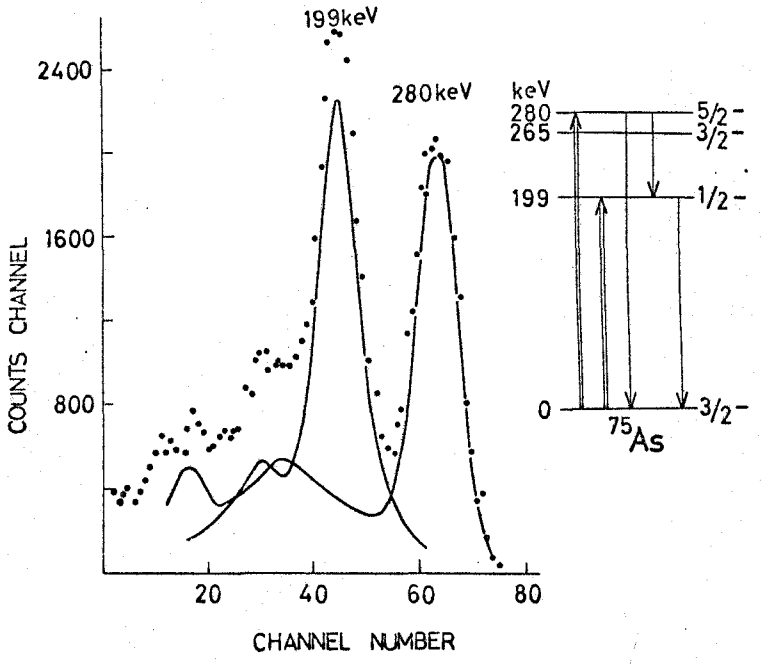

Fig. 6-2. Gamma ray spectra of ^{45}Sc [a] and ^{75}As [b] following Coulomb excitation with ^{14}N ions.

excitation of ^{165}Ho and ^{23}Na were also used as other standards. They were

^{165}Ho	94.7 keV
^{23}Na	438 keV.

The total gamma ray yield for each transition was obtained by integrating the number of photopeak counts and correcting the intrinsic peak efficiency of the present crystal. The correction was also done for the absorption effect of the target material, holder and surrounding wall. The effect due to the angular anisotropy of emitted gamma rays was smaller than a few percent in the case of the present geometry and targets.

The total number of projectiles must be measured accurately to obtain the B(E2) values. When heavy ions pass through a long duct, some of them collide with the residual gas molecules and change their charge numbers. In our experiment, the extracted 11.5 MeV N^{3+} ions from the cyclotron fly about five meters to reach the target. Therefore, we measured the charge distribution by a magnetic analysis method and estimated the average charge number to be 3.05.

6-2-3. Extraction of B(E2)

In case of the present combination of projectile, bombarding energy and targets, the semiclassical treatment of the Coulomb excitation process is sufficiently good.

The total cross section for the E2 excitation is expressed as

$$\sigma_{E2}(E) = 4.819\left(\frac{A_2}{A_1 + A_2}\right)^2 \frac{A_1}{Z_2^2} (E - \Delta E') B(E2)\uparrow f_{E2}(\xi) \quad b \tag{6-8}$$

where A_1 and A_2 are the mass numbers of the projectile and target, respectively. The notation Z_2 is the atomic number of the target nucleus. The E denotes the projectile energy and $\Delta E' = (1+A_1/A_2)\Delta E$, where ΔE represents the excitation energy. The function $f_{E2}(\xi)$ is the classical total excitation cross section function and treated in unit of e^2b^2. These notations are referred to Alder et al. (Al56).

The total thick target gamma ray yield Y_{th} of a given transition is obtained by integrating Eq. (6-1) over the trajectory of a projectile in the target and multiplying the decay factor ε of this mode. Therefore we obtain

$$T_{th} = \frac{N_A a I \varepsilon}{A} \int^{E_{max}} \sigma_{E2}(E) \frac{dE}{dE/dX} + \left(\begin{array}{c}\text{contributions from} \\ \text{higher excited levels}\end{array}\right). \tag{6-9}$$

Here, N_A is Avogadro number; a is the number of target nuclei per molecule; A is the molecular weight of the target and I is the number of projectile incident on the target. The stopping power dE/dx is expressed in unit of MeV/g/cm^2. The second term in Eq. (6-9) is the contri-

bution of cascade decays from higher levels. The evaluation of this term can be easily done by analysing first the transitions from the highest excited level in the experiment and successively those from the lower states.

By combining Eq. (6-8) with (6-9), the yield Y of given gamma rays from the directly excited level may be written as

$$Y = \varepsilon B(E2)\uparrow I\left[\frac{4.819N_A a}{A}\,\frac{A_2}{A_1+A_2Z_2^2}\,\frac{A_1}{}\left(\int^{E_{max}}(E-\Delta E')f_{E2}(\xi)\frac{dE}{dE/dX}\right)\right] \cdot 10^{-24}. \qquad (6\text{-}10)$$

The partial reduced transition probability $\varepsilon B(E2)\uparrow$ for the excitation is obtained by determining Y/I experimentally and calculating numerically the term of the square bracket in the above equation. In this calculation, it is necessary to know the stopping power dE/dx as a function of projectile energy E. In the energy range of 0.1~2 MeV/amu, however, there are neither experimental nor theoretical prediction on the stopping powers of the present targets.

For light ions such as protons and alpha particles, the relation $dE/dx \propto E^{-0.55}$ has been used so far. However this relation is not applicable for heavy ions. One method used for heavy ions is to assume constant stopping power over the wide range of energy, but this assumption

is inadequate for the present energy range. Another method is to apply the proton stopping power data to heavy ions, by correcting the effective charge. The effective charge is estimated using the experimental Papineau curve (Pa56) on the assumption that it is independent of the kind of material medium. But our experiment on the charge changing collision of heavy ions has shown that the effective charge is dependent on the material medium and its deviation amounts to about ten percent (Im65). Therefore, in the present analysis, we estimated the stopping power by the following consideration:

For heavy ions of about 2 MeV/amu energies, Bethe's formula on the stopping power of a single material seems to hold vely well (Fa63), and that of a compound may be

$$-\frac{dE}{dX} = (\gamma Z_1)^2 \frac{0.307}{A\beta^2} \sum_i \left[a_i Z_i \ln\left(\frac{1.022 \cdot 10^6 \beta^2}{I_i}\right) \right] \text{MeV} \cdot \text{cm}^2/\text{g}, \qquad (6\text{-}11)$$

where γZ_1 is the effective charge of the incident ions; A is the molecular weight of absorbing material; a_i and I_i are the number of the atom i per molecule and the mean ionization potential in unit of eV, respectively. $\beta = v/c$ where v is the velocity of the insident ions.

Furthermore, it has been shown experimentally that the ratio of the stopping powers of media whose atomic numbers are slightly different from each other, is approximately constant over the wide range of energy (No63). From

these facts, the stopping power of a compound material $(dE/dx)_m$ may be expressed as

$$(dE/dX)_m = C(dE/dX)_r \qquad (6\text{-}12)$$

where $(dE/dx)_r$ is the stopping power for the reference medium which lies near the atom of average atomic number of the compound. The constant C can be evaluated from the data at energies above 2 MeV/amu. In this way, one obtains the relations

$$\begin{aligned} dE/dX &= 0.98\ (dE/dX)_{Al} \qquad \text{for } Sc_2O_3 \\ &= 1.17\ (dE/dX)_{Ag} \qquad \text{for As,} \end{aligned} \qquad (6\text{-}13)$$

here aluminium and silver are used as the reference media.

In order to carry out numerically the integration of Eq. (6-10), we used the expression

$$-\frac{dE}{dX} = Z_1^2 \exp\Big[\sum_{j=0}^{4} P_j \ln\Big(\frac{E}{A_1}\Big)^j\Big], \qquad (6\text{-}14)$$

where the coefficients p_j were adjusted so as to fit the experimental data in the energy range of interest.

6-2-4 Discussions about B(E2)

i) ^{45}Sc nucleus

From the reaction studies (Yn64) and the conversion coefficient (Jo66), it has been inferred that the first

excited state at 12 keV is a $d_{3/2}$ hole state with $I = 3/2+$. Schwartz, Alford and Marinor (Sc67) have assigned the spin of the second excited state at 378 keV to be 1/2 - or 3/2 - from DWBA analysis of the reaction $^{44}Ca(^{3}He,d)^{45}Sc$. As shown in Fig. 6-2, a large number of 360 keV gamma rays were observed in our experiment, which should be attributed to the transition from the 378 keV to 12 keV level. Therefore I^{π} of the 378 keV state may not be 1/2 -, but 3/2 -. The yield of the 360 keV gamma rays is 3.89×10^{-9} per incident particle, which corresponds to $\epsilon B(E2) = 0.0086 \pm 0.0017$.

The internal conversion coefficient for the 360 keV E1 transition is estimated by extrapolating the calculated values of Sliv and Band (Sl65), and is smaller than 0.01. Consequently, the upward reduced transition probability B(E2) is 0.0086 ± 0.0017. This is in fairly good agreement with the value of 0.0093 obtained by Alkhazov et al (Al64).

Table 6-1 shows the theoretical and experimental results of B(E2). The theoretical values are calculated by using the best fit wave functions obtained in Chapter 5. The experimental results for higher levels are those by Afonin et al. (Af67).

The experimental $B(E2)\uparrow$ for the 378 keV level is enhanced by a factor of seven over the single particle estimate. The single particle estimate $B(E2)^{sp}$ is given by

Table 6-1. Experimental and theoretical B(E2) values for ^{45}Sc nucleus in units of e^2b^2.

Transition I^{π}(energy keV)	Experiment e^2b^2	Theory e^2b^2	Collective contribution e^2b^2
3/2-(376) ---- 7/2-(0)	0.017[a)]	0.011	0.007
5/2-(722) ---- 7/2-(0)	0.0071[b)]	0.0001	0.00003
11/2-(1238) -- 7/2-(0)	0.0062[b)]	0.007	0.005

a). Ref. (Im67)

b). Ref. (Af67)

$$B(E2)^{sp} = e^2 \frac{2I_f+1}{4\pi} \langle f|r^2|i\rangle (I_i \tfrac{1}{2} 20 | I_f \tfrac{1}{2})^2$$

where the notations are the same as those by Sorensen (So64).

A large part of the B(E2) value comes from the collective contribution. The experimental B(E2) cannot be reproduced at all, when only the quasiparticle contribution is considered. The agreement between the theoretical and experimental results is rather good for the 378 and 1238 keV levels. But in order to reproduce better the 725 keV state, a stronger mixing between the wave functions must be introduced.

ii) ^{75}As nucleus

As seen in Fig. 6-2, the gamma ray spectrum in the arsenic experiment is composed of the 199 and 280 keV gamma rays. The 260 keV radiation cannot be drawn out.

The yield of the 280 keV radiation is 1.61×10^{-8} per incident particle, which corresponds to $B(E2)\uparrow$ of 0.050 ± 0.012. By combining this value with the measured life time (Sh59) of the 280 keV level, the internal conversion coefficient α is decided as 0.01. Consequently one obtains $B(E2)\uparrow = 0.051 \pm 0.012$. Taking into account of the transition from the 280 keV to 199 keV state, the yield of the 199 keV gamma rays is estimated as 1.3×10^{-8} per insident particle. Similarly to the above agreement, we

obtain $\alpha = 0.02$ and $B(E2)\uparrow = 0.015 \pm 0.003$.

The reported values of $B(E2)\uparrow$ for the 199 and 280 keV levels are tabulated in Table 6-2. Some of these are in accordance with the present observation. (Kamitsubo's data may contain a systematic error.)

More recently Robinson, McGowan, Stelson and Milner (Ro67a) obtained the B(E2) values for the higher levels by Coulomb excitation with alpha and oxigen ions. They deduced the values for the 468.8 (1/2 -), 572.3 (5/2 or 7/2 -), 617.7 (3/2 or 1/2 -) and 821.8 (7/2 -) keV transitions to the ground state and obtained 0.0066, (0.049 or 0.037), (0.0011 or 0.0022) and 0.054, respectively.

Using the best fit wave functions derived in Chap. 5, we calculate the B(E2) values for the various levels of ^{75}As and compare them with the experimental data of Robinson et al. These are shown in Table 6-3.

The theoretical B(E2) values are composed of two terms; one is the contribution of collective motion and the other is that of quasiparticle motion. As already pointed out, the factor $(U_{\nu_i} U_{\nu_f} - V_{\nu_i} V_{\nu_f})$ comes from the pairing effect and diminishes the contribution of quasi-particles especially at low-lying states. Therefore the experimental B(E2) values cannot be reproduced at all, when only the quasiparticle contribution is considered. Then a large part of the reduced E2 transition probability results from the collective contribution. This tendency

Table 6-2. B(E2)↑ values for the 198.6 and 279.5 keV levels in ^{75}As nucleus in units of e^2b^2.

Level energy (keV)	Ritter et al. (Ri62)	Paul et al. (NDS60)	Kamitsubo (Ka62)	Present (Im67)
198.6	0.015	0.016	0.025	0.015 ± 0.003
279.5	0.052	0.050	0.071	0.051 ± 0.012

Table 6-3. Experimental and theoretical B(E2) values for ^{75}As nucleus in units of e^2b^2.

Transition I^{π}(energy keV)	Experiment e^2b^2	Theory e^2b^2	Collective contribution e^2b^2
1/2-(198.6) -- 3/2-(0)	0.034[a)]	0.007	0.006
3/2-(264.6) -- 3/2-(0)	0.0054[b)]	0.0075	0.008
5/2-(279.5) -- 3/2-(0)	0.032[a)]	0.062	0.064
1/2-(468.5) -- 3/2-(0)	0.007[b)]		
5/2- or (572.1) -- 3/2-(0)	0.049[b)]	0.007	0.011
7/2-	0.037[b)]	0.027	0.027
3/2-(617.7) -- 3/2-(0)	0.0017[b)]	0.002	0.003
7/2-(821.8) -- 3/2-(0)	0.037[b)]	0.008	0.008

a). Ref. (Im67)

b). Ref. (Ro67a)

is readily seen in Table 6-3. The last column of this table gives the magnitudes of the collective contribution.

The spins of the 572.1 keV has not been clearly determined, but possibly believed 5/2 - or 7/2 -. The theoretical B(E2) values are calculated for both spins and the B(E2) for 7/2 - is found closer to the experimental value. The theoretical values for a few levels are a little smaller than the experimental ones. This probably implies that the actual deformation may be larger or the real states may mix more strongly with each other owing to another interaction ——— rotation-vibration or neutron-proton interaction. However, since the calculation is done without using effective charges, the overall agreement with the experiment seems worth noting.

iii) ^{79}Br nucleus

Historically, Heydenburg and Temmer(He54) first deduced the B(E2) values for the levels of ^{79}Br by means of Coulomb excitation, but their results have not been well refined. Recently, however, Robinson, McGowan, Stelson and Milner (Ro67a) have investigated more precisely the properties of the low-lying levels of this nucleus. They used 2.5 ~ 7.0 MeV alpha particles and 36 MeV oxygen ions. These results are shown in Table 6-4.

We calculated the B(E2) values similarly to the preceding analysis and tabulate the results in the table.

Considering the experimental, theoretical and collective magnitudes, the same discussions as for ^{75}As could be done.

Table 6-4. Experimental and theoretical B(E2) values for ^{79}Br nucleus in units of e^2b^2.

Transition I^{π}(energy keV)	Experiment (Ro67a) e^2b^2	Theory e^2b^2	Collective contribution e^2b^2
5/2-(217.2) -- 3/2-(0)	0.0263	0.12	0.12
3/2-(261.4) -- 3/2-(0)	0.007	0.005	0.005
1/2- or (306.4) -- 3/2-(0)	0.0422	0.005	0.005
3/2-	0.0211		
3/2-(397.2) -- 3/2-(0)	0.0033		
5/2-(522.8) -- 3/2-(0)	0.063	0.008	0.008
3/2-(605.9) -- 3/2-(0)	0.0152	0.005	0.005
5/2- Or (761.2) -- 3/2-(0)	0.085	0.014	0.013
7/2-	0.064	0.003	0.003
1/2- or (831.6) -- 3/2-(0)	0.0012	0.005	0.005
3/2-	0.0006		
3/2- or (1332.3)-- 3/2-(0)		0.002	0.002
1/2-			

6-3. Quadrupole Moment

The nuclear deformation is reflected on the values of intrinsic quadrupole moment Q_o and electric quadrupole moment Q. For doubly even nuclei, Q_o is related to B(E2) by the following formula (ND65).

$$Q_o = \left[\frac{16\pi}{5} B(E2;0 \rightarrow 2)\right]^2 \qquad (6\text{-}15)$$

Therefore one can obtain easily the intrinsic quadrupole moment from the experimental B(E2) value.

When we assume that the deformation for an odd-mass nucleus might not differ from that for the neighbouring doubly-even nuclei, we can compare the Q_o value evaluated by Eq. (6-4) with the experimental values for the doubly-even nuclei. These results are shown in Table 6-5. Here, ^{44}Ca, ^{46}Ti, ^{74}Ge, ^{76}Se and ^{78}Se are used as the neighbouring doubly-even nuclei. The agreement between the two Q_o values is sufficiently good, and this fact also supports the present theory.

The quadrupole moment Q can be also related to the wave function and the deformation as follows:

$$Q = \sum_{K\xi} |C^I_{K\xi}|^2 \frac{3K^2 - I(I+1)}{(I+1)(2I+3)} Q_o \qquad (6\text{-}16)$$

The Q value are calculated for the ground states of ^{45}Sc, ^{75}As and ^{77}Br, and compared with the experimental values. These are tabulated in Table 6-6. An overall accordance

is seen, which means the present wave function for each nucleus is sufficiently adequate.

Table 6-5. Theoretical intrinsic quadrupole moment Q_o compared with that of doubly-even-mass nucleus.

Nucleus	Present theory (in barn)	Experiment (ND65) (in barn)	
^{45}Sc	0.45	0.60(^{44}Ca)	0.90(^{46}Ti)
^{75}As	1.56	1.78(^{74}Ge)	2.17(^{76}Se)
^{79}Br	2.17	1.94(^{78}Se)	

Table 6-6. Theoretical and experimental quadrupole moment Q.

Nucleus	Present theory (in barn)	Experiment (in barn)
^{45}Sc	-0.10	-0.22 (Fr59)
^{75}As	0.28	0.29 (ND66a)
^{79}Br	0.40	0.31 (ND66b)

CHAPTER 7. SUMMARY AND CONCLUSION

We have studied the nuclear structure of some off-magic isotopes, ^{71}As, ^{73}As, ^{75}As, ^{77}As, ^{77}Br, ^{79}Br, ^{81}Br, ^{81}Rb, ^{83}Rb, ^{45}Sc and ^{47}Sc. Here, we have considered that each nucleus is composed of a doubly-even core plus an unpaired quasiparticle. Furthermore we have assumed that the core subjects a quadrupole distortion and the unpaired quasiparticle moves in the quadrupole field under the background of pairing force. Then we have introduced a non-adiabatic model, where the motion of the quasiparticle moving in Nilsson's deformed orbital is coupled by a Coriolis force with the rotational motion. It was found that the quasiparticle formalism leads to a reduction of the off-diagonal part of H_{coup} as well as a compression of the low energy spectrum, when compared with the single particle picture.

In order to know about the quasiparticle motion, one quasiparticle energy and the wave function, we determined accurately, at first, the single particle energy ε_ν and the wave function $|\nu\rangle$ for N = 3 shell and then the chemical potential λ and the energy gap Δ.

We have used Nilsson Hamiltonian to represent a single particle motion in a quadrupole field. This Hamiltonian has four parameters, $\mathring{\omega}_o$, κ, μ and η. Among them, a reasonable value for $\mathring{\omega}_o$ has been obtained by taking the

root mean square radius for all the nucleons to be equal to $\frac{3}{5}\cdot 1.2\cdot A^{1/3}$ fm, which gives $\hbar\mathring{\omega}_0 = 41\ A^{-1/3}$ MeV for all nuclei. We determined other two parameters κ and μ for N = 3 shell, referring to the observed single particle level spectrum of ^{57}Ni isotope which is composed of doubly-magic core plus one nucleon. The obtained values of κ and μ are 0.034 and 0.284, respectively. We then calculated the eigenvalues ε_ν and eigenfunctions $|\nu\rangle$ as a function of η. These results are presented in a figure and a table.

Two parameters λ and Δ were determined by introducing a pairing strength G and a true particle number n. Here the constancy of G for the same A have been assumed and the value of 19/A MeV has been chosen according to Kisslinger and Sorensen. They obtained the value by applying the following three methods to nickel isotopes: first, a comparison of the experimental odd-even mass differences with the theoretical ground state energy differences between odd- and doubly even-mass nuclei; second, a comparison of the theoretical with the experimental energy levels for odd-mass nuclei; third, similar comparison for doubly even-mass nuclei. The final results of these parameters λ and Δ are shown in figures for the present groups of isotopes; arsenic, bromine, rubidium and scandium. It was found that λ changes rapidly but Δ slowly with η.

We could then calculate the present model spectra by diagonalizing the Coriolis interaction with the rotational

wave functions built on a number of intrinsic states. These states are attributed to the motion of a single "quasi-proton" in No. 15, 16, 17, 19, 20 or 26 orbital for so called $p_{3/2}$ or $f_{5/2}$ shell nuclei and in No. 10, 12, 13 or 14 orbital for so called $f_{7/2}$ shell nuclei. These calculations were done by using only two free parameters η and $\frac{\hbar^2}{2\mathcal{J}}$, which were determined by the best fit procedure between the calculated and the observed level locations.

Among arsenic isotopes, the ^{75}As level scheme has been well established by ^{75}As Coulomb excitation and ^{75}Ge and ^{75}Se decays. The level calculation for ^{75}As was done with and without Coriolis interaction and/or pairing force. It was found that only the calculation including both Coriolis and pairing forces can reproduce the experimental level scheme. A characteristic feature in this calculation is that several levels located nearby one another and seem to form apparent groups. For instances, four levels of $I^{\pi} = 3/2\,-$, $3/2\,-$, $1/2\,-$ and $5/2\,-$ appeared at low excitation energy and three levels of $I^{\pi} = 5/2\,-$, $3/2\,-$ and $7/2\,-$ at a little higher excitation energy. This feature is distinctly found in the experimental level scheme. The order of the lower four levels is dependent strongly on the deformation and slightly on the rotational constant. The best agreement with experiment was obtained for $\eta = 6$ and $\frac{\hbar^2}{2\mathcal{J}} = 60$ keV. Previous theories can not reproduce the ^{75}As level spectrum, but the present theory explains rather well both spins and locations of the low-lying odd-parity levels. The exception

is found for the 468.8 keV 1/2 - state.

For ^{73}As and ^{77}As, the spin and parity assignment has been done to only a few levels and we can not execute the best fitting procedure. We present here only the tentative level spectra calculated using a set of parameters η = 2.7 and $\frac{\hbar^2}{2\mathcal{I}}$ = 60 keV and a set of η = 6 and $\frac{\hbar^2}{2\mathcal{I}}$ = 60 keV, respectively. The ground state in ^{71}As has been known (5/2 -), which suggests η smaller than 2.5 according to the present model.

Among bromine isotopes the level scheme of ^{79}Br has been established, and so we carried out a least-squares fit to this nucleus. The best agreement was obtained for η = 7.5 and $\frac{\hbar^2}{2\mathcal{I}}$ = 60 keV. As previously noted for ^{75}As, the three levels form an apparent triplet. The similar but not so clear feature is also found in the 5/2 -, 3/2 - and 1/2 - states of ^{79}Br, but the level order is different from that in ^{75}As. We found that this grouping feature is clearly reproduced by the present theory, and other higher states are fitted, too, within the root mean square deviation of about 20 keV from the observed levels. For other nuclei of bromine, we presented only tentative theoretical level spectra.

One of the distinct features of the ^{83}Rb level scheme is that the ground state is 5/2 - and at only 5 keV above the ground state the 3/2 - level is located. This feature was reproduced by choosing η = 6 and $\frac{\hbar^2}{2\mathcal{I}}$ = 60 keV.

Furthermore, other levels with lower spin values could be fitted very well with the corresponding observed states within about 40 keV deviation. However, the levels with higher spins, i.e. 7/2, which appear in the calculated spectrum, are not found in the lower energy region of the experimental scheme.

For ^{45}Sc and ^{47}Sc isotopes, the best fit was obtained for a set of the parameters $\eta = 4$ and $\frac{\hbar^2}{2\vartheta} = 170$ keV and for $\eta = 3$ and $\frac{\hbar^2}{2\vartheta} = 240$ keV, respectively. Previous shell model or other models cannot account for the low-lying levels, but the present model predicts rather well all these levels. The 7/2 - ground state was found to belong mainly to K = 1/2 band. The trend of each parameter is reasonable, when one compares their 3/2 + first excited states with the filling of $1f_{7/2}$ neutron shell.

In order to check the validity of the present wave functions, we investigated in detail the reduced electric transition probability B(E2). This probability is enhanced many times over the single particle rate by the deformation of nucleus, and is also dependent upon the wave function of individual nuclear state. Therefore, the comparison of the experimental with the theoretical probability is one of the most valuable methods.

We presented the general formula to calculate the B(E2) value. It was found that the pairing effect diminishes the contribution of quasiparticles and almost of the E2 transition probability comes from the collective part. Since the

experimental B(E2) value is generally extracted from the Coulomb excitation experiment, we also carried out the experiment using nitrogen ions as projectiles and obtained the values for ^{45}Sc and ^{75}As. In the extraction procedure, it is necessary to know the stopping power as a function of projectile energy. Since the stopping power data have been obtained only for a few combinations of projectiles and targets, we present a semiempirical method to evaluate the stopping powers.

Finally, we compared the experimental with the theoretical B(E2) values, and obtained an overall agreement. For a few levels, the theoretical values are smaller than the experimental ones. This probably implies that real states may mix more strongly with one another owing to other interactions — rotation-vibration or neutron-proton interaction. Since the calculation has been done without using effective charges, the overall agreement seems worth noting.

The nuclear deformation is reflected on the values of intrinsic quadrupole moment Q_o and electric quadrupole moment Q. We calculated them using the deformation and the wave functions obtained by the present theory. We compared the calculated Q_o and Q with the experimental Q_o values for the nearest doubly even-nuclei and the experimental ground state Q values, respectively, and a satisfactory accordance was found.

In conclusion, we have studied the nuclear structure of

As, Br, Rb and Sc isotopes from the point of deformation. The quantities we calculated are level energies, B(E2), Q_o and Q values. As for the level energies, we obtain satisfactory agreement between the calculated and the experimental results. The B(E2) values are predicted well for most of the transitions, but the prediction is poor for a few cases. This means that some of the theoretical wave functions are not always correct and additional interactions must be considered as higher order perturbations. The obtained Q_o and Q values, which do not depend so much on the wave functions, are reasonable.

To confirm the present model more, the experimental informations about the properties for ^{71}As, ^{73}As, ^{77}Br, ^{81}Br and ^{81}Rb nuclei are expected. The experimental B(E2) values for the transitions of unstable nuclei are also necessary to refine the interaction Hamiltonian.

Some nuclei in the isotopes such as Ge, Se, Kr, Tc, Rh, Pd and Ru probably suffer incipient deformations but they have been hardly treated theoretically. In future, we intend to apply the present model to the odd-mass nuclei of these regions which locate away from the closed shells.

ACKNOWLEDGEMENTS

I would like to express my deepest appreciation to Professor M. Sakisaka for his wise counsel and encouragement during the course of the work. Association with Dr. F. Fukuzawa is a unique and impressive experience. Appreciation is also expressed for his contribution to my education in scientific and other fields. I would like to thank Messrs. M. Tomita, K. Ogino, S. Okumura, K. Yoshida, K. Shima, K. Tsuji, T. Yamazaki and N. Ide for their cordial help in carrying out the Coulomb excitation experiment. I am very grateful for having studied at Department of Nuclear Engineering and am indebted to many other peoples, too.

I would like to express my sincere gratitude to Professor T. Nishi for his many productive suggestions and encouragement. Without his support, I could not pursue this work at Engineering Research Institute. Association with Drs. I. Fujiwara, M. Ishibashi, H. Nakahara and Mr. H. Okamoto is very fruitful. Their help and friendship made it possible to carry out the decay scheme experiment. Name of Mr. K. Hotta is also remembered.

This work involves the first heavy ion experiment in Japan. I am indebted to Dr. Y. Uemura, Mr. H. Fujita and others for the acceleration of heavy ions in the Kyoto University Cyclotron. Thanks are extended to Professor T. Yanabu for his interest and encouragement.

In addition, I appreciate the allotment of time on the KDC II computer granted by the Kyoto University Computation Center.

I owe to the members of my family the continuation of my education. The constant support of my wife Taeko has always been of great value to me.

APPENDIX COMPUTER PROGRAMS

1. PROGRAM NILSR computes the eigenvalues and eigenfunctions for Nilsson Hamiltonian (3-3). This program calls JAC and VCCOEF.
2. FORTRAN IV SUBROUTINE JAC diagonalizes the real symmetric matrix. This is prepared by Hitachi Ltd.
3. FUNCTION VCCOEF computes the vector coupling coefficients $\langle J_1 M_1 J_2 M_2 | JM \rangle$. This function calls FACTO.
4. FUNCTION FACTO is called by VCCOEF to compute the factorials x!.
5. PROGRAM QPFEEG computes particle numbers and pairing strengths for given sets of chemical potential and energy gap.
6. PROGRAM CORIOJ computes and diagonalizes the Hamiltonian (2-11) with rotational wave functions which are built on a number of intrinsic states, for given sets of deformation and rotational constant. This program calls JAC and VCCOEF.
7. PROGRAM COBE2 reads the wave functions calculated by PROGRAM CORIOJ and computes the reduced quadrupole transition probability by Eq. (6-2). This program calls EXVR2 and VCCOEF.
8. FUNCTION EXVR2 computes the radial matrix element $\langle N'l' | r^2 | Nl \rangle$.

```
¥NILSR                          HARP
      WRITE(6,4201)
 4201 FORMAT(1H1,78HNILSSON MODEL,ORTHOGONALIZATION OF R FUNCTION,EIGEN
     1FUNCTIONS AND EIGEN VALUES///)
      DIMENSION ETA(99),TNNI(15),OMNI(15),SRNI(15),SLON(15,7),SMU(99),
     1GLAON(15,7),SIGON(15,7),ALLON(15,7),JS(15),A(15,15),U(15,15)
      DO 4001 IE=1,99
      READ(5,4101)SMU(IE),IS
 4101 FORMAT(F10.5,I5)
      WRITE(6,4202)SMU(IE)
 4202 FORMAT(1H ,24HPARAMETER SMALL MU=2*D/C,F15.7)
      IF(SMU(IE).EQ.-1.1)GO TO 4301
      DO 4002 I=1,IS
      READ(5,4102)TNNI(I),OMNI(I),JS(I),ID
 4102 FORMAT(2F10.5,2I5)
      WRITE(6,4215)TNNI(I),OMNI(I)
 4215 FORMAT(1H0,1HN,F10.5,5X,5HOMEGA,F10.5/)
      JSI=JS(I)
      DO 4003 J=1,JSI
      READ(5,4103)SLON(I,J),GLAON(I,J),SIGON(I,J)
 4103 FORMAT(3F10.5)
 4003 CONTINUE
C     DATA WHICH ARE CONTAINED IN N(I) AND OMEGA(I) HAVE BEEN READ.
      READ(5,4100)(ETA(IDE),IDE=1,ID)
 4100 FORMAT(7F10.5)
      DO 4000 JD=1,ID
      WRITE(6,4200)ETA(JD)
 4200 FORMAT(1H ,21HDEFORMATION PARAMETER,9X,F15.7)
      EPS=0.001
      ITMAX=111
      IND=1
      DO 4004 JL=1,JSI
      DO 4005 JC=1,JSI
      U(JL,JC)=0.
      A(JL,JC)=0.
 4005 CONTINUE
 4004 CONTINUE
      N=JSI
C     CALCULATION OF MATRIX ELEMENTS A(I,J) IS BEING DONE.
      DO 4006 JL=1,JSI
      DO 4007 JC=1,JSI
      ERS=0.
      EY20=0.
      ELS=0.
      ELL=0.
C     ERS,EY20,ELS,AND ELL REPRESENT EIGEN VALUES OF SMALL R**2,Y20,LS,
C     AND LL,RESPECTIVELY.
      IF(SLON(I,JL).NE.SLON(I,JC))GO TO 4302
      IF(GLAON(I,JL).NE.GLAON(I,JC))GO TO 4303
      IF(SIGON(I,JL).NE.SIGON(I,JC))GO TO 4304
C     FOR SAME SLON,GLAON AND SIGON
      ERS=TNNI(I)+1.5
      VCA=SLON(I,JL)
```

```
      VCB=2.
      VCC=VCA
      VCX=GLAON(I,JL)
      VCY=0.
      VCZ=VCX
      VCXX=0.
      VCZZ=0.
      EY20=SQRT(5./4./3.1415926)*VCCOEF(VCA,VCX,VCB,VCY,VCC,VCZ)*
     1VCCOEF(VCA,VCXX,VCB,VCY,VCC,VCZZ)
      ELS=SIGON(I,JC)*GLAON(I,JC)
      ELL=SLON(I,JC)*(SLON(I,JC)+1.)
      GO TO 4303
 4304 WRITE(6,4203)
 4203 FORMAT(1H ,31HTHIS COMBINATION IS IMPROBABLE.)
 4303 IF(GLAON(I,JL).NE.GLAON(I,JC)+1.)GO TO 4305
      IF(SIGON(I,JL).NE.SIGON(I,JC)-1.)GO TO 4306
C     FOR SAME SLON  DIFFERENT GLAON AND SIGON
      ELS=0.5*SQRT((SLON(I,JL)-GLAON(I,JC))*(SLON(I,JC)+GLAON(I,JC)+1.))
      GO TO 4305
 4306 WRITE(6,4203)
 4305 IF(GLAON(I,JL).NE.GLAON(I,JC)-1.)GO TO 4302
      IF(SIGON(I,JL).NE.SIGON(I,JC)+1.)GO TO 4307
C     FOR SAME SLON DIFFERENT GLAON AND SIGON
      ELS=0.5*SQRT((SLON(I,JL)+GLAON(I,JC))*(SLON(I,JC)-GLAON(I,JC)+1.))
      GO TO 4302
 4307 WRITE(6,4203)
 4302 IF(ABS(SLON(I,JL)-SLON(I,JC)).NE.2.)GO TO 4308
      IF(GLAON(I,JL).NE.GLAON(I,JC))GO TO 4308
      SLONL=SLON(I,JL)
      SLONC=SLON(I,JC)
      SLONM=AMAX1(SLONL,SLONC)
      ERS=SQRT((TNNI(I)-SLONM+2.)*(TNNI(I)+SLONM+1.))
      VCA=SLON(I,JC)
      VCB=2.
      VCC=SLON(I,JL)
      VCX=GLAON(I,JC)
      VCY=0.
      VCZ=VCX
      VCXX=0.
      VCZZ=0.
      EY20=SQRT(5./4./3.1415926*(2.*SLON(I,JC)+1.)/(2.*SLON(I,JL)+1.))*
     1VCCOEF(VCA,VCX,VCB,VCY,VCC,VCZ)*VCCOEF(VCA,VCXX,VCB,VCY,VCC,VCZZ)
 4308 A(JL,JC)=-ETA(JD)*4./3.*SQRT(3.1415926/5.)*ERS*EY20-2.*ELS-SMU(IE)
     1*ELL
 4007 CONTINUE
 4006 CONTINUE
      WRITE(6,4204)(SLON(I,J),GLAON(I,J),SIGON(I,J),J=1,JSI)
 4204 FORMAT(1H ,7HSMALL L,F10.5,5X,11HLARGE LAMDA,F10.5,5X,5HSIGMA,F10.
     15)
      WRITE(6,4205)
 4205 FORMAT(1H ,41HDIAGONAL AND OFF DIAGONAL MATRIX ELEMENTS)
      WRITE(6,4206)((A(JL,JC),JC=1,JSI),JL=1,JSI)
 4206 FORMAT(1H ,8F15.7)
```

```
      DO 4010JL=1,JSI
      DO 4011 JC=1,JSI
      A(JL,JC)=A(JC,JL)
 4011 CONTINUE
 4010 CONTINUE
      CALL EIG1(A,U,N,EPS,ITMAX,IND)
      WRITE(6,4217)
 4217 FORMAT(1H ,12HEIGEN VALUES)
      GO TO(4309,4309,4310,4311,4321),JSI
 4309 WRITE(6,4207)((A(JL,JC),JC=1,JSI),JL=1,JSI)
      GO TO 4318
 4310 WRITE(6,4208)((A(JL,JC),JC=1,JSI),JL=1,JSI)
      GO TO 4318
 4311 WRITE(6,4209)((A(JL,JC),JC=1,JSI),JL=1,JSI)
      GO TO 4318
 4321 WRITE(6,4218)((A(JL,JC),JC=1,JSI),JL=1,JSI)
      GO TO 4318
 4207 FORMAT(1H ,2F15.7)
 4208 FORMAT(1H ,3F15.7)
 4209 FORMAT(1H ,4F15.7)
 4218 FORMAT(1H ,5F15.7)
 4318 WRITE(6,4210)
 4210 FORMAT(1H ,28HEIGEN VECTOR SMALL A L LAMDA)
      GO TO (4312,4312,4313,4314,4322),JSI
 4312 WRITE(6,4207)((U(JL,JC),JC=1,JSI),JL=1,JSI)
      GO TO 4319
 4313 WRITE(6,4208)((U(JL,JC),JC=1,JSI),JL=1,JSI)
      GO TO 4319
 4314 WRITE(6,4209)((U(JL,JC),JC=1,JSI),JL=1,JSI)
      GO TO 4319
 4322 WRITE(6,4218)((U(JL,JC),JC=1,JSI),JL=1,JSI)
 4319 WRITE(6,4228)
 4228 FORMAT(1H ,28HEIGEN VECTOR LARGE A L LAMDA)
      DO 4008 JL=1,JSI
      DO 4009 JC=1,JSI
      ALLON(JL,JC)=U(JL,JC)/U(1,JC)
 4009 CONTINUE
 4008 CONTINUE
      GO TO(4315,4315,4316,4317,4323),JSI
 4315 WRITE(6,4207)((ALLON(JL,JC),JC=1,JSI),JL=1,JSI)
      GO TO 4320
 4316 WRITE(6,4208)((ALLON(JL,JC),JC=1,JSI),JL=1,JSI)
      GO TO 4320
 4317 WRITE(6,4209)((ALLON(JL,JC),JC=1,JSI),JL=1,JSI)
      GO TO 4320
 4323 WRITE(6,4218)((ALLON(JL,JC),JC=1,JSI),JL=1,JSI)
 4320 WRITE(6,4211)N,EPS,ITMAX,IND
 4211 FORMAT(1H ,9HN OF E1G1,I9,3X,3HEPS,F9.3,3X,5HITMAX,I9,3X,3HIND,I9)
      WRITE(6,4212)
 4212 FORMAT(1H ,40HCALCULATION FOR THIS DEFORMATION IS OVER//)
 4000 CONTINUE
      WRITE(6,4213)
 4213 FORMAT(1H ,40HCALCULATION FOR THIS N AND OMEGA IS OVER//)
```

```
 4002 CONTINUE
      WRITE(6,4214)
 4214 FORMAT(1H ,26HCALCULATION FOR MU IS OVER//////)
 4001 CONTINUE
 4301 STOP
      END

¥JAC

¥VCCDEF                          HARP
      FUNCTION VCCDEF(VCA,VCX,VCB,VCY,VCC,VCZ)
      DIMENSION VCS(99)
      COMMON VCI(99)
      IF(VCA+VCB-VCC.LT.-0.00001)GO TO 2012
      IF(VCB+VCC-VCA.LT.-0.00001)GO TO 2012
      IF(VCC+VCA-VCB.LT.-0.00001)GO TO 2012
      IF(VCA-VCX.LT.-0.00001)GO TO 2012
      IF(VCB-VCY.LT.-0.00001)GO TO 2012
      IF(VCC-VCZ.LT.-0.00001)GO TO 2012
      IF(ABS(VCX+VCY-VCZ).GT.0.00001)GO TO 2012
      VCI(1)=0.
      DO 2001 IV=1,98
      VCI(IV+1)=VCI(IV)+1.
 2001 CONTINUE
      ABCM=VCA+VCB-VCC
      AXM=VCA-VCX
      BYM=VCB-VCY
      CZ=VCC+VCZ
      CZM=VCC-VCZ
      ABC1=VCA+VCB+VCC+1.
      ABMC=VCA-VCB+VCC
      AMBC=VCB+VCC-VCA
      AX=VCA+VCX
      BY=VCB+VCY
      SQVCP=SQRT((2.*VCC+1.)*FACTO(ABCM)*FACTO(AXM)*FACTO(BYM)*FACTO(CZ)
     1*FACTO(CZM)/(FACTO(ABC1)*FACTO(ABMC)*FACTO(AMBC)*FACTO(AX)*
     2FACTO(BY)))
      VCS(1)=0.
      SMVCP=0.
      DO 2002 JV=1,99
      AXS=VCA+VCX+VCS(JV)
      BCXMSM=VCB+VCC-VCX-VCS(JV)
      S=VCS(JV)
      AXMSM=VCA-VCX-VCS(JV)
      CZMSM=VCC-VCZ-VCS(JV)
      BCMXS=VCB-VCC+VCX+VCS(JV)
      IF(CZMSM.LT.-0.00001)GO TO 2011
      IF(AXMSM.LT.-0.00001)GO TO 2011
      IF(BCMXS.LT.-0.00001)GO TO 2017
      SMVCP=SMVCP+(-1.)**(VCS(JV)+VCA-VCX)*FACTO(AXS)*FACTO(BCXMSM)/
     1(FACTO(S)*FACTO(AXMSM)*FACTO(CZMSM)*FACTO(BCMXS))
 2017 VCS(JV+1)=VCS(JV)+1.
```

```
 2002 CONTINUE
 2011 VCOEF=SQVCP*SMVCP
      GO TO 2013
 2012 VCOEF=0.
 2013 RETURN
      END
¥FACTO                          HARP
      FUNCTION FACTO(VF)
      COMMON VCI(99)
      FACTO=1.
      IF(ABS(VF).LT.0.00001)GO TO 4001
      IF(VF.LT.-0.00001)GO TO 4002
      DO 4003 IV=1,99
      FACTO=FACTO*(VF-VCI(IV))
      IF(VF-VCI(IV).LT.1.00001)GO TO 4001
 4003 CONTINUE
      WRITE(6,4201)FACTO
 4201 FORMAT(1H ,30HFACTO REPEATED TOO MUCH.      ,E17.8)
      GO TO 4001
 4002 WRITE(6,4202)VF
 4202 FORMAT(1H ,35HTHIS ARGUMENT IN FACTO IS INVALID. ,E17.8)
 4001 RETURN
      END
```

```
¥QPFEEG                    HARP
      WRITE(6,5201)
 5201 FORMAT(1H1,62HCALCULATION OF FERMI ENERGY AND ENERGY GAP FOR QUASI
     1 PARTICLES///)
      DIMENSION DTA(99),LN(99),TNNI(99),SRNI(99),ENU(99),FERM(99),
     1ENEGP(99),PAIRE(99),PARNO(99),SKAP(9,9),AM(99)
      DO 5001 K=1,9
      READ(5,5101)KS,IES
 5101 FORMAT(2I5)
      READ(5,5104)(SKAP(K,KN),KN=1,KS)
      IF(KS.EQ.-1)GO TO 5304
      DO 5002 IE=1,IES
      READ(5,5102)DTA(IE),IS
 5102 FORMAT(F10.5,I5)
      DO 5003 I=1,IS
      READ(5,5103)LN(I),TNNI(I),SRNI(I)
 5103 FORMAT(I5,2F10.5)
 5003 CONTINUE
      DO 5004 IA=1,98
      READ(5,5104)AM(IA),FERMI,FERMF,FERMN,ENEGPI,ENEGPF,ENEGPN
 5104 FORMAT(7F10.5)
C     UPPER VARIABLES EXCEPT AM ARE GIVEN IN UNITS OF MEV.
      IF(AM(IA).LE.-1.)GO TO 5303
      WRITE(6,5203)AM(IA),DTA(IE)
 5203 FORMAT(1H ,11HMASS NUMBER,9X,F15.7,15X,25HDEFORMATION PARAMETER DT
     1A,F15.7/1H ,12HLEVEL NUMBER,2X,26HHARMONIC OSCILLATOR NUMBER,2X,25
     2HEIGENVALUES OF FUNCTION R,2X,20HNILSSON LEVEL ENERGY,2X,12HLSCOUP
     3LING K)
      DO 5005 I=1,IS
      KI=INT(TNNI(I))+1
      ENU(I)=41./AM(IA)**0.33333*(1./(1.-4./3.*DTA(IE)**2-
     116./27.*DTA(IE)**3)**0.166667*(TNNI(I)+1.5)+SRNI(I)*
     2SKAP(K,KI))
      WRITE(6,5204)LN(I),TNNI(I),SRNI(I),ENU(I),SKAP(K,KI)
 5204 FORMAT(1H ,I5,9X,F15.7,13X,F15.7,12X,F15.7,9X,F15.7)
 5005 CONTINUE
      FERM(1)=FERMI
      DO 5006 LL=1,98
      WRITE(6,5205)FERM(LL)
 5205 FORMAT(1H ,18HFERMI ENERGY LAMDA,F15.7/1H ,10HENERGY GAP,5X,14HPAI
     1RING ENERGY,1X,15HPARTICLE NUMBER)
      1ENEGP(1)=ENEGPI
      LDS=0
      DO 5007 LD=1,98
      LDS=LDS+1
      PARNO(LD)=0.
      PAIREI=0.
      DO 5008 I=1,IS
      PAIREI=PAIREI+(1./SQRT((ENU(I)-FERM(LL))**2+ENEGP(LD)**2))
      PARNO(LD)=PARNO(LD)+1.-(ENU(I)-FERM(LL))/
     1SQRT((ENU(I)-FERM(LL))**2+ENEGP(LD)**2)
 5008 CONTINUE
      PAIRE(LD)=2./PAIREI
```

```
      ENEGP(LD+1)=ENEGP(LD)+ENEGPN
      IF(ENEGP(LD+1).GT.ENEGPF)GO TO 5301
  007 CONTINUE
  301 WRITE(6,5206)(ENEGP(LD),PAIRE(LD),PARNO(LD),LD=1,LDS)
  206 FORMAT(1H ,5(F5.2,F8.4,F10.4))
      FERM(LL+1)=FERM(LL)+FERMN
      IF(FERM(LL+1).GT.FERMF)GO TO 5302
  006 CONTINUE
  302 WRITE(6,5207)
  207 FORMAT(1H ,36HCALCULATION FOR THIS NUCLEUS IS OVER/////)
  004 CONTINUE
  303 WRITE(6,5208)
  208 FORMAT(1H ,40HCALCULATION FOR THIS DEFORMATION IS OVER//////////)
  002 CONTINUE
      WRITE(6,5209)
  209 FORMAT(1H ,41HCALCULATION FOR THIS IS PARAMETER IS OVER//////////)
  001 CONTINUE
  304 STOP
      END
```

```
¥CORIOJ                    HARP
      WRITE(6,211)
  211 FORMAT(1H1,23HCORIOLIS COUPLING MODEL///)
      DIMENSION AM(19),ZN(19),HBI(19),ETA(9),TNNI(15),OMNI(15),ZNNI(15),
     1GLANI(15),SRNI(15),SLON(15,7),GLAON(15,7),SIGON(15,7),ALLON(15,7),
     2SALLON(15,7),CJON(15,7),SJON(15,7),PHNI(15),ROI(15),ROK(15),M(15)
     3,JS(15),SUMAS(15),SQSUMA(15),CLS(15),EOMNU(15),EPONU(15),A(15,15),
     4DCCOE(15),VCCO(15),U(15,15),AB(15,15),CLL(15),SKAP(19),FERM(99),
     5ENEGP(19),NINOC(99),SUMJJ(15),EOMNJ(15)
      DIMENSION NINOR(99),NNIN(19),TNNIR(99),OMNIR(99),ZNNIR(99),
     1GLANR(99) ,SLONR(99,7),GLAOR(99,7),SIGOR(99,7),JSR(99),ISR(99),
     2SRNIR(19)
      READ(5,120)IN
  120 FORMAT(I5)
      DO 53 N=1,IN
      READ(5,121)NINOR(N), JSR(N),TNNIR(N),OMNIR(N),ZNNIR(N),GLANR(N)
  121 FORMAT(2I5,F5.0,F5.1,2F5.0)
      JSI=JSR(N)
      READ(5,122)(SLONR(N,J),GLAOR(N,J),SIGOR(N,J),J=1,JSI)
  122 FORMAT(4(2F5.0,F5.1))
   53 CONTINUE
      DO 11 IA=1,19
      READ(5,123)AM(IA),ZN(IA),SKAP(IA),ISR(IA)
  123 FORMAT(3F5.0,I5)
      IF(AM(IA).EQ.0.)GO TO 1110
      SKPP=SKAP(IA)
      IS=ISR(IA)
      READ(5,124)(NNIN(I),I=1,IS)
  124 FORMAT(7I10)
      WRITE(6,212)AM(IA),ZN(IA),SKAP(IA)
  212 FORMAT(1H ,11HMASS NUMBER,9X,F16.7/1H ,13HATOMIC NUMBER,7X,F16.7/1
     1H ,35HSTRENGTH PARAMETER OF LS COUPLING K,F15.7)
      DO 12 IE=1,9
      READ(5,125)ETA(IE),FERM(IE),ENEGP(IE)
  125 FORMAT(3F10.5)
      IF(ETA(IE).EQ.-1.)GO TO 1109
      WRITE(6,213)ETA(IE),FERM(IE),ENEGP(IE)
  213 FORMAT(1H ,21HDEFORMATION PARAMETER,9X,F16.7/1H ,18HFERMI ENERGY L
     1AMDA,12X,F16.7/1H ,10HENERGY GAP,20X,F16.7)
      READ(5,126)(SRNIR(I),I=1,IS)
  126 FORMAT(7F10.5)
      DO 55 I=1,IS
      DO 56 N=1,IN
      IF(NINOR(N).NE.NNIN(I))GO TO 56
      JS(I)=JSR(N)
      JSI=JS(I)
      READ(5,126)(ALLON(I,IJ),IJ=1,JSI)
      TNNI(I)=TNNIR(N)
      OMNI(I)=OMNIR(N)
      ZNNI(I)=ZNNIR(N)
      GLANI(I)=GLANR(N)
      SRNI(I)=SRNIR(I)
      NINOC(I)=NNIN(I)
```

```
      DO 57 J=1,JSI
      SLON(I,J)=SLONR(N,J)
      GLAON(I,J)=GLAOR(N,J)
      SIGON(I,J)=SIGOR(N,J)
   57 CONTINUE
   56 CONTINUE
   55 CONTINUE
      WRITE(6,238)
  238 FORMAT(1HO,33HNILSSON MODEL WITH QUASI PARTICLE)
      DO 15 I=1,IS
      SUMAS(I)=0.
      JSI=JS(I)
      WRITE(6,214)TNNI(I),OMNI(I),ZNNI(I),GLANI(I),SRNI(I),NINOC(I)
  214 FORMAT(1HO,11HN,F9.3,3X,5HOMEGA,F9.3,3X,8HSMALL NZ,F9.3,3X,11HLARGE
     1 LAMDA,F9.3,3X,7HSMALL R,F12.5,3X,11HORBITAL NO.,I5)
      DO 16 J=1,JSI
      SUMAS(I)=SUMAS(I)+ALLON(I,J)**2
   16 CONTINUE
      SQSUMA(I)=SQRT(SUMAS(I))
      DO 17 J=1,JSI
      SALLON(I,J)=ALLON(I,J)/SQSUMA(I)
      WRITE(6,215)SLON(I,J),GLAON(I,J),SIGON(I,J),ALLON(I,J),SALLON(I,J)
  215 FORMAT(1H ,7HSMALL L,F9.3,3X,11HLARGE LAMDA,F9.3,3X,5HSIGMA,F9.3,3
     1X,7HALLAMDA,F12.5,3X,13HSMALL ALLAMDA,F12.7)
   17 CONTINUE
      SJON(I,1)=SLON(I,1)+0.5
      DO 18 K=1,JSI
      CJON(I,K)=0.
      DO 19 J=1,JSI
      IF(SLON(I,J).EQ.SJON(I,K)-0.5)GO TO 1111
      IF(SLON(I,J).NE.SJON(I,K)+0.5)GO TO 19
 1111 VCA=SLON(I,J)
      VCX=GLAON(I,J)
      VCB=0.5
      VCY=SIGON(I,J)
      VCC=SJON(I,K)
      VCZ=OMNI(I)
      CJON(I,K)=CJON(I,K)+SALLON(I,J)*VCCOEF(VCA,VCX,VCB,VCY,VCC,VCZ)
   19 CONTINUE
      WRITE(6,217)SJON(I,K),CJON(I,K)
  217 FORMAT(1H ,7HSMALL J,F9.3,3X,8HSMALL CJ,F12.7)
      SJON(I,K+1)=SJON(I,K)-1.
      IF(SJON(I,K+1).LT.OMNI(I))GO TO 1112
   18 CONTINUE
 1112 CLS(I)=0.
      DO 20 K=1,JSI
      DO 21 J=1,JSI
      IF(GLAON(I,J).NE.GLAON(I,K))GO TO 1113
      CLSP=SIGON(I,J)*GLAON(I,J)
      IF(SLON(I,J).NE.SLON(I,K))GO TO 1113
      CLL(I)=CLL(I)+SLON(I,J)*(SLON(I,J)+1.)*SALLON(I,J)**2
 1113 IF(GLAON(I,J).NE.GLAON(I,K)+1.)GO TO 1114
      CLSP=0.5*SQRT((SLON(I,J)-GLAON(I,J))*(SLON(I,J)+GLAON(I,J)+1.))
```

```
 1114 IF(GLAON(I,J).NE.GLAON(I,K)-1.)GO TO 1115
      CLSP=0.5*SQRT((SLON(I,J)+GLAON(I,J))*(SLON(I,J)-GLAON(I,J)+1.))
 1115 CLS(I)=CLS(I)+CLSP*SALLON(I,K)*SALLON(I,J)
   21 CONTINUE
   20 CONTINUE
      EOMNU(I)=41./AM(IA)**0.33333*(1./(1.-4./3.*(SKPP*ETA(IE))**2-
     116./27.*(SKPP*ETA(IE))**3)**0.16667*(TNNI(I)+1.5)+SRNI(I)*
     2SKPP)
   15 CONTINUE
      READ(5,117)IHS
      READ(5,118)(HBI(IH),IH=1,IHS)
      READ(5,117)IIS
  117 FORMAT(I5)
      DO 43 I=1,IS
      SUMJJ(I)=0.
      JSI=JS(I)
      DO 52 K=1,JSI
      SUMJJ(I)=SUMJJ(I)+CJON(I,K)**2*SJON(I,K)*(SJON(I,K)+1.)
   52 CONTINUE
      EOMNJ(I)=EOMNU(I)+SUMJJ(I)*HBI(IH)*1.
      EPONU(I)=SQRT((EOMNJ(I)-FERM(IE))**2+ENEGP(IE)**2)
      WRITE(6,218)EPONU(I),SKAP(IA)
  218 FORMAT(1H ,85HEPSIRON OMEGA NU,RELATIVE GROUND STATE ENERGY IN MEV
     1 NOT CONSIDERED DECOUPLING FACTOR,3X,F17.7/1H ,4HSKAP,F12.5)
   43 CONTINUE
      READ(5,118)(ROI(II),II=1,IIS)
  118 FORMAT(7F10.5)
      DO 44 IH=1,IHS
      WRITE(6,247)HBI(IH)
      DO 22 II=1,IIS
      ROK(1)=ROI(II)
      WRITE(6,219)ROI(II)
  219 FORMAT(1H ,21HSPIN OF NUCLEAR LEVEL,3X,F17.7)
  247 FORMAT(1H ,19HROTATIONAL CONSTANT,5X,F17.7)
      N=0
      DO 39 I=1,IS
      DO 40 J=1,IS
      AB(I,J)=0.
   40 CONTINUE
   39 CONTINUE
      DO 23 K=1,15
      DO 24 I=1,IS
      JSI=JS(I)
      IF(OMNI(I).EQ.ROK(K))GO TO 1118
      IF(OMNI(I).NE.-ROK(K))GO TO 1119
 1118 N=N+1
      AB(I,I)=HBI(IH)*(ROI(II)*(ROI(II)+1.)-2.*ROK(K)**2)+EPONU(I)
      IF(ABS(ROK(K)).NE.0.5)GO TO 1120
      DCCOE(I)=0.
      DO 25 IC=1,JSI
      DCCOE(I)=DCCOE(I)+(-1.)**(SJON(I,IC)-0.5)*(SJON(I,IC)+0.5)*CJON(I,
     1IC)**2
   25 CONTINUE
```

```
      AB(I,I)=AB(I,I)+HBI(IH)*DCCOE(I)*(-1.)**(ROI(II)+0.5)*(ROI(II)+0.5
     1)
 1120 DO 26 J=1,IS
      IF(OMNI(J).GT.ROK(1))GO TO 26
      JSJ=JS(J)
      IF(ROK(K).GT.0.)GO TO 1121
      IF(OMNI(J).EQ.-(ROK(K)-1.))GO TO 1122
      IF(OMNI(J).EQ.-(ROK(K)+1.))GO TO 1123
      IF(ABS(OMNI(J)+ROK(K)).NE.1.)GO TO 1124
 1122 VCCO(I)=0.
      DO 27 JC=1,JSI
      JDD=0
      DO 28 JD=1,JSJ
      JDD=JDD+1
      IF(SJON(J,JD).EQ.SJON(I,JC))GO TO 1125
   28 CONTINUE
      IF(JC.EQ.JSI)GO TO 1126
      IF(SJON(J,JDD).NE.SJON(I,JC))GO TO 27
 1125 VCCO(I)=VCCO(I)+CJON(I,JC)*CJON(J,JDD)*(-1.)**(ROI(II)-0.5)*SQRT((
     1SJON(I,JC)+ROK(K))*(SJON(I,JC)-ROK(K)+1.))
   27 CONTINUE
 1126 AB(I,J)=-HBI(IH)*SQRT((ROI(II)+ROK(K))*(ROI(II)-ROK(K)+1.))*VCCO(I
     1)
      GO TO 26
 1123 VCCO(I)=0.
      DO 29 JC=1,JSI
      JDD=0
      DO 30 JD=1,JSJ
      JDD=JDD+1
      IF(SJON(J,JD).EQ.SJON(I,JC))GO TO 1127
   30 CONTINUE
      IF(JC.EQ.JSI)GO TO 1128
      IF(SJON(J,JDD).NE.SJON(I,JC))GO TO 29
 1127 VCCO(I)=VCCO(I)+CJON(I,JC)*CJON(J,JDD)*(-1.)**(ROI(II)-0.5)*SQRT((
     1SJON(I,JC)-ROK(K))*(SJON(I,JC)+ROK(K)+1.))
   29 CONTINUE
 1128 AB(I,J)=-HBI(IH)*SQRT((ROI(II)-ROK(K))*(ROI(II)+ROK(K)+1.))*VCCO(I
     1)
 1124 GO TO 26
 1121 IF(OMNI(J).EQ.ROK(K)+1.)GO TO 1129
      IF(OMNI(J).EQ.ROK(K)-1.)GO TO 1130
      IF(ABS(OMNI(J)-ROK(K)).NE.1.)GO TO 1131
 1129 VCCO(I)=0.
      DO 31 JC=1,JSI
      JDD=0
      DO 32 JD=1,JSJ
      JDD=JDD+1
      IF(SJON(J,JD).EQ.SJON(I,JC))GO TO 1132
   32 CONTINUE
      IF(JC.EQ.JSI)GO TO 1133
      IF(SJON(J,JDD).NE.SJON(I,JC))GO TO 31
 1132 VCCO(I)=VCCO(I)+CJON(I,JC)*CJON(J,JDD)*(-1.)**(ROI(II)-0.5)*SQRT((
     1SJON(I,JC)-ROK(K))*(SJON(I,JC)+ROK(K)+1.))
   31 CONTINUE
```

```
1133 AB(I,J)=-HBI(IH)*SQRT((ROI(II)-ROK(K))*(ROI(II)+ROK(K)+1.))*VCCO(I
     1)
      GO TO 26
1130 VCCO(I)=0.
      DO 33 JC=1,JSI
      JDD=0
      DO 34  JD=1,JSJ
      JDD=JDD+1
      IF(SJON(J,JD).EQ.SJON(I,JC))GO TO 1134
   34 CONTINUE
      IF(JC.EQ.JSI)GO TO 1135
      IF(SJON(J,JDD).NE.SJON(I,JC))GO TO 33
1134 VCCO(I)=VCCO(I)+CJON(I,JC)*CJON(J,JDD)*(-1.)**(ROI(II)-0.5)*SQRT((
     1SJON(I,JC)+ROK(K))*(SJON(I,JC)-ROK(K)+1.))
   33 CONTINUE
1135 AB(I,J)=-HBI(IH)*SQRT((ROI(II)+ROK(K))*(ROI(II)-ROK(K)+1.))*VCCO(I
     1)
1131 GO TO 26
   26 CONTINUE
1119 GO TO 24
   24 CONTINUE
      ROK(K+1)=ROK(K)-2.
      IF(ABS(ROK(K+1)).GT.ROK(1))GO TO 1136
   23 CONTINUE
1136 EPS=0.001
      ITMAX=111
      IND=1
      DO 35 IU=1,N
      DO 36 JU=1,N
      U(IU,JU)=0.
      A(IU,JU)=0.
   36 CONTINUE
   35 CONTINUE
      NI=0
      DO 37 I=1,IS
      IF(AB(I,I).EQ.0.)GO TO 37
      NI=NI+1
      M(I)=NI
      A(NI,NI)=AB(I,I)
      WRITE(6,220)TNNI(I),OMNI(I),ZNNI(I),AB(I,I)
  220 FORMAT(1H ,1HN,F9.3,3X,5HOMEGA,F9.3,3X,8HSMALL NZ,F9.3,3X,35HENERG
     1Y OF LEVEL I N OMEGA NZ IN MEV,F16.7)
   37 CONTINUE
      DO 41 I=1,IS
      DO 38 J=1,IS
      IF(AB(I,J).EQ.0.)GO TO 38
      NJ=M(J)
      NI=M(I)
      A(NI,NJ)=0.5*AB(I,J)*(SQRT((1.+(EOMNJ(I)-FERM(IE))/EPONU(I))*
     1(1.+(EOMNJ(J)-FERM(IE))/EPONU(J)))+SQRT((1.-(EOMNJ(I)-FERM(IE)
     2)/EPONU(I))*(1.-(EOMNJ(J)-FERM(IE))/EPONU(J))))
   38 CONTINUE
   41 CONTINUE
```

```
      WRITE(6,235)
  235 FORMAT(1H ,41HDIAGONAL AND OFF DIAGONAL MATRIX ELEMENTS)
      WRITE(6,236)((A(I,J),J=1,N),I=1,N)
  236 FORMAT(1H ,15F8.4)
      DO 45 I=1,N
      DO 46 J=1,N
      A(I,J)=A(J,I)
   46 CONTINUE
   45 CONTINUE
      CALL EIG1(A,U,N,EPS,ITMAX,IND)
      WRITE(6,230)
  230 FORMAT(1H ,44HLEVEL ENERGIES CONSIDERING CORIOLIS COUPLING)
      WRITE(6,231)((A(I,J),J=1,N),I=1,N)
  231 FORMAT(1H ,15F8.4)
      WRITE(6,232)
  232 FORMAT(1H ,25HEIGEN VECTOR,LARGE C K NU)
      WRITE(6,233)((U(I,J),I=1,N),J=1,N)
  233 FORMAT(1H ,15F8.4)
      WRITE(6,234)N,EPS,ITMAX,IND
  234 FORMAT(1H ,9HN OF EIG1,I9,3X,3HEPS,F9.3,3X,5HITMAX,I9,3X,3HIND,I9)
      WRITE(6,221)
  221 FORMAT(1H ,33HCALCULATION OF THIS LEVEL IS OVER//)
   22 CONTINUE
      WRITE(6,248)
  248 FORMAT(1H ,48HCALCULATION FOR THIS ROTATIONAL CONSTANT IS OVER//)
   44 CONTINUE
      WRITE(6,222)
  222 FORMAT(1H ,40HCALCULATION FOR THIS DEFORMATION IS OVER//)
   12 CONTINUE
 1109 WRITE(6,223)
  223 FORMAT(1H ,36HCALCULATION FOR THIS NUCLEUS IS OVER//)
   11 CONTINUE
 1110 WRITE(6,224)
  224 FORMAT(1H ,19HCALCULATION IS OVER//)
      STOP
      END

¥JAC

¥VCCOEF

¥FACTO
```

```
¥CORBE2 HARP
      WRITE(6,3201)
 3201 FORMAT(1H1,88HREDECED TRANSITION PROBABILITIES DEDUCED FROM CORIOL
     1IS COUPLING MODEL IN UNITS OF E2FM-4/////)
      DIMENSION AM(19),ZN(19),QO(19),SN(5),ETA(19),BETA(19),ROIE(19),
     1ROIKE(20,10),ROCKE(20,10),SLONE(20,10,5),GLAONE(20,10,5),
     2SIGONE(20,10,5),TNNIE(20,10),LBS(20),LCS(20,10),ALLONE(20,10,5)
     3,FERM(19),ENEGP(19),EOMNU(20,10),EPONU(20,10),SRNI(20,10),
     4NINO(20,10),SKAP(19),HBI(19)
      DIMENSION NIN(39),LCSN(39),TNNI(39),ROIK(39),SLON(39,9),
     1SIGON(39,9),GLAON(39,9),LBSN(39),NNIN(39),SRN(39),ALLON(39,9),
     2ENER(20)
      READ(5,2101)IN
 2101 FORMAT(I5)
      DO 2001 N=1,IN
      READ(5,2102)NIN(N),LCSN(N),TNNI(N),ROIK(N)
 2102 FORMAT(2I5,F5.0,F5.1)
      LS=LCSN(N)
      READ(5,2103)(SLON(N,L),GLAON(N,L),SIGON(N,L),L=1,LS)
 2103 FORMAT(4(2F5.0,F5.1))
 2001 CONTINUE
      DO 3001 IA=1,19
      READ(5,3101)AM(IA),ZN(IA),SKAP(IA),LBSN(IA)
 3101 FORMAT(3F5.0,I5)
      IF(AM(IA).EQ.0.)GO TO 3306
      SKPP=SKAP(IA)
      LS=LBSN(IA)
      READ(5,3102)(NNIN(L),L=1,LS)
 3102 FORMAT(7I10)
      WRITE(6,3202)AM(IA),ZN(IA)
 3202 FORMAT(1H ,11HMASS NUMBER,F12.5,17X,13HATOMIC NUMBER,F12.5//)
      H2MW=2.*(1.05443)**2/0.41/1.67239/1.60206*AM(IA)**(1./3.)
      DO 3002 IE=1,19
      READ(5,3103)ETA(IE),FERM(IE),ENEGP(IE),HBI(IE),LAS
 3103 FORMAT(4F10.5,I5)
      IF(ETA(IE).EQ.-1.)GO TO 3301
      READ(5,3104)(SRN(L),L=1,LS)
 3104 FORMAT(7F10.5)
      DO 2003 L=1,LS
      DO 2004 N=1,IN
      IF(NIN(N).NE.NNIN(L))GO TO 2004
      NLCS=LCSN(N)
      READ(5,3104)(ALLON(L,LC),LC=1,NLCS)
 2004 CONTINUE
 2003 CONTINUE
      BETA(IE)=4./3.*SQRT(3.1416/5.)*ETA(IE)*SKPP*(1.-4./3.*(ETA(IE)*
     1SKPP)**2-16./27.*(ETA(IE)*SKPP)**3)**(1./6.)
      QO(IA)=0.8*ZN(IA)*(1.2*AM(IA)**0.33333)**2* 3./4.*SQRT(5./3.1416)*
     1BETA(IE)*(1.+0.5*SQRT(5./3.1416)*BETA(IE))
      WRITE(6,3203)ETA(IE),BETA(IE),FERM(IE),ENEGP(IE),SKAP(IA),HBI(IE)
 3203 FORMAT(1H ,20HDEFOR. PARAM. ETA   ,20HDEFOR. PARAM. BETA  ,20HFERM
     1I ENE. LAMDA MEV,20HENE. GAP DELTA MEV  ,20HHLS STRENGTH       ,2
     20HROTATIONAL CONSTANT /1H ,6(F12.5,5X))
```

```
      WRITE(6,3212)QO(IA)
 3212 FORMAT(1H ,25HINTRINSIC QUAD. MOMENT    ,F12.5)
      WRITE(6,3211)
 3211 FORMAT(1HO,33HNILSSON MODEL WITH QUASI PARTICLE)
      DO 3003 LA=1,LAS
      READ(5,3114)ROIE(LA),ENER(LA)
 3114 FORMAT(2F10.5)
      READ(5,3104)(ROCKE(LA,LB),LB=1,LS)
      DO 3004 LB=1,LS
      DO 3005 N=1,IN
      IF(NIN(N).NE.NNIN(LB))GO TO 3005
      LBS(LA)=LBSN(IA)
      TNNIE(LA,LB)=TNNI(N)
      ROIKE(LA,LB)=ROIK(N)
      SRNI(LA,LB)=SRN(LB)
      LCS(LA,LB)=LCSN(N)
      NIND(LA,LB)=NNIN(LB)
      LCSAB=LCS(LA,LB)
      SALL=0.
      DO 2005 LC=1,LCSAB
      SLONE(LA,LB,LC)=SLON(N,LC)
      GLAONE(LA,LB,LC)=GLAON(N,LC)
      SIGONE(LA,LB,LC)=SIGON(N,LC)
      SALL=SALL+ALLON(LB,LC)**2
 2005 CONTINUE
      DO 2006 LC=1,LCSAB
      ALLONE(LA,LB,LC)=ALLON(LB,LC)/SQRT(SALL)
 2006 CONTINUE
 3005 CONTINUE
 3004 CONTINUE
 3003 CONTINUE
      WRITE(6,3204)ROIE(1)
 3204 FORMAT(1H ,28HNUCLEAR SPIN OF GROUND STATE,9X,F12.5)
      DO 3006 LA=2,LAS
      RENER=ENER(LA)-ENER(1)
      WRITE(6,3205)ROIE(LA),RENER
 3205 FORMAT(1H ,44HNUCLEAR SPIN AND ENERGY OF THE EXCITED LEVEL,2F12.5)
      LBS1=LBS(1)
      LBSLA=LBS(LA)
      QP=0.
      QPC=0.
      SN(1)=-2.
      SN(2)=-1.
      SN(3)=0.
      SN(4)=1.
      SN(5)=2.
      DO 3007 N=1,5
      QK=0.
      QKI=0.
      QKC=0.
      DO 3008 LB1=1,LBS1
      IF(ROIE(1)-ROIKE(1,LB1).LT.-0.00001)GO TO 3008
      EOMNU(1,LB1)=41./AM(IA)**0.33333*(1./(1.-4./3.*(SKPP*ETA(IE))**2
     1-16./27.*(SKPP*ETA(IE))**3)**0.16667*(TNNIE(1,LB1)+1.5)+
     2SRNI(1,LB1)*SKPP)
```

```
      EPONU(1,LB1)=SQRT((EOMNU(1,LB1)-FERM(IE))**2+
     1ENEGP(IE)**2)
      DO 3009 LBL=1,LBSLA
      IF(ROIE(LA)-ROIKE(LA,LBL).LT.-0.00001)GO TO 3009
      EOMNU(LA,LBL)=41./AM(IA)**0.33333*(1./(1.-4./3.*(SKPP*ETA(IE))**2
     1-16./27.*(SKPP*ETA(IE))**3)**0.16667*(TNNIE(LA,LBL)+1.5)+
     2SRNI(LA,LBL)*SKPP)
      EPONU(LA,LBL)=SQRT((EOMNU(LA,LBL)-FERM(IE))**2+ENEGP(IE)**2)
      IF(ABS(ROIKE(1,LB1)-ROIKE(LA,LBL)-SN(N)).GT.0.00001)GO TO 3303
      QL=0.
      LCS1B=LCS(1,LB1)
      LCSAB=LCS(LA,LBL)
      DO 3010 LC1=1,LCS1B
      DO 3011 LCL=1,LCSAB
      IF(ABS(SLONE(LA,LBL,LCL)-SLONE(1,LB1,LC1)).GT.2.)GO TO 3011
      IF(ABS(SIGONE(LA,LBL,LCL)-SIGONE(1,LB1,LC1)).GT.0.00001)GO TO 3011
      IF(ABS(GLAONE(1,LB1,LC1)-GLAONE(LA,LBL,LCL)-SN(N)).GT.0.00001)
     1GO TO 3011
      VCA=SLONE(LA,LBL,LCL)
      VCB=2.
      VCC=SLONE(1,LB1,LC1)
      VCX=GLAONE(LA,LBL,LCL)
      VCY=SN(N)
      VCZ=VCX+VCY
      VCXX=0.
      VCYY=0.
      VCZZ=0.
      R2N=TNNIE(LA,LBL)
      R2LP=SLONE(1,LB1,LC1)
      R2L=SLONE(LA,LBL,LCL)
      QL=QL+EXVR2(R2N,R2LP,R2L)*SQRT((2.*R2L+1.)/(2.*R2LP+1.))*
     1VCCOEF(VCA,VCXX,VCB,VCYY,VCC,VCZZ)*ALLONE(1,LB1,LC1)*
     2ALLONE(LA,LBL,LCL)*VCCOEF(VCA,VCX,VCB,VCY,VCC,VCZ)
3011  CONTINUE
3010  CONTINUE
      UV=0.5*(SQRT((1.+(EOMNU(1,LB1)-FERM(IE))/EPONU(1,LB1))*
     1(1.+(EOMNU(LA,LBL)-FERM(IE))/EPONU(LA,LBL)))-SQRT((1.-(EOMNU(1,LB1
     2)-FERM(IE))/EPONU(1,LB1))*(1.-(EOMNU(LA,LBL)-FERM(IE))/EPONU(LA,LB
     3L))))
      VCA=ROIE(LA)
      VCB=2.
      VCC=ROIE(1)
      VCX=ROIKE(LA,LBL)
      VCY=SN(N)
      VCZ=VCX+VCY
      QK=QK+ROCKE(LA,LBL)*ROCKE(1,LB1)*VCCOEF(VCA,VCX,VCB,VCY,VCC,VCZ)*
     1(UV*(-1.)**(SN(N)*(ROIE(1)-0.5))*(1.+ZN(IA)/AM(IA)**2)*H2MW*
     2QL)
      IF(ABS(VCY).GT.0.00001)GO TO 3303
      IF(NINO(1,LB1).NE.NINO(LA,LBL))GO TO 3303
      QKC=QKC+ROCKE(LA,LBL)*ROCKE(1,LB1)*VCCOEF(VCA,VCX,VCB,VCY,VCC,VCZ)
     1*QO(IA)
      FEOCCV=VCCOEF(VCA,VCX,VCB,VCY,VCC,VCZ)
```

```
      WRITE(6,3221)QKC,ROCKE(LA,LBL),ROCKE(1,LB1),FEOCCV
 3221 FORMAT(4F12.5)
 3303 IF(ABS(ROIKE(1,LB1)-(-ROIKE(LA,LBL)-SN(N))).GT.0.00001)GO TO 3009
      QLI=0.
      LCS1B=LCS(1,LB1)
      LCSAB=LCS(LA,LBL)
      DO 3012 LC1=1,LCS1B
      DO 3013 LCL=1,LCSAB
      IF(ABS(SLONE(LA,LBL,LCL)-SLONE(1,LB1,LC1)).GT.2.)GO TO 3013
      IF(ABS(SIGONE(LA,LBL,LCL)+SIGONE(1,LB1,LC1)).GT.0.00001)GO TO 3013
      IF(ABS(GLAONE(LA,LBL,LCL)+GLAONE(1,LB1,LC1)+SN(N)).GT.0.00001)
     1GO TO 3013
      VCA=SLONE(LA,LBL,LCL)
      VCB=2.
      VCC=SLONE(1,LB1,LC1)
      VCX=GLAONE(LA,LBL,LCL)
      VCY=SN(N)
      VCZ=VCX+VCY
      VCXX=0.
      VCYY=0.
      VCZZ=0.
      R2N=TNNIE(LA,LBL)
      R2LP=SLONE(1,LB1,LC1)
      R2L=SLONE(LA,LBL,LCL)
      QLI=QLI+EXVR2(R2N,R2LP,R2L)*SQRT((2.*R2L+1.)/(2.*R2LP+1.))*
     1VCCOEF(VCA,VCXX,VCB,VCYY,VCC,VCZZ)*ALLONE(1,LB1,LC1)*
     2ALLONE(LA,LBL,LCL)*VCCOEF(VCA,VCX,VCB,VCY,VCC,VCZ)
 3013 CONTINUE
 3012 CONTINUE
      VCA=ROIE(LA)
      VCB=2.
      VCC=ROIE(1)
      VCC=ROIE(1)
      VCX=ROIKE(LA,LBL)
      VCY=SN(N)
      VCZ=VCX+VCY
      UV=0.5*(SQRT((1.+(EOMNU(1,LB1)-FERM(IE))/EPONU(1,LB1))*
     1(1.+(EOMNU(LA,LBL)-FERM(IE))/EPONU(LA,LBL)))-SQRT((1.-(EOMNU(1,LB1
     2)-FERM(IE))/EPONU(1,LB1))*(1.-(EOMNU(LA,LBL)-FERM(IE))/EPONU(LA,LB
     3L))))
      QKI=QKI+ROCKE(LA,LBL)*ROCKE(1,LB1)*VCCOEF(VCA,VCX,VCB,VCY,VCC,VCZ)
     1*(UV*(1.+ZN(IA)/AM(IA)**2)*H2MW*QL)*(-1.)**(SN(N)*(ROIE(1)-0.5)+
     22.*ROIKE(1,LB1)+0.5+TNNIE(1,LB1)+ROIE(1))
 3009 CONTINUE
 3008 CONTINUE
      QP=QP+QK+QKI+QKC
      QPC=QPC+QKC
 3007 CONTINUE
      BE2=5./16./3.141592*QP**2
      BE2C=5./16./3.141592*QPC**2
      WRITE(6,3206)BE2,BE2C
 3206 FORMAT(1H ,56HREDUCED TRANSITION PROBABILITY BE2 IF IN UNITS OF E2
     1FM-4,10X,E17.8/1H ,23HCOLLECTIVE CONTRIBUTION,43X,E17.8)
```

```
      WRITE(6,3207)
 3207 FORMAT(1H ,43HCALCULATION FOR THIS EXCITED LEVEL IS OVER.)
 3006 CONTINUE
 3302 WRITE(6,3208)
 3208 FORMAT(1H ,41HCALCULATION FOR THIS DEFORMATION IS OVER./)
 3002 CONTINUE
 3301 WRITE(6,3209)
 3209 FORMAT(1H ,37HCALCULATION FOR THIS NUCLEUS IS OVER.)
 3001 CONTINUE
 3306 STOP
      END
¥EXVR2   HARP
      FUNCTION EXVR2(R2N,R2LP,R2L)
      IF(R2LP.NE.R2L)GO TO 3501
      EXVR2=R2N+1.5
      GO TO 3502
 3501 IF(R2LP.NE.R2L-2.)GO TO 3503
      EXVR2=SQRT((R2N-R2L+2.)*(R2N+R2L+1.))
      GO TO 3502
 3503 IF(R2LP.NE.R2L+2.)GO TO 3504
      EXVR2=SQRT((R2N-R2L)*(R2N+R2L+3.))
      GO TO 3502
 3504 EXVR2=0.
 3502 RETURN
      END

¥VCCOEF

¥FACTO
```

REFERENCES

Af67 O. F. Afonin, A. P. Grinberg, I. Kh. Lemberg and I. N. Chugunov, Yad. Fiz. 6 219 (1967)

Al56 K. Alder et al., Rev. Mod. Phys. 28 432 (1956)

Al64 D. G. Alkhazov et al., Izv. Akad. Nauk. SSSR, 28 1683 (1964)

Ba57 J. Bardeern, L. N. Cooper and J. R. Schrieffer, Phys. Rev. 108 1175 (1957)

Ba60 M. Baranger, Phys. Rev. 120 957 (1960)

Be59 S. T. Beliaev, Mat. Fys. Medd. Dan. Vid. Selsk. 31 No. 11 (1959)

Bj64 I. H. Bjerregaard et al., Nucl. Phys. 51 641 (1964)

Bo52 A. Bohr, Mat. Fys. Medd. Dan. Vid. Selsk. 26 No. 14 (1952)

Bo53 A. Bohr and B. Mottelson, ibid. 27 No. 16 (1953)

Bo58 A. Bohr, B. Mottelson and D. Pines, Phys. Rev. 110 936 (1958)

Bo58a H. L. van den Bold, H. C. Geijin and P. M. Endt, Physica 24 23 (1958)

Bo62 A. Bohr and B. Mottelson, Lecture on Nuclear Structure and Energy Spectra (Inst. for Theoretical Physics and NORDITA, Copenhargen 1962)

Bo64 E. C. O. Bonacalza, Arkiv. Fysik. 26 141 (1964)

Bu58 Buchner and Mazari, Revista Mexicana de Fisica 7 117 (1958)

Cl69 F. M. Clikeman, V. C. Roger and L. E. Beghian, Bull. Am. Phys. Soc. 14 55 (1969)

Co67 S. Cohen et al., Phys. Rev. 160 903 (1967)

Cr60 M. de Croes and G. Backstrom, Ark. Fysik. 16 567 (1960)

Do68 D. P. Donnelly, J. J. Reidy and M. L. Miedenbeck, Nucl. Phys. A112 145 (1968)

Ed61 W. F. Edwards and C. J. Gallager, Nucl. Phys. 26 649 (1961)

En67 P. M. Endt and C. van der Leun, Nucl. Phys. A105 1 (1967)

Et68 R. C. Etherton, L. M. Beyer, W. H. Kelley and D. J. Horen, Phys. Rev. 168 1249 (1968)

Ev67 K. R. Evans et al., Nucl. Phys. A102 237 (1967)

Fa63 V. Fano, Ann. Rev. Nucl. Sci. 13 1 (1963)

Fr59 G. Fricke et al., Z. Physik 156 416 (1959)

Fr63 M. S. Freedman, F. T. Porter and F. Wagner, Phys. Rev. 152 1005 (1966)

Fu67 F. Fukuzawa, N. Imanishi, M. Sakisaka, K. Yoshida, Y. Uemura, S. Kakigi and H. Fujita, Bull. Inst. Chemi. Res. Kyoto Univ. 45 363 (1967)

Gr61 E. P. Grigoriev and A. V. Zolotain, Nucl. Phys. 22 689 (1961)

Ha49 O. Haxel, J. H. D. Jensen and H. E. Suess, Phys. Rev. 75 1766 (1949)

He54 N. D. Heydenburg and G. M. Temmer, Phys. Rev. 93 906 (1954)

Im65 N. Imanishi, M. Sakisaka, F. Fukuzawa and Y. Uemura, J. Phys. Soc. Japan 20 2100 (1965)

Im67 N. Imanishi, F. Fukuzawa, M. Sakisaka and Y. Uemura, Nucl. Phys. A101 654 (1967)

Im69 N. Imanishi, H. Nakahara, M. Ishibashi, I. Fujiwara and T. Nishi, J. Inorg. Nucl. Chem. 31 2284 (1969)

Im69a N. Imanishi, M. Sakisaka and F. Fukuzawa, Nucl. Phys. A125 626 (1969)

Im70 N. Imanishi et al. (To be published)

Jo66 K. W. Jones and A. Schwarzshild, Phys. Rev. 148 1148 (1966)

Ka62 H. Kamitsubo, J. Phys. Soc. Japan 17 252 (1962)

Ke56 A. K. Kerman, Mat. Fys. Medd. Dan. Vid. Selsk. 30 No. 6 (1956)

Ki60 L. S. Kisslinger and R. A. Sorensen, ibid. 32 NO. 9 (1960)

Ki63 L. S. Kisslinger and R. A. Sorensen, Revs. Mod. Phys. 35 853 (1963)

Ki67 L. S. Kisslinger and K. Kumar, Phys. Rev. Lett. 19 1239 (1967)

Ko65 J. B. van der Kooi and H. J. van den Bold, Nucl. Phys. 70 449 (1965)
Ku60 T. Kuroyanagi, J. Phys. Soc. Japan 15 2179 (1960)
Ku61 T. Kuroyanagi, ibid. 16 2363 (1961)
La66 H. Langhoff, L. Frevert, W. Schott and A. Flammersfeld, Nucl. Phys. 79 145 (1966)
La67 H. Langhoff and M. Schumacher, Bull. Am. Phys. Soc. 12 129 (1967)
Ma49 M. G. Mayer, Phys. Rev. 75 1969 (1949)
Ma62 V. Maxisa, W. H. Kelley and D. J. Horen, J. Inorg. Nucl. Chem. 24 1175 (1962)
Ma66 F. B. Marik and W. Scholz, Phys. Rev. 150 919 (1966)
Mc64 J. O. McCullen, B. F. Bayman and L. Zamik, Phys. Rev. 134 B515 (1964)
Me62 F. R. Metzger, Phys. Rev. 127 220 (1962)
Mo59 B. Mottelson and S. G. Nilsson, Mat. Fys. Medd. Dan. Vid. Selsk. 1 No. 8 (1959)
ND65 P. H. Stelson and L. Grodzins, Nuclear Data A1-1-21 (1965)
ND66 S. C. Pancholi, K. Way and Ikegami, ibid. B1-6-47 (1966)
ND66a S. C. Pancholi and H. Ikegami, ibid. B1-6-79 (1966)
ND66b A. Artna, ibid. B1-4-49 (1966)
ND66c A. Artna, ibid. B1-4-125 (1966)
Pa56 M. A. Papineau, Compt. Rend. 242 2933 (1956)
Pl65 H. S. Plendl, L. J. Defelice and R. K. Sheline, Nucl. Phys. 73 131 (1965)
Po66 F. T. Porter, M. S. Freedmann, F. Wagner and K. A. Orlandini, Phys. Rev. 146 774 (1966)
Pr67 S. Prawirosoehardjo, Phys. Rev. 157 995 (1967)
Ra66 P. V. Rao and R. W. Fink, priv. comm. (1966)
Ra66a P. V. Rao, D. K. McDaniels and B. Crasemann, Nucl. Phys. 81 296 (1966)
Ra67 P. V. Rao and R. W. Fink, Phys. Rev. 154 1208 (1967)
Re64 K. R. Reddy, A. S. Johnston and S. Jha, Bull. Am. Phys. Soc. 9 17 (1964)

Ri60 R. A. Ricci, R. van Lieshout and H. J. van den Bold, Physica 26 1014 (1960)

Ri62 R. C. Ritter, P. H. Stelson, F. K. McGowan and R. L. Robinson, Phys. Rev. 128 2320 (1962)

Ro64 R. L. Robinson, F. K. McGowan and P. H. Stelson, ORNL 3582 112 (1964)

Ro67 R. L. Robinson, F. K. McGowan, P. H. Stelson and W. T. Milner, Nucl. Phys. A104 401 (1967)

Ro67a R. L. Robinson, F. K. McGowan, P. H. Stelson and W. T. Milner, Nucl. Phys. A96 26 (1967)

Sc55 A. W. Schardt and J. P. Welker, Phys. Rev. 99 810 (1955)

Sc66 J. J. Schwartz and W. P. Alford, Phys. Rev. 149 820 (1966)

Sc67 W. Scholz and F. B. Malik, Bull. Am. Phys. Soc. 12 66 (1967)

Sc67a J. J. Schwartz, Phys. Rev. Lett. 18 174 (1967)

Sc67b J. J. Schwartz, W. P. Alford and A. Marinor, Phys. Rev. 153 1248 (1967)

Sh59 E. N. Shipley, F. J. Lynch and R. E. Holland, Bull. Am. Phys. Soc. 4 404 (1959)

Sl65 L. A. Sliv and I. M. Band, Alpha-, beta-, and gamma-ray spectroscopy ed. by K. Siegbarn (North Holland Publ. Co. Amsterdam 1965) 1639

So64 R. A. Sorensen, Phys. Rev. 133 B281 (1964)

Sp68 K. H. Speidel et al., Nucl. Phys. A115 421 (1968)

Te56 G. M. Temmer and N. P. Heydenburg, Phys. Rev. 104 967 (1956)

Th55 S. Thulin, Arkiv Fysik 9 137 (1955)

Va62 J. Varma and M. A. Eswaran, Phys. Rev. 125 652 (1962)

Yt60 C. Ythier and R. van Lieshout, J. Phys. radium 21 476 (1960)

Yn64 I. L. Yntema and G. R. Sachler, Phys. Rev. 134 B976 (1964)